



PHD

**The adsorption of methane and ethane on type 5A molecular sieve.**

Robinson, K. S.

*Award date:*  
1978

*Awarding institution:*  
University of Bath

[Link to publication](#)

## Alternative formats

If you require this document in an alternative format, please contact:  
[openaccess@bath.ac.uk](mailto:openaccess@bath.ac.uk)

### General rights

Copyright and moral rights for the publications made accessible in the public portal are retained by the authors and/or other copyright owners and it is a condition of accessing publications that users recognise and abide by the legal requirements associated with these rights.

- Users may download and print one copy of any publication from the public portal for the purpose of private study or research.
- You may not further distribute the material or use it for any profit-making activity or commercial gain
- You may freely distribute the URL identifying the publication in the public portal ?

### Take down policy

If you believe that this document breaches copyright please contact us providing details, and we will remove access to the work immediately and investigate your claim.

THE ADSORPTION OF METHANE AND ETHANE

ON TYPE 5A MOLECULAR SIEVE

Submitted by K. S. Robinson

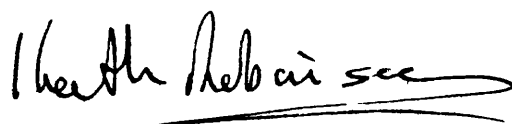
for the degree of Ph.D. of the University of Bath

1978

COPYRIGHT

Attention is drawn to the fact that copyright of this thesis rests with its author. This copy of the thesis has been supplied on condition that anyone who consults it is understood to recognise that its copyright rests with its author and that no quotation from the thesis and no information derived from it may be published without the prior written consent of the author.

This thesis may be made available for consultation within the University Library and may be photocopied or lent to other libraries for the purposes of consultation.

A handwritten signature in black ink, appearing to read 'Keith Robinson', with a horizontal line underneath.

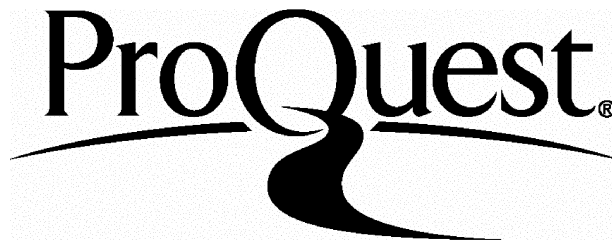
ProQuest Number: U641804

All rights reserved

INFORMATION TO ALL USERS

The quality of this reproduction is dependent upon the quality of the copy submitted.

In the unlikely event that the author did not send a complete manuscript and there are missing pages, these will be noted. Also, if material had to be removed, a note will indicate the deletion.



ProQuest U641804

Published by ProQuest LLC(2015). Copyright of the Dissertation is held by the Author.

All rights reserved.

This work is protected against unauthorized copying under Title 17, United States Code.  
Microform Edition © ProQuest LLC.

ProQuest LLC  
789 East Eisenhower Parkway  
P.O. Box 1346  
Ann Arbor, MI 48106-1346

UNIVERSITY OF BATH  
LIBRARY

Q1 20 FEB 1981

PHD

## PREFACE

The author would like to express his sincere thanks to his supervisor, Professor W. J. Thomas, for his patience and timely encouragement.

Thanks are also due to Mr. A. D. Lockett, who modified the recorder and supervised connections to the P.D.P8, Dr. J. W. Thompson, who modified Real Time Focal and to Mr. J. Stainer and Mr. M. Wilkes for their help.

Financial support was provided by the S.R.C. and this is gratefully acknowledged.

CONTENTS

	<u>Page No.</u>
<u>SUMMARY</u> .. .. .	1
 <u>CHAPTER ONE</u>	
<u>INTRODUCTION AND LITERATURE SURVEY</u>	
1.1 Introduction .. .. .	3
1.2 Isotherm Equations .. .. .	6
1.2.1 Single Component Models .. .. .	6
1.2.1a Langmuir Adsorption Isotherm .. .. .	6
1.2.1b Statistical Thermodynamic Model .. .. .	8
1.2.1c Polanyi Adsorption Potential Theory .. .. .	9
1.2.2 Multi-component Models .. .. .	11
1.2.2a Extended Langmuir Isotherm .. .. .	11
1.2.2b Ideal Adsorbed Solution Theory .. .. .	11
1.2.2c Statistical Thermodynamic Model .. .. .	12
1.2.2d Polanyi Adsorption Potential Theory .. .. .	13
1.3 Mathematical Modelling of Fixed-bed Breakthrough	14
1.4 Experimental Methods .. .. .	15
1.4.1 Gravimetric Method .. .. .	15
1.4.2 Volumetric Method .. .. .	15
1.4.3 Fixed-bed Flow Cell .. .. .	16
 <u>CHAPTER TWO</u>	
<u>APPARATUS AND EXPERIMENTAL</u>	
2.1 Introduction .. .. .	17
2.2 Apparatus .. .. .	17
2.3 Gas Sample Analysis .. .. .	19
2.4 Data Link to P.D.P.8 Computer .. .. .	20
2.5 Automatic Attenuation Switching .. .. .	21
2.6 Calibration .. .. .	22
2.7 Determination of Apparatus Dead-time .. .. .	22
2.8 Materials .. .. .	22
2.9 Gas Sample Preparation .. .. .	24
2.10 Adsorbent Regeneration .. .. .	24
2.11 Adsorbent Weight Loss on Regeneration .. .. .	25
2.12 Experimental Procedure .. .. .	25
2.13 Variation in Outlet Flowrate with Adsorbate Concentration .. .. .	27
 <u>CHAPTER THREE</u>	
<u>ADSORPTION DATA ANALYSIS PROGRAM</u>	
3.1 Data Input .. .. .	29
3.2 Calculation Sequence .. .. .	29

ADSORPTION ISOTHERM EXPERIMENTAL RESULTS AND MATHEMATICAL MODELLING

4.1	Single Component Adsorption Isotherm .. .. .	33
4.1.1	On 4A Molecular Sieve .. .. .	33
4.1.2	On 5A Molecular Sieve .. .. .	33
4.1.2a	Methane .. .. .	34
4.1.2b	Ethane .. .. .	35
4.1.3	Polanyi Adsorption Potential Theory Correlation ..	35
4.1.4	On Activated Carbon .. .. .	36
4.1.4a	Methane .. .. .	36
4.1.4b	Ethane .. .. .	36
4.1.5	Polanyi Adsorption Potential Theory Correlation ..	37
4.1.6	Conclusions .. .. .	37
4.2	Binary Adsorption Isotherm Results on 5A Molecular Sieve	38
4.3	Mathematical Modelling of Binary Adsorption Data ..	39
4.3.1	Extended Empirical Langmuir Equation .. .. .	39
4.3.2	Kidnay-Meyers Model .. .. .	39
4.3.3	Two Component Statistical Thermodynamic Model ..	40
4.3.4	Polanyi Adsorption Potential Theory Correlation ..	40
4.4	Conclusions .. .. .	40
4.5	Modified Coefficient Single Component Empirical Langmuir Model .. .. .	42

CHAPTER FIVEMATHEMATICAL MODELLING OF FIXED-BED BREAKTHROUGH

5.1.1	Derivation of Equations .. .. .	45
5.1.2	Mass Transfer Rate Controlling Mechanism .. .. .	46
5.1.2a	Micro-pore Diffusion Control .. .. .	46
5.1.2b	Surface Diffusion Control .. .. .	47
5.1.2c	Gas Phase Mass Transfer Control .. .. .	47
5.1.2d	Conclusions .. .. .	48
5.1.3	Finite Difference Approximations .. .. .	49
5.1.4	Boundary Conditions .. .. .	50
5.1.5	Bed Axial Flow Profile .. .. .	51
5.1.6	Calculation Sequence .. .. .	52
5.2	Single Component Breakthrough .. .. .	53
5.2.1	Stability and Convergence .. .. .	54
5.2.1a	Equilibrium Control Model .. .. .	54
5.2.1b	Linear Lumped Parameter Model .. .. .	58
5.2.2	The Effect of Various Bed Axial Flow Profiles and the Mole Fraction of Adsorbate in the Gas Phase .. .. .	59
5.2.2a	No Axial Flow Profile .. .. .	59
5.2.2b	Linear Axial Flow Profile .. .. .	59
5.2.2c	Equal Fractional Axial Concentration and Flow Profiles ..	60
5.2.3	The Effect of the Change in Outlet Flowrate with Gas Phase Composition .. .. .	60
5.2.3a	Equilibrium Model .. .. .	60
5.2.3b	Linear Lumped Parameter Model .. .. .	60
5.2.4	The Effect of a Non-step Change in Inlet Adsorbate Concentration .. .. .	61
5.3	Results .. .. .	61
5.4	Conclusions .. .. .	62
5.5	Binary Adsorption Breakthrough .. .. .	63
5.6	Results .. .. .	64
5.7	Conclusions .. .. .	64

DESORPTION SEPARATION OF BINARY MIXTURES ON 5A MOLECULAR SIEVE

6.1	Introduction	..	..	..	..	65
6.2	Experimental	..	..	..	..	66
6.3	Results	..	..	..	..	66
6.4.1	Mathematical Modelling of the Experimental Adsorption-Desorption Cycles	..	..	..	..	67
6.4.2	Results	..	..	..	..	67
6.4.3	Conclusions	..	..	..	..	68
6.5.1	The Computer Simulation of Adsorption-Desorption Cycles	..	..	..	..	68
6.5.2	Results	..	..	..	..	69
6.5.3	Conclusions	..	..	..	..	69
<u>SUGGESTIONS FOR FURTHER WORK</u>						70
<u>NOMENCLATURE</u>						71
<u>REFERENCES</u>						74
<u>FIGURES AND TABLES</u>						
<u>APPENDIX ONE</u>						

Flow diagram and listing of Data Acquisition Program

<u>APPENDIX TWO</u>						
---------------------	--	--	--	--	--	--

Flow diagram, listing and typical results for the  
Adsorption Data Analysis Program

<u>APPENDIX THREE</u>						
-----------------------	--	--	--	--	--	--

Flow diagram, listing and typical results for the  
Binary Adsorption Breakthrough Modelling Program



SUMMARY

The subject of this dissertation is the adsorption of methane and ethane on a 5A molecular sieve. An experimental method, based on the fixed-bed flow-cell, was developed covering a wide range of adsorbate partial pressures in a continuous sequence.

A Laporte type 4A molecular sieve failed to adsorb methane or ethane.

Single component isotherms were established for a 5A molecular sieve and an activated carbon at 20°C. Binary isotherms were obtained for the 5A molecular sieve, at high fractional saturation, at 20°C. The results obtained for single components agreed well with an established mathematical model. Single component isotherms on the activated carbon were of the same order as have been found by other workers.

All the single component isotherms could be expressed in terms of an empirical Langmuir model. None of the models used to describe the binary adsorption data on the 5A molecular sieve, from the single component model coefficients, gave satisfactory results. An empirical method was employed to model the binary adsorption data using single component empirical Langmuir models to express the isotherm of each component in each mixture. The Langmuir model coefficients were then expressed as a function of the gas phase mole fraction of the interfering species.

Adsorbent particle macro-pore spectra and volume were determined using mercury porosimetry. Isothermal fixed bed experiments were carried out, and data from the isotherm experiments were used, to obtain breakthrough data for single and two component mixtures over a range of component relative mole fractions, total adsorbate mole fraction of the total flow, adsorbate concentration and flow rate.

Mathematical models, using finite difference techniques, were used to model the fixed bed breakthrough data. In the instances where the total adsorbate concentration was a significant proportion of the total gas phase concentration a constant flow rate through the bed could not be assumed. A mathematical method was developed whereby a bed axial flow profile was calculated and used in the solution of the fixed bed flow equations with excellent results. Stability criteria were derived for equilibrium and linear lumped parameter kinetic models which gave more accurate predictions of the finite difference step lengths and also explained instability in the equilibrium control model at what were previously thought to be suitable step lengths. An equilibrium control model was found to give good results over the whole range of experimental conditions.

Isothermal fixed bed experiments were carried out to determine the desorption kinetics of methane-ethane mixtures. A linear lumped parameter model was used to describe the desorption of both components. A series of computer simulations were run, using the results from these experiments to examine the feasibility of using the desorption step to effect a further separation, especially when the initial gas feed contained a small fraction of ethane.

CHAPTER ONE

INTRODUCTION AND LITERATURE SURVEY

1.1 INTRODUCTION

The recent sharp rise in crude oil prices and the subsequent increase in the manufacturing costs of the many products for which it is the starting material has stimulated research towards finding alternative sources of starting materials for these products. Ethylene is a product derived from crude oil, which has a very important role as the starting material for a large number of widely used products. Not only can ethylene be produced in the catalytic cracking of crude oil but also by the high temperature reforming of ethane. An alternative source of hydrocarbon starting material, which is receiving increasing attention is natural gas. The deposits in Western Europe contain typically 3% by volume of ethane as well as smaller quantities of heavier hydrocarbons (1). Throughout the rest of the world natural gas deposits containing up to 8% by volume of ethane have been found (2). An industrial plant to manufacture a wide variety of hydrocarbon based products has been designed to operate on a feedstock of natural gas (3). Large volumes of light hydrocarbons, including ethane, are produced during the refining of crude oil and could be used as a feedstock for the production of ethylene and other more complex products.

A plant using ethane as a feedstock requires a feed as rich as possible in ethane to reduce plant size, pumping costs and heating costs.

The enrichment or separation of gas mixtures is normally achieved by low temperature (cryogenic) distillation (4), adsorption (5), or absorption (6). Which method is to be used is a matter to be decided by an economic evaluation concerned not only with the composition of the supply and the required concentration of the product but also on the siting of the plant. The separation of a small quantity of ethane from

a large volume flow of methane, such as natural gas, would be very difficult by absorption owing to the chemical and physical similarity of the two species involved. Cryogenic distillation requires a large capital outlay for compressors and heat exchange equipment. Adsorption is already used to remove trace impurities from natural gas. It was decided, therefore, that this work should concentrate on the separation of methane-ethane mixtures by adsorption-desorption on 5A or 4A molecular sieves.

Molecular sieves comprise porous aluminosilicate frameworks, as their calcium, sodium or potassium salts, constructed from tetrahedral units stacked to form larger polyhedra. Access to the inside of the polyhedra is via the windows in the tetrahedra, thus limiting the size of molecule that can enter. The window size is small ( $3 - 10 \text{ \AA}$  diameter) when compared with the pore size of other adsorbents ( $10 - 10,000 \text{ \AA}$ ;  $40 - 100 \text{ \AA}$  average diameter) and can be manufactured to a specific size by the substitution of various cations within the structure.

Molecular sieves (usually type 5A;  $\sim 5 \text{ \AA}$  diameter window) are used in the gas processing industry to remove water, sulphur bearing compounds, carbon dioxide and oxygen from natural gas (2). 4A and 5A molecular sieves were chosen as the adsorbents in this work as it was hoped that the small pore size would maximise the difference in desorption rates between molecules of a similar volume and shape, thereby producing a second separation on desorption. These molecular sieves would also eliminate the branched chain heavier hydrocarbons (8) present in natural gas which would produce unwanted compounds when the adsorbates were desorbed and processed.

The necessary first step in the research program was the study of gas-solid equilibrium between methane or ethane on the molecular sieves followed by the acquisition of binary adsorption equilibrium data. A mathematical model had then to be found which would express the binary data, in a form suitable for the computer modelling of fixed bed

breakthrough, preferably in terms of single component models only. For simplicity, this initial investigation was carried out under isothermal conditions, at 20°C. As an industrial process subject to overall plant economic viability would be required to operate in such a way that the maximum use is made of an adsorbent, the single component and binary isotherms were determined up to a high level of adsorbent saturation. No work has been reported for methane as a single component or as binary mixtures with ethane, on molecular sieves in this region.

The acquisition of gas-solid equilibrium data has been time consuming, especially when more than one adsorbate is present. It was therefore decided to develop an experimental method, based on the fixed-bed flow cell, that would produce up to 10 or 12 experimental equilibrium data points in each run and which would be suitable for on-line computer control. Single component isotherms for methane and ethane were obtained using an activated carbon adsorbent to further test the experimental method developed. The next step involved the mathematical modelling of fixed-bed break through over a range of experimental conditions and the determination of the gas-solid mass transfer model which gave the best fit between experimental and computer model results. Desorption kinetics were then studied and a series of computer simulations were run to demonstrate the feasibility of a second separation step on desorption over a range of initial gas feed compositions. Although an industrial adsorption-desorption process would probably be non-isothermal, it was thought that the isothermal experiments would provide the basic data and give an indication of the feasibility of such a process.

## 1.2 ISOTHERM EQUATIONS

The equilibrium that exists between a single adsorbate in the gas phase and its concentration on the surface of a solid adsorbent with which it is in contact varies with the gas phase concentration of the adsorbate and the temperature of the adsorbent as well as with the chemical and structural nature of the adsorbent and adsorbate. Several mathematical models have been proposed to describe gas-solid equilibrium for a given adsorbate-adsorbent system.

### 1.2.1 SINGLE COMPONENT MODELS

#### 1.2.1a The Langmuir Adsorption Isotherm (8)

The model is based on the following assumptions:

- 1) mono-layer adsorption.
- 2) localised adsorption on active sites.
- 3) the heat of adsorption is independent of surface coverage.

Let  $V_e$  equal the equilibrium volume of gas adsorbed per unit mass of adsorbent at a pressure  $p$  and  $V_m$  equal the volume of gas required to cover unit mass of adsorbent with a complete mono-layer.

The rate of adsorption is directly proportional to:

- a) the rate of collision between active sites and gas molecules, which is directly proportional to the pressure  $p$ .
- b) the probability of striking an active site  $(1 - V_e/V_m)$ .
- c) an activation term,  $\exp(-E_A/RT)$ , where  $E_A$  is the activation energy for adsorption.

The rate of desorption is directly proportional to:

- a) the fraction of the surface that is covered,  $V_e/V_m$ .
- b) an activation term,  $\exp(-E_D/RT)$ , where  $E_D$  is the activation energy for desorption.

Therefore, at equilibrium:

$$p(1-V_e/V_m) \times \text{EXP}(E_A/RT) = k \times (V_e/V_m) \times \text{EXP}(-E_D/RT) \quad (1.1)$$

where  $k$  is a constant of proportionality:

$$\text{i.e. } p = k \times \exp\{\Delta H_{\text{ADS}}/RT\} \times \frac{V_e/V_m}{(1 - V_e/V_m)} \quad (1.2)$$

where  $\Delta H_{\text{ADS}} = E_A - E_D =$  heat of adsorption and is independent of surface coverage. Therefore,

$$k \times \exp(\Delta H_{\text{ADS}}/RT) = \frac{1}{b} \quad (1.3)$$

where  $b$  is a constant.

From equations 1.1 and 1.3 it can be seen that

$$b \propto \frac{\text{Rate of desorption}}{\text{Rate of absorption}} \quad (1.4)$$

Substituting equation 1.3 in equation 1.2 and rearranging gives:

$$V_e = \frac{V_m \times b \times p}{1 + b \times p} \quad (1.5)$$

By considering equation 1.5 and equation 1.4 we can see that:

- a) If Rate of adsorption  $\gg$  Rate of desorption, then  $V_e \approx V_m \times b \times p$ , and a linear isotherm results.
- b) If the rate of desorption is significant when compared with the rate of adsorption, then as the degree of coverage increases desorption will play an increasingly important role and the isotherm will be non-linear (equation 1.5).

Equation 1.5 is usually expressed as

$$q = \frac{A \times B \times c}{1 + B \times c} \quad (1.6)$$

The coefficients A and B are normally found empirically by a least squares fit of the model to experimental data. This form of equation has found wide use, describing chemisorption and physical adsorption on a wide variety of adsorbents (9, 10, 11, 12). The coefficient B, expressing the degree of non-linearity of the isotherm, can be expressed as a function of temperature in an Arrhenius type of equation (13). The coefficient A, giving a value for the number of active sites on the surface area, is normally unaffected by temperature.

The simple form of the Langmuir isotherm equation is ideally suited to the large number of computer calculations necessary for the modelling of fixed-bed breakthrough.

#### 1.2.1b Statistical Thermodynamic Model (14)

Adsorption within the regular micro-porous structure of molecular sieves has been described by Ruthven et al. (14), for type 4A and 5A molecular sieves, with the following assumptions:

- 1) Adsorption is not limited to active sites within each cavity.
- 2) there is no interchange of occluded molecules between cavities.

The sorbate molecule must obviously be small enough to enter through the cavity window.

The derivation of the theoretical isotherm from a simple idealised statistical thermodynamic analysis involves the definition of the grand partition function for each cavity subsystem. An expression for the average number of molecules in each cavity, with the use of an approximation for the configuration integral in terms of measurable physical properties, yields:

$$Q = \frac{K \times P + (K \times P)^2 \times \left(1 - \frac{2 \times \beta}{\gamma}\right)^2 + \dots + \frac{(K \times P)^m}{(m-1)!} \times \left(1 - \frac{m \times \beta}{\gamma}\right)^m}{1 + K \times P + \frac{1}{2!} \times (K \times P)^2 \times \left(1 - \frac{2 \times \beta}{\gamma}\right)^2 + \dots + \frac{(K \times P)^m}{m!} \times \left(1 - \frac{m \times \beta}{\gamma}\right)^m} \quad (1.7)$$



where  $Q$  has the units of molecules/cavity.

Temperature dependence is taken into account by expressing the Henry's Law constant  $K$  in the form of an Arrhenius equation thus:

$$K = K_0 \times \exp (\Delta H_0/RT) \quad 1.8$$

where  $\Delta H_0$  and  $K_0$  are determined from experimental data. The effective molecular volume  $\beta$  is found by curve-matching graphs of  $Q$  vs.  $K \times P$  with  $\beta/\gamma$  as the third variable, where  $\gamma$  is the volume of a molecular sieve cavity.  $M$  is an integer approximation to  $\gamma/\beta$ , the saturation limit expressed as a whole number of molecules per cavity.

Although this form of isotherm equation has been successfully applied to a number of adsorbates in type 4A and 5A molecular sieves, over a wide range of temperatures and gas phase adsorbate concentration, up to 1 atmosphere, (14), the computational effort required is too large for the modelling of fixed bed breakthrough. The model was used, however, to test the accuracy of the experimental method developed for the adsorption of methane and ethane, as single components, on 5A molecular sieve.

#### 1.2.1c Polanyi Adsorption Potential Theory (8)

The assumptions forming the basis for this model, in its simplest and most often used form, are:

- 1) The adsorbed phase is confined within the adsorption space between the solid surface and the gas phase.
- 2) The chemical potential of a point in this space is a measure of the work done by the surface forces in bringing one molecule of adsorbate to this point, from a point where the forces have no influence.
- 3) The free energy change in passing from liquid to adsorbed phase state is small compared with the change in free energy in passing from gas to liquid state.

i.e. the adsorbed state is considered to behave as a liquid.

With the above assumptions and the modification of Lewis et al. (15), who substituted fugacity for pressure, the adsorption potential of a given surface for an adsorbate is given by:

$$R \times T \times \ln \frac{f_0}{f} \quad \text{I.9}$$

The Polanyi Adsorption Potential Theory postulates that there is a unique relationship between the adsorbed phase volume,  $V$ , and the adsorption potential.

The most frequently used relationship is:

$$\ln V = g \left( R \times T \times \ln \left( \frac{f_0}{f} \right) \right) \quad \text{1.10}$$

Although this model involves a great deal of calculation there is a large amount of experimental evidence to indicate that it may be used to describe the adsorption of a range of similar compounds, on a given adsorbate, by a single relationship, over a wide range of temperature and gas phase adsorbate concentrations (15, 16, 17, 18). This being the case, by a series of strategically planned experiments, with one or two adsorbates, a relationship could be obtained which would provide equilibrium data over a wide range of components, temperature and gas phase adsorbate concentration. Data thus obtained could be fitted by a simpler empirical model, such as the Langmuir isotherm, for use in the computation of fixed bed breakthrough data.

The form of equation 1.10, modified to provide a single correlation for more than one single adsorbate on a particular adsorbent, is:

$$\ln V = g(I)$$

where  $I = \frac{R \times T \times \ln \left( \frac{f_0}{f} \right)}{D}$  1.11

Lewis et al. (15) and Grant et al. (17) used the molar saturated liquid volume at the temperature at which the vapour pressure of the liquid is equal to the adsorption pressure as the correlating divisor,  $D$ . Later, Manes and Smith (18) applied a simpler model using the normal liquid boiling point molar volume, with a correction factor for various adsorbates.

Either method produces satisfactory results but the simpler model of Manes and Smith (18) was adopted for the work in this thesis.

### 1.2.2 MULTI-COMPONENT MODELS

#### 1.2.2a The Extended Langmuir Isotherm

Provided that  $A_1 = A_2 = \dots = A_N$ , implying a constant separation factor between all components, and that the adsorbed phase behaves ideally, then the Langmuir model for mixed adsorption can be expressed, in terms of the single component coefficients, as:

$$q_i = \frac{A_i \times B_i \times c_i}{N \left( 1 + \sum_{i=1} B_i \times c_i \right)} \quad 1.12$$

The above provisions are rarely met in practice but an empirical form of equation 1.12 can be used when the deviations from the model are small.

For a binary mixture equation 1.12 becomes

$$q_1 = \frac{A_1 \times B_1 \times c_1}{1 + B_1 \times c_1 + B_{e1} \times c_2} \quad 1.13$$

where  $B_{e1}$  is found by a least squares fit of experimental data to the model. This form of binary isotherm has been used by Thomas and Lombardi (10) for toluene in toluene-benzene mixtures on activated carbon.

#### 1.2.2b The Ideal Adsorbed Solution Theory

This theory, due to Meyers and Prausnitz (20), treats the adsorbed state in a manner similar to Raoult's Law for vapour-liquid equilibrium and proposes a surface potential or spreading pressure,  $\pi$ , for each pure component, of the form:

$$\pi = \frac{a}{R \times T} \times \int_0^p \frac{q}{p} \cdot dp \quad 1.14$$

This method has successfully predicted binary adsorption equilibrium at equal values of the spreading pressure,  $\pi$ , for all components (21).

The amount of computation required is large and a great deal of experimental data at low values of  $\rho$  is required for the accurate calculation of  $\pi$ . The simplest method of calculating binary equilibria using the Ideal Adsorbed Solution Theory is a graphical one. The assumption of ideal adsorbed phase behaviour limits its application, although, for small deviations from ideality, this theory has been used to calculate adsorbed phase activity coefficients (22, 23).

A simplification of the Ideal Adsorbed Solution Theory, due to Kidnay and Meyers (24), can be applied when the adsorbed phase concentration of each component is related to its spreading pressure by the same function, i.e.  $A_1 = A_2$ . This is a necessary but not sufficient condition, as ideal adsorbed phase behaviour is required for an accurate description of binary adsorption.

### 1.2.2c Statistical Thermodynamic Model (25)

Ruthven et al. (25) have extended the single component model (14) to include binary adsorption on type A zeolites, thus:

$$Q_1 = \frac{K_1 \times P_1 \times \sum_{i=1}^M \sum_{j=1}^N \frac{(K_1 \times P_1)^j \times (K_2 \times P_2)^j \times (1-i \times \beta_1 - j \times \beta_2)^{i+j}}{(i-1)! \times j!}}{1 + K_1 \times P_1 + K_2 \times P_2 \sum_{i=1}^M \sum_{j=1}^N \frac{(K_1 \times P_1)^i \times (K_2 \times P_2)^j \times (1-i \times \beta_1 - j \times \beta_2)^{i+j}}{i! \times j!}} \quad 1.15$$

with a similar expression for  $Q_2$ .

Where  $i + j > 2$  and  $i \times \beta_1 + j \times \beta_2 < \gamma$ .

This model has successfully predicted binary gas-solid equilibria at low total sorbate concentrations but failed to give accurate results at high fractional saturation for methane-nitrogen mixtures on 5A molecular sieve (25).

This failure was thought to be due to a change in the adsorbate volumes at the high pressures used (up to 30 atmospheres partial pressure of methane). At sufficiently low levels of adsorbate concentration, i.e. approx. 2-3 molecules/cavity, the terms in the summation series in equation 1.15 may be neglected and the equation reduces to a two component extended Langmuir isotherm equation. When  $\beta_1 = \beta_2$  it has been shown that (25) equation 1.15 gives the same results as the Ideal Adsorbed Solution Theory.

The multi component statistical thermodynamic model also assumes ideal adsorbed phase behaviour.

#### 1.2.2d Polanyi Adsorption Potential Theory

Manes and Smith (18) have used the Polanyi Adsorption Potential Theory to predict binary adsorption on an activated carbon.

Assuming ideal adsorbed phase behaviour, at equal adsorption potential for a binary mixture:

$$\frac{R \times T}{D_1} \times \ln\left(\frac{wX_1 \times f_1^0}{f_1}\right) = \frac{R \times T}{D_2} \times \ln\left(\frac{wX_2 \times f_2^0}{f_2}\right) \quad 1.16$$

Equation 1.16 can be solved implicitly for the adsorbed phase mole fractions,  $wX$ , which with the single component correlation, given by equation 1.11 gives the multi component equilibrium adsorbed phase concentrations.

The results calculated in this manner by Manes and Smith (18) were typically within  $\pm 3\%$  of the experimental values for methane-propane; methane-hexane on activated carbon.

Lewis et al. (19), however, using a similar procedure failed to obtain a satisfactory agreement between calculated and experimental values for relative volatility for several binary mixtures on various adsorbents. For adsorption on activated carbon the calculated values of relative volatility were approximately one third the experimental values. The correlation was better when silica gel was the adsorbent.

### 1.3 MATHEMATICAL MODELLING OF FIXED-BED BREAKTHROUGH

When an inert carrier gas, containing a proportion of an adsorbate, flows through a fixed-bed of adsorbent, a number of processes, either singly or in some combination, limit the rate at which equilibrium is attained between the solid and gas phases:

- 1) micro-pore diffusion.
- 2) macro-pore diffusion.
- 3) Surface diffusion.
- 4) Inter-particle mass transfer.
- 5) Combination of all or any of 1) - 4).
- 6) Axial diffusion in the gas or solid phase.
- 7) No resistance to mass transfer - equilibrium control.

Assuming plug flow, isothermal operation and a constant cross-sectional area for flow within the bed, a gas-solid phase rate equation, a mass balance over a section of the bed and a gas-solid equilibrium relationship provide a set of 3 equations to be solved to give bed exit breakthrough data, (see Chapter 5.1.1). Analytical solutions for all the above constraints, and several of the possible combinations, have been obtained when the flow rate through the bed was constant and a simple, single component gas-solid equilibrium relationship obtained (8, 26, 27).

In the situation where the adsorbate is a significant proportion of the total flow, the flow rate along the bed axis is not constant and no analytical solution is possible unless an expression is found relating the change in axial flow rate with bed axial position and time. Such an expression, if one could be derived, would be complex and make the solution of the fixed-bed breakthrough equations very difficult.

Asymptotic, or constant pattern, solutions have been obtained for many of the listed cases for both single component and binary adsorption (8, 28, 29, 30, 31).

Numerical methods, using finite difference approximations for the partial derivatives, have been used to solve the fixed-bed breakthrough equations (27, 32).

Although it might have been possible to use an asymptotic approximation to the bed axial flow profile, it was decided to use finite difference methods to solve the fixed-bed breakthrough partial differential equations as this method offered greater flexibility.

By solving a mass balance over the whole bed, at the end of each time-step, the inlet gas flow rate can be calculated. For a short bed length, such that the flow profile is predominantly due to adsorption, one can assume a fractional axial flow profile identical to the fractional axial total adsorbate concentration profile (Chapter 5). This formed the basis of the mathematical modelling of fixed-bed breakthrough to include cases when the adsorbate was a significant proportion of the total flow.

#### 1.4 EXPERIMENTAL METHODS

Three methods are generally used for the acquisition of gas-solid equilibrium data.

##### 1.4.1 Gravimetric Method (17, 31, 32)

This method involves the direct measurement of the increase in weight of a sample of adsorbent, at a constant temperature, exposed to an adsorbate, at constant pressure. A buoyancy correction is often required.

##### 1.4.2 Volumetric Method (15, 22, 23)

The gas phase pressure is recorded when a measured volume of adsorbate is added to a cell containing adsorbent, at constant temperature. The difference between the amount of gas added to the cell and the amount present in the gas phase, calculated from the measured pressure, gives the amount adsorbed. A correction for adsorbed phase volume may be necessary.

#### 1.4.3 Fixed-bed Flow Cell (26, 33, 34)

Adsorbate and carrier gas, at constant pressure, are passed over a fixed bed of adsorbent, at constant temperature. The cell effluent is monitored until breakthrough is complete. The difference between the amount of adsorbate flowing into and out of the cell gives the amount adsorbed and accumulated within the bed. A correction for the adsorbate volume and the adsorbate accumulated within the pellet macro-pores and the intergranular voids is not normally necessary as the total voidage is a small proportion of the total flow through the cell (Chapter 4.1.3).

As one of the objectives of this work was to obtain and model the fixed-bed breakthrough of methane-ethane mixtures, the fixed-bed flow cell was a natural choice as a basis for the experimental method that was developed. This method is easier to run at high pressure than the gravimetric method and the most suitable method for computer control.



CHAPTER TWO

APPARATUS AND EXPERIMENTAL

2.1 Introduction

Previous work using the fixed-bed flow-cell has involved single experiments, performed at one set of experimental conditions (26, 33, 34). An extension of this method was envisaged that could be used to cover a range of gas phase concentrations, enabling several points on the isotherm to be obtained in one experiment. As a preliminary step towards the control of the experiment and on-line data analysis by computer, the integration of the gas chromatograms obtained from the analysis of the bed effluent were performed on a Digital Equipment Corporation P.D.P.8 computer. Complete on-line data analysis was not possible as the P.D.P.8 store was not large enough to hold the data analysis program. It was therefore necessary to produce a punched paper tape of the chromatogram peak areas and run the data analysis program on the University I.C.L.-450 computer. It was thought unwise to install computer control of the adsorption cell pressure and gas sampling at this stage, as a degree of manual control was thought necessary when testing a new experimental technique.

2.2 Apparatus

Equipment designations refer to Figure 1. The extension to the fixed-bed flow-cell method was as follows: when breakthrough of all species was complete at the initial pressure, rather than starting a new experiment with fresh adsorbent and a different adsorbate concentration, the concentration of adsorbate was increased by raising the gas pressure in the flow cell, 4, by means of the cylinder-head pressure regulator, PR1, on the gas sample cylinder, 1. Cell effluent analysis continued as the adsorbate concentration was increased, after completion of each breakthrough, in a series of step changes in cell pressure to within approximately 80% of the

sample cylinder pressure.

Outlet flow rate was set by a needle valve, V10, and measured by a bubble flow meter, FM. The pressure in the sample loop and upstream of the outlet flow control valve was maintained constant by a chromatography grade pressure regulator, PR2. The pressure in the sample loop was maintained constant at 28 psig. to match the carrier gas pressure at the chromatography column inlet, to minimise flow surges and injection peaks. A high pressure needle valve, V9, was used as a pressure reducing valve, upstream from the outlet pressure regulator, PR2, to prevent the upstream pressure exceeding the maximum operating pressure of the pressure regulator, at high adsorption cell pressures (greater than 200 psig.).

All pipework downstream from the change over valve, V11, with the exception of the connections between V9 and V13, was of  $\frac{1}{16}$ " O.D. x  $\frac{1}{32}$ " I.D. stainless steel, to withstand the high temperature regeneration - high pressure adsorption cycles and to minimise the apparatus dead time. The flexibility of the tubing allowed 'in situ' regeneration of the adsorbent by moving the adsorption tube between the water bath, 2, and the regeneration furnace, 5. All other pipework was  $\frac{1}{4}$ " O.D. x  $\frac{3}{16}$ " I. D. copper pipe. All pipe joints were brazed or soldered, depending on their maximum operating temperature, except for the minimum number of joints required for the removal of the adsorption tube, valves and pressure gauges. The adsorption cell was an 18" length of  $\frac{1}{4}$ " O.D. x  $\frac{3}{16}$ " I.D. stainless steel tube. The ends were plugged with glass wool and any dead space remaining after the addition of the adsorbent was filled with 30-60 mesh glass beads. All materials for high temperature duty were tested, before use, in a furnace at 500°C. Vacuum for regeneration, VS, was provided by means of an oil diffusion pump, with an extra condenser packed with copper gauze to eliminate oil carry-over, backed by an Edwards Rotary Vacuum Pump. The adsorption cell was immersed in a continuously stirred, lagged water bath, 2. The water bath temperature was maintained constant by means of a Fisons

Fi-monitor Regulator and Red Rod immersion heaters, at  $20^{\circ}\text{C} \pm 0.05^{\circ}\text{C}$  as measured by a mercury in glass thermometer, T1. When the adsorption tube was placed in the water bath the excess piping, approximately 2' long, was coiled, 3, and immersed in the bath to preheat the inlet gas stream.

The regeneration furnace temperature was controlled with a Pye-Ether Mini Temperature Regulator, 6, using a chromed-alumed thermocouple, T2, without cold junction compensation. After 12 hours regeneration under vacuum overnight, the furnace was automatically switched off using an electric time switch, 7, which simultaneously connected the laboratory compressed air supply, CA, to the base of the furnace by means of a solenoid valve, V12. The adsorbent bed was therefore cool and ready for use the next morning.

Adsorption cell effluent was sampled using a Pye six port rotary sampling valve, V13, with a  $0.5\text{ cm}^3$  sample loop, 8.

### 2.3 Gas Sample Analysis

Gas-solid chromatography, based on a Pye 104 unit, was used to analyse the adsorption cell effluent gas samples. A  $4' \times \frac{3}{16}"$  I.D. column containing 80-120 mesh uncoated Porasil B glass beads was used at a temperature of  $50^{\circ}\text{C}$  with a carrier gas flow rate of  $70\text{ cm}^3/\text{min}$ . at an inlet pressure of 28 psig. An identical flow rate was applied to the reference side of the katharometer detector, which was maintained at a temperature of  $200^{\circ}\text{C}$  with a supply current of typically 160 ma. Helium was used as the carrier gas for the adsorption experiments and the chromatography. Neither methane nor ethane peaks were symmetrical and the addition of 3% w/w dinonyl phthalate to the solid phase made no improvement.

The separation obtained in the two component analysis was adequate, Figure 2, except in cases of relative adsorbate concentrations requiring attenuation switching.

Although, in the case of single component experiments, it would have been possible to pass the adsorption cell effluent directly through a calibrated katherometer, it was decided to use the chromatographic analysis to test the peak integration and data analysis programs for systems that had already been described.

#### 2.4 Data Link to the P.D.P.8 Computer

A block diagram of the data link to the P.D.P.8 computer is given in Figure 3. Katherometer output signals were supplied to the P.D.P.8 computer by means of voltage signals in the range 0 - 4.8 volts, proportional to the percentage full scale deflection, obtained from the recorder slide-wire, which were fed into the computer analogue to digital convertor (A.D.C.).

Peak height samples were taken every 200 ms. after a 0.25% full scale deflection threshold had been exceeded, which was detected in a free running loop. This rate of sampling gave approximately 40 data points for the response to either component. Sampling at a faster rate did not alter the values of the peak areas obtained until samples were taken at 60 ms. intervals at which point samples were lost owing to aliasing. To avoid any possibility of aliasing the data were integrated by Simpsons Rule at the end of the sampling sequence. A flow diagram and listing of the P.D.P.8 data acquisition program are given in Appendix 1.

Sample peak areas were reproducible to  $\pm 0.14\%$  for ten replicate samples. Peak areas calculated by on-line computer were in good agreement with those calculated manually (Figure 4). In the case of two component analysis the 0.25% full scale deflection threshold was used to distinguish between the sample peaks. In the worst case the 0.25% full scale deflection threshold represented approximately 5% of the maximum peak height, but in most cases was approximately 0.5% of the maximum peak height. Although difficult to calculate accurately, the error due to the threshold was thought to be negligible.

A digital input push-button switch and digital output light were installed near the apparatus gas sampling valve so that the data acquisition program could be started and stopped by external command and a visible indication of the receipt of the commands was available.

## 2.5 Automatic Attenuation Switching

In order that two component experiments could be performed with a total adsorbate mole fraction of ethane less than 0.1, a series of tests were carried out to investigate the feasibility of switching katharometer output attenuation resistors by commands from the P.D.P.8 computer, triggered by the 0.25% full scale deflection threshold between sample peaks. The circuit employed is shown in Figure 5. Single pole change over reed switches, R1 - R4, with gold plated contacts were used for their high speed of operation. To avoid thermoelectric effects, switch contacts were included in the zero volts line.

S1 was the attenuation selector supplied with the instrument and S2 a single pole 12 way switch connected in parallel with S1 to select the second attenuation setting. There was no offset after switching between the two attenuation values set by S1 and S2. However, when operating the pairs of switches so that contact was either make before break or break before make, a spike of up to 10% full scale deflection occurred on the recorder as the contacts were broken. The decay time of the spike was such that accurate analysis of methane-ethane mixtures, where a change of attenuation was required, was not possible as the spike persisted for longer than the maximum obtainable separation time between peaks. Nevertheless, it was thought that this system could be used successfully when the separation time between peaks was greater than approximately 20 s.

## 2.6 Calibration

The katherometer responses to methane and ethane were found by injecting 0.1 - 1.0 cm<sup>3</sup> samples of each gas. A linear relationship was found between gas volume and peak area, calculated by on-line computer, for both gases over the range investigated (Figure 6). A katherometer response check was performed at the end of each experiment by connecting the appropriate gas cylinder upstream from PR2 and taking a 0.5 cm<sup>3</sup> sample.

Pressure gauges P1 and P2 were calibrated using a Budenburg Standard Test Gauge, before and halfway through the series of experiments. The pressure drop across the adsorption cell was found to be negligible over the range of flow rates used throughout the experiments.

## 2.7 Determination of Apparatus Dead Time

The apparatus dead time was determined with the adsorption cell packed with 30-60 mesh glass beads. The bed effluent response was sampled at 30 s intervals after changing from pure helium to a low mole fraction methane-helium mixture at the initial pressure to be used in the isotherm experiments. The same outlet flow rate was used as that for the isotherm experiments. The gas phase fractional breakthrough obtained at the bed exit is shown in Figure 7.

Integration of 1- fractional breakthrough versus time, by Simpsons Rule, gave the apparatus dead time. The determination was carried out in triplicate and repeated halfway through the series of experiments. An average of the six values , 1.61 min, was used in the data analysis computer program.

## 2.8 Materials

The gases were supplied by Air Products Limited at the following stated purities:

helium	-	99.99 %
methane	-	99.9 %
ethane	-	99.7 %

The methane and ethane purities were checked quantitatively by gas-solid chromatography and qualitatively by mass spectrometer. No contaminants could be detected in the methane. Ethane was found to contain approximately 0.2% by volume of methane. Throughout this work pure ethane refers to ethane at 99.8% containing methane at 0.2% approximately. This level of impurity was not detected at the katheterometer output attenuations used in any of the experiments carried out.

The molecular sieve adsorbents were supplied by Laporte Industries Limited as 1mm - 2mm spherical pellets, made from 1 $\mu$ m - 5 $\mu$ m molecular sieve crystals with approximately 20% by weight of binder, calcined at 650°C. The pellets were crushed in a ball mill and sieved to produce a 30 - 44 mesh cut. The activated carbon adsorbent was supplied by The Lancashire Chemical Company Ltd., in a wide size range. A 30 - 44 mesh cut was obtained by sieving. A visual inspection showed that the 30 - 44 mesh cut 5A molecular sieve pellet and activated carbon particles were similar in shape. Both 5A molecular sieve and activated carbon macro-pore spectra and volume were determined using a Carlo Erba 1500 Mercury Porosimeter. Pore diameters down to 50Å could be determined. A mercury compressibility correction was applied. Calculations were performed using a computer program from the literature (35). A typical porosimeter chart and calculated results are shown in Figure 8 and Table 1 respectively.

For 5A molecular sieve:

$$\text{Average pore diameter} = 603\text{Å}^{\circ}$$

$$\text{Total pore volume: } E_{\text{MACRO}} = 0.322 \text{ cm}^3/\text{gm}$$

For the activated carbon:

$$\text{Average pore diameter} = 962\text{Å}^{\circ}$$

$$\text{Total pore volume: } E_{\text{MACRO}} = 0.282 \text{ cm}^3/\text{gm}.$$

The virtual absence of hysteresis in the porosimeter chart, Figure 8, shows the lack of pores having narrower necks than bodies. The chart for the activated carbon showed only slightly more hysteresis.

Adsorbent bed bulk densities for 5A molecular sieve and activated carbon were determined by measuring the length of a packed bed of adsorbent (after tapping), of known weight, in a  $\frac{1}{4}$ " O.D. x  $\frac{3}{16}$ " I.D. glass tube.

The average of 5 results for each adsorbent, corrected for weight loss on regeneration, were:

$$\begin{aligned} \text{5A molecular sieve: } \rho_{\text{bulk}} &= 0.734 \text{ gm/cm}^3 \\ \text{activated carbon: } \rho_{\text{bulk}} &= 0.494 \text{ gm/cm}^3 \end{aligned}$$

## 2.9 Gas Sample Preparation

Prior to the series of experiments, sample gas cylinder feed lines were flushed to remove water vapour and the whole apparatus was evacuated for 48 hrs. Whenever a gas sample was made-up the sample cylinder feed lines were flushed and the sample cylinder evacuated for 12 hrs.

Samples were made-up as follows:

- a) V3 was closed, V1 opened and the sample cylinder filled with methane and/or ethane to the required pressure.
- b) V1 was closed, V2 opened and the cylinder filled with helium to the required pressure.
- c) V2 and V5 were then closed.

The sample was then analysed to obtain the best katherometer output attenuation settings.

## 2.10 Adsorbent Regeneration

A weighed sample of adsorbent was placed in the adsorption cell which was put into the regeneration furnace. A slow helium purge was passed through the apparatus until the regeneration temperature had been reached, typically 45 min. The helium supply was then switched off (V2) and, with



V9 closed, the adsorption cell was evacuated for 12 hrs as described previously, (Section 2.2 of this Chapter).

### 2.11 Adsorbent Weight Loss on Regeneration

Both the 5A molecular sieve and the activated carbon were tested for weight loss at their respective regeneration temperatures. Samples were analysed in triplicate, in two batches at an interval of 10 days, with no significant change in the percentage weight loss obtained. The average figures used in subsequent calculations were:

5A molecular sieve: 5.10% @ 450°C

activated carbon: 11.00% @ 250°C

### 2.12 Experimental Procedure

It has been shown that the adsorption equilibrium of binary mixtures is independent of the order of contact of the adsorbates for a variety of gases and vapours on several adsorbents (19, 23). Methane-ethane mixtures have not, however, been investigated for the dependence of adsorption equilibrium on the order of contact but as the molecules are simple and non-polar, it was assumed that no such dependence existed on 5A molecular sieve.

After the adsorbent had been regenerated and cooled, the adsorption cell was placed in the water bath, the vacuum switched off and the apparatus pressure tested to 1000 psig. with helium. The helium pressure was then lowered to that required for the first adsorption step and the flow rate set by V10 and measured by the bubble flow meter, FM. The preheater coil was placed in the water bath and helium passed through the apparatus for 2 hrs. to ensure that the adsorbent bed was at the temperature of the water bath. The gas chromatography unit was switched on and allowed to warm up. The peak height data acquisition and integration program was loaded into Real Time Focal K on the P.D.P.8 computer. This modification of Real Time Focal had

the equals sign suppressed to make its output format compatible with the ICL-450 input format.

The pipework from the sample cylinder to V11 was flushed out via V8 at a pressure, P2, equal to that of the helium carrier gas, P1. Before changing over to the gas sample, a number of bed effluent samples were analysed, without using the peak area integration program, to ensure that regeneration was complete and that no impurities were being desorbed by the carrier gas. The peak area integration program was started, V11 switched to connect the sample cylinder to the adsorption cell and the first effluent sample taken. The helium supply was switched off. Adsorption cell effluent samples were then taken and analysed at 30s intervals for single component experiments and 60s intervals for binary adsorption experiments, until breakthrough of all the adsorbate species was complete. At this point the adsorption cell pressure and therefore the adsorbate partial pressure was increased by means of PR1. Bed effluent samples were subsequently taken and analysed as before. The gas phase adsorbate concentration fell to a constant level and then rose again during breakthrough. The experiment continued in a series of pressure steps up to a maximum of 1000 psig. As the adsorption cell pressure was increased above 150 psig., valve V9 was adjusted to maintain P3 below 150 psig. The maximum operating pressure of PR2 was 200 psig. Typical adsorbent bed outlet adsorbate fractional breakthrough, calculated inlet flow rate (for single component only, as binary adsorption results were almost identical) and calculated rates of sorption, for a series of pressure steps, are given for single component and binary adsorption in Figures 9 to 13. The sample and calculated data points have been joined together for ease of representation. Ambient temperature and pressure were measured during the experiment and the outlet flow rate was measured at the end of the experiment.

### 2.13 Variation in Outlet Flowrate with Adsorbate Concentration

In order that high gas phase concentrations of adsorbate could be investigated, while at the same time keeping the total gas phase pressure in the adsorption cell to a reasonable level, gas phase mole fractions of adsorbate up to 0.55 were used. This meant that the amount adsorbed could be a significant proportion of the total flow and hence the inlet flowrate would vary with the rate of sorption (see Figures 10 and 11).

The outlet flowrate, set initially with pure helium, was found to vary with gas phase composition at a constant setting of  $V_{10}$ . Consideration of the isothermal flow through an orifice with a constant discharge coefficient indicated that the outlet volumetric flowrate should decrease with an increase in the gas phase density, or in this case, an increase in adsorbate concentration (36).

However, the gas phase volumetric flowrate was found to increase with adsorbate concentration (Figure 14). Nevertheless, by consideration of the rate of fluid flow through a variable area flowmeter with a constant annulus area and float characteristics it is possible to see that a gas of higher density but lower viscosity can flow at a higher volumetric flowrate than a less dense gas of higher viscosity (37). At one atmosphere pressure and  $20^{\circ}\text{C}$  the viscosity of helium, methane and ethane are:

$2 \times 10^{-6} \text{ N s m}^{-2}$ ;  $1.1 \times 10^{-6} \text{ N s m}^{-2}$ ;  $1.2 \times 10^{-6} \text{ N s m}^{-2}$  respectively (38).

As the viscosity of helium, the least dense gas, is approximately twice that of either methane or ethane it was thought that the increase in outlet gas phase volumetric flowrate with increasing concentration of adsorbate was due to the decrease in gas viscosity producing an increase in the effective discharge coefficient of the outlet flow control valve.

Rather than attempt to model this behaviour in terms of a mathematical expression based on gas flow through an orifice, an empirical relationship was obtained from the experimental data obtained from the isotherm experiments. A least squares straight line fit through the origin

was obtained to the data in Figure 14.

$$\frac{F_o}{F_o \text{ INITIAL}} = 0.35 \times Y_T \quad \dots \quad 2.1$$

where  $F_o$  and  $F_o \text{ INITIAL}$  represent the outlet gas phase flowrate at any time,  $t$ , and that set initially using helium.  $Y_T$  is the mole fraction of total adsorbate in the outlet flow. Although there is some error involved with this model the simple expression was thought adequate as the fractional increases in flow rate were small and the breakthrough of adsorbates lasted a relatively short period of time.

CHAPTER THREE

ADSORPTION DATA ANALYSIS PROGRAM

A fully annotated computer program listing, flow diagram and typical results for binary adsorption are given in Appendix 2.

3.1 Data Input

The basic input data file was created on the I.C.L.-450 computer from the punched tape of experimental peak areas. The additional data required was added after file creation.

3.2 Calculation Sequence

The gas phase mole fractions of each component were calculated assuming a linear relationship between chromatogram peak area and gas volume for each adsorbate (Figure 6).

The apparatus dead time was calculated, taking into account the increased dead volume due to the macro pore volume of the adsorbent. As the average diameter of the adsorbent pellet macro-pores ( $\approx 600 \text{ \AA}$ ) was at least two orders of magnitude larger than the molecular diameter of either adsorbate ( $\approx 5 \text{ \AA}$ ) and was of the same order of magnitude as the mean free path of the gas phase components ( $\approx 500 \text{ \AA}$  at 50 psig and  $20^\circ\text{C}$  (39)), it was decided to include the pellet macro-pore volume in the total bed voidage (see chapter 5.1.5).

The apparatus dead volume, with non-porous glass beads instead of adsorbent, was calculated thus: dead time = 1.61 min. at a flowrate of  $0.97 \times 10^{-3}$  mol/min and 64.7 psig. At this pressure, assuming ideal gas behaviour, the gas density is  $1.97 \times 10^{-4}$  gmol/cm<sup>3</sup>,

$$\therefore \text{dead volume} = \frac{1.61 \times 0.97 \times 10^{-3}}{1.97 \times 10^{-4}} = 7.94 \text{ cm}^3. \quad 3.1$$

$$\therefore \text{dead time with adsorbent in tube} = 1.61 \times \frac{(7.94 + E_{\text{MACRO}} \times \text{WT})}{7.94} \quad 3.2a$$

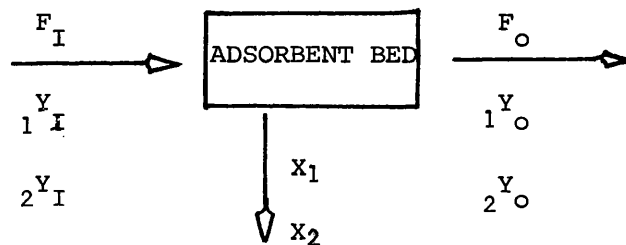
The dead time for flowrates other than that at which the apparatus was

calibrated is given by:

$$\text{deadtime} = \frac{(\text{deadtime at } 0.97 \times 10^{-3} \text{ gmol/min.}) \times 0.97 \times 10^{-3}}{\text{Experimental molar flowrate}} \quad 3.2b$$

Adsorption cell outlet gas phase fractional responses were calculated. Initial and final outlet molar flowrates were calculated, assuming ideal gas behaviour.

The next section calculates the instantaneous rates of sorption and inlet flowrate at each sample time. Using a side-stream to represent the amount of adsorbate adsorbed and accumulated:



A mass balance over the adsorbent bed for component 1 gives:

$$F_I \times \frac{DT}{60} \times Y_{1I} = X_1 + F_O \times \frac{DT}{60} \times Y_{1O} \quad \dots \quad 3.3$$

Similarly for component 2:

$$F_I \times \frac{DT}{60} \times Y_{2I} = X_2 + F_O \times \frac{DT}{60} \times Y_{2O} \quad \dots \quad 3.4$$

An overall mass balance yields:

$$F_I = F_O + (X_1 + X_2) \times \frac{60}{DT} \quad 3.5$$

Assuming a linear relationship between the fractional increase in outlet flowrate and the total adsorbate fractional breakthrough (Chapter 2.13) and putting

$$DF = F_{O \text{ FINAL}} - F_{O \text{ INITIAL}} \quad 3.6$$

one obtains

$$F_O = F_{O \text{ INITIAL}} \times (1 + DF \times (Y_{1O} + Y_{2O})/2) \quad 3.7$$

$$\text{Putting } F_o \times \frac{DT}{60} = F \dots \quad 3.8$$

and substituting equation 3.5 in equation 3.3 and rearranging gives:

$$X_1 \times (1 - {}_1Y_I) - X_2 \times {}_1Y_I = Fx ({}_1Y_I - {}_1Y_O) \quad 3.9$$

Substituting equation 3.5 in equation 3.4 gives:

$$- X_1 \times {}_2Y_I + X_2 (1 - {}_1Y_I) = Fx ({}_1Y_I - {}_1Y_O) \quad 3.10$$

Multiplying equation 3.9 by  ${}_2Y_I$  and equation 3.10 by  $(1 - {}_1Y_I)$ , adding the resulting equations and further algebraic manipulation yields:

$$X_2 = \frac{Fx ( ({}_1Y_I - {}_1Y_O) \times {}_2Y_I + ({}_2Y_I - {}_2Y_O) \times (1 - {}_1Y_I) )}{(1 - {}_1Y_I) \times (1 - {}_2Y_I) - {}_1Y_I \times {}_2Y_I} \quad 3.11$$

Substituting equation 3.11 in equation 3.9 gives:

$$X_1 = Fx \frac{ ( ({}_1Y_I - {}_1Y_O) + X_2 \times {}_1Y_I ) }{(1 - {}_1Y_I)} \quad 3.12$$

Therefore, using equations 3.11, 3.12 and 3.5 the instantaneous rates of sorption and inlet flow rate may be calculated.

The amount of each component adsorbed during each pressure step was calculated by integrating the instantaneous rates of sorption for each pressure step, using Simpsons Rule. A correction was applied to the amount adsorbed in the first pressure step to account for the apparatus dead time. Account was taken of an experimental flow rate different from that at which the dead time was determined. The total amount adsorbed at each pressure step was calculated by summing the amounts adsorbed up to and including that step.

The next section of the program calculated the gas phase densities and fugacities at their partial pressure in the adsorption cell via the subroutine EXEC. This subroutine selected which method was to be used for the calculation. For partial pressures greater than 1 atmosphere the Benedict, Ruben and Webb equation of state (40) was used to calculate the adsorbate density and fugacity in subroutine HPFUG. For partial pressures

less than 1 atmosphere ideal gas behaviour was assumed for the calculation of gas phase density and accentric factors (41) used for the calculation of fugacity in subroutine LPFUG.

Adsorbate 'liquid' molar volumes were calculated within subroutine EXEC, using the model of Cook and Basmadjian (42) for use in the Polanyi Adsorption Potential Theory correlation.

The molar volume of methane and ethane as a function of temperature and partial pressure versus temperature data required for Clausius-Clapeyron plots were obtained from the literature (39). Clausius-Clapeyron plots of pressure-temperature data for single components were required to determine:

- a) the temperature at which the 'liquid' adsorbate pressure is equal to the adsorbate partial pressure, (required for the Cook and Basmadjian model for adsorbate 'liquid' molar volume).
- b) the pressure that the 'liquid' adsorbate would exert at the adsorption temperature (used to calculate  $f^0$  for the Polanyi Adsorption Potential).

In the case of ethane the value of  $f^0$  was calculated using the Benedict, Ruben and Webb equation of state. The adsorbed phase 'liquid' partial pressure of methane, at the adsorption temperature of 20°C, was above the maximum pressure that could be used accurately with the Benedict, Ruben and Webb equation of state and the adsorbed phase fugacity was calculated using a fugacity coefficient (43).

Subroutine SOLVE was then called which, in the case of single component isotherms, calculated the Polanyi Adsorption Potential (equation 1.11) and for the binary adsorption isotherm experiments the adsorbate mole fraction of methane was calculated (equation 1.16). The main program was then re-entered and the results written.



CHAPTER FOUR

ADSORPTION ISOTHERM EXPERIMENTAL RESULTS AND MATHEMATICAL MODELLING

4.1 SINGLE COMPONENT ADSORPTION ISOTHERM RESULTS

4.1.1 On 4A molecular sieve

Three experiments were performed with pure methane, pure ethane and a methane-ethane mixture at 20°C. The experimental conditions were the same as those for the first three pressure steps in experiments 2, 6 and 9 given in Tables 3, 7 and 10 respectively.

In no case was there significant adsorption. In all cases breakthrough, at the initial pressure, was similar to that obtained for the determination of the apparatus dead time, within experimental error. A subsequent increase in pressure produced very small but measurable adsorption possibly due to adsorption on the external surfaces of the molecular sieve crystals and on the binder.

Prior to these experiments, Laporte Industries were of the opinion (44) that there might be some difficulty in adsorbing ethane on their 4A molecular sieve owing to a window shrinkage of approximately 5% in each linear dimension, at the pellet calcining temperature of 650°C. As was evident from the results of the above experiments neither methane nor ethane were adsorbed within the 4A molecular sieve crystals. As the critical diameter of the adsorbates are nearly equal it is not surprising that neither species was adsorbed.

4.1.2 On 5A molecular sieve

Two experiments were carried out with pure methane as the adsorbate and one with pure ethane. Experimental conditions and results are given in Tables 3, 4 and 6.

#### 4.1.2a Methane

The results for the low mole fraction and high mole fraction of adsorbate in the total adsorption cell gas phase give a single isotherm, shown in Figure 15. The isotherm was in good agreement with the single component Statistical Thermodynamic model over the whole range of adsorbate concentrations. The parameters for this model are given in Table 11. The small error between the model and experimental data was thought to be due to:

- 1) The approximate value for the percentage binder used in making the pellets, as quoted by the manufacturer.
- 2) Experimental error due to:
  - a) errors in the Simpsons Rule integration of the experimental data in the data analysis program (Appendix 2). This was likely to have been greatest for the binary adsorption experiments when samples were analysed at 60s intervals.
  - b) errors in the operation and reading of pressure gauges.
  - c) temperature differences between the water bath and the adsorbent.
  - d) variations in the ambient conditions during the experiments.
  - e) errors in the operation of the peak height integration program (Appendix 1).

The local error included in the use of Simpson's Rule was much less than would have been encountered if the Trapezoidal Rule had been used for the integration of the experimental data and approximately the same as that involved with the use of the more complex Milne's or Adam's Method (45). The errors listed in 2b to 2e above were minimised by the design and/or calibration of the relevant pieces of equipment.

- 3) errors in the model parameters.

There did not appear to be any significant effect of pressure on the molecular volume up to an adsorbate partial pressure of 550 psig.

The experimental isotherm could also be expressed in terms of an empirical single component Langmuir model over the whole range of adsorbate concentrations. The constants for this model, calculated by a least squares fit to experimental data, are given in Table 12.

#### 4.1.2b Ethane

The results of this experiment formed a single isotherm with data interpolated from the work of Antonson and Dranoff (12) and were well represented by both the single component Statistical Thermodynamic and empirical Langmuir models over the whole range of adsorbate concentrations, see Figure 15. Tables 11 and 12 give the various model parameters. The error between the Statistical Thermodynamic model and the experimental isotherm was thought to be due to the same reasons as were given in the previous section (4.1.2a). Again there was no evidence of a significant reduction in molecular volume with increased pressure.

The single component isotherms on 5A molecular sieve show the saturation limit for each adsorbate.

#### 4.1.3 Polanyi Adsorption Potential Theory.

No unique relationship was found between adsorbate volume and Polanyi Adsorption Potential for methane and ethane on the 5A molecular sieve (Figure 17). A similar result was obtained by Lederman and Williams (46) for the adsorption of methane and nitrogen on 5A molecular sieve. Inaccuracies in this, the simplest form of the Polanyi Adsorption Potential Theory, could result from a number of sources:

- a) an inaccurate value for the free energy change on adsorption.
- b) an inappropriate correlating divisor.
- c) an inaccurate value for the adsorbate volume.

Initially a correction was applied to the isotherm results to account for the adsorbate accumulated within the pellet macro-pores and intergranular voids. It was found, however, that the correction was very small; at a partial pressure of methane of 550 psig. the correction was less than 0.1% and was therefore ignored.

Adsorption within molecular sieves is thought to occur both at active sites and by occlusion within the sieve cavity. This assumption has formed the basis of the Statistical Thermodynamic model. The two modes of adsorption, especially at high fractional saturation, would lead to an adsorbate whose average density and free energy do not correspond to those of the adsorbed 'liquid' state used in the version of the Polanyi Adsorption Potential used in this work. This would account for any or all of the possible errors listed previously. No other form of the Polanyi Adsorption Theory could be used to account for two modes of adsorption.

#### 4.1.4 On Activated Carbon

Two experiments were performed with pure methane as the adsorbate and one with pure ethane. Experimental conditions and results are given in Tables 2, 5 and 7.

##### 4.1.4a Methane

The results for the low and high mole fraction of adsorbate give a single isotherm (Figure 16). A single component empirical Langmuir model gave a good representation of the results. The model coefficients, obtained by a least squares fit of the model to experimental data, are given in Table 12.

##### 4.1.4b Ethane

The experimental data were well represented by a single component empirical Langmuir model (Figure 16). Table 12 lists the model coefficients obtained by a least squares fit.

In contrast to the adsorption of methane and ethane on 5A molecular sieve, the experimental isotherms on activated carbon showed no saturation limit,

at similar adsorbate concentrations, due to their higher adsorption capacity. The values obtained were of a similar magnitude as has been found on an activated carbon at 20°C, by Szepezy and Illés (47).

#### 4.1.5 Polanyi Adsorption Potential Theory.

A unique relationship was found between adsorbate volume and the Polanyi Adsorption Potential for methane and ethane on the activated carbon (Figure 17). In this case, therefore, the assumption of 'liquid' adsorbate behaviour would appear to be correct.

#### 4.1.6 Conclusions.

The results demonstrated the ability of the experimental method to obtain gas-solid equilibrium data over a wide range of adsorbate concentrations and mole fractions of the total gas phase composition, in a small number of experiments.

The accuracy of the mathematical model used to calculate the gas-solid equilibrium data from experimental breakthrough data, over a range of adsorbate mole fractions of the total gas phase composition was shown in the case of 5A molecular sieve by the good agreement with the Statistical Thermodynamic model.

The simplest form of the Polanyi Adsorption Potential Theory, assuming 'liquid' adsorbate behaviour, as modified by Lewis et al. (15) and Grant and Manes (13) can be applied to the adsorption of methane and ethane, as a single component, on the activated carbon used in this work. The assumption of liquid like behaviour of the adsorbed species appears not to apply when the adsorbent is a 5A molecular sieve where the correlation between adsorbed phase volume and the Polanyi Adsorption Potential is not unique.

The adsorption of methane and ethane, as single components, on both 5A molecular sieve and the activated carbon, was well represented by an empirical single component Langmuir model over a wide range of adsorbate concentrations.

#### 4.2 BINARY ADSORPTION ISOTHERM RESULTS ON 5A MOLECULAR SIEVE.

Figure 12 shows the fractional gas phase response at the adsorbent bed exit for a typical example of two component adsorption. The inhibition of the weakly adsorbed species by the more strongly adsorbed component was demonstrated by the desorption of a proportion of the less strongly adsorbed species during the period between its breakthrough and the breakthrough of the stronger adsorbed component. This phenomenon has been demonstrated by Thomas and Lombardi (10) and Gariepy and Zwiebel (48). After complete breakthrough at the initial pressure, the gas phase pressure and hence the adsorbate partial pressures were increased. As can be seen from Figure 12 the bed effluent concentration of both species fell, rose to a constant value which persisted until breakthrough of the more strongly adsorbed component occurred. Experimental conditions and results for the binary adsorption of methane and ethane on 5A molecular sieve are given in Tables 8, 9 and 10.

The isotherms obtained are shown in Figure 18 together with the pure component data. Mutual inhibition between the adsorbed species can be seen as the amount of each component adsorbed (at the same gas phase concentration of that component) decreased with an increase in the gas phase concentration of the second adsorbate.

4.3

MATHEMATICAL MODELLING OF THE BINARY ADSORPTION ISOTHERMS ON 5A MOLECULAR SIEVE.

4.3.1 The Extended Empirical Langmuir Equation.

An extended empirical Langmuir model (equation 1.7) was used to represent the binary adsorption isotherms using the coefficients obtained from the single component isotherms.

Figure 19 shows the poor fit obtained with this model, especially in the case of methane. No Langmuir correlation exists with respect to ethane gas phase mole fraction for the adsorption of methane. In the case of the adsorption of ethane, although no single relationship was found between the degree of inhibition and the gas phase concentration of methane, there is a trend showing a dependence on both the gas phase concentration of methane and the mole fraction of ethane. The higher the mole fraction of ethane the less the inhibition due to the gas phase mole fraction of methane.

A modified extended empirical Langmuir equation (equation 1.8) was used to express the binary adsorption isotherms. The results obtained were similar to those for the previous model.

4.3.2 Kidnay-Meyers Model.

The results obtained using this model are shown in Figure 20. The equations relating gas and solid phase adsorbate concentrations were those derived by Thomas and Lombardi (10) using the single component empirical Langmuir coefficients:

$$q_1 = \frac{A_1 \times B_1 \times c_1 \times \left[ 1 + \left( 1 - \frac{A_2}{A_1} \right) \times B_2 \times c_2 \right]}{1 + B_1 \times c_1 + B_2 \times c_2} \tag{4.2}$$

with a similar expression for  $q_2$ .

Once again the fit obtained was poor and the trends were similar to those obtained with the extended empirical Langmuir model.

#### 4.3.3 Two Component Statistical Thermodynamic Model.

The parameters used in this equation (1.10) were those used for the single component models given in Table 11. The comparison between model and experimental results is shown in Figure 21. Again, no single relationship was found between the inhibition in the adsorbed phase concentration of one component and the gas phase concentration of the other. However, unlike the other models investigated, there is a similar trend in the results for both adsorbates. The inhibition in the adsorbed phase concentration is a function of the gas phase concentration of the second species but decreases with an increase in the gas phase mole fraction of the adsorbate under consideration. The calculated solid phase adsorbate concentration of ethane was less than the experimental value in all cases, except that for 0.903 mole fraction of methane where the fit was good. In the case of methane, the calculated adsorbed phase concentration was generally greater than the experimental data.

#### 4.3.2 Polanyi Adsorption Potential Theory

An attempt to use the Polanyi Adsorption Potential Theory to predict the binary adsorption equilibrium after the manner of Grant and Manes (14), produced results which underestimated the adsorbed phase mole fraction of methane by approximately 50%. A bad correlation between experiment and theory was to be expected in the light of the single component correlations obtained on the 5A molecular sieve. However there did appear to be an almost constant relationship between the calculated and experimental values for the adsorbed phase mole fraction of methane (Figure 22). This is possibly a fortuitous correlation and should be approached with caution in the absence of any further experimental evidence.

#### 4.4 Conclusions.

There is no 'a priori' method of predicting binary adsorption equilibrium of methane and ethane (over the range of gas phase adsorbate



concentrations studied) on a 5A molecular sieve from the single component isotherm coefficients. Although the criterion that the empirical Langmuir coefficients (equation 1.5)  $A_1$  and  $A_2$  are approximately equal for the system studied is satisfied, the extended empirical Langmuir and Kidnay and Meyers models did not accurately predict the experimental binary equilibrium data. This criterion is necessary but not sufficient to ensure a good fit between the model and experimental data as adsorbed phase ideality is assumed in both models.

The two component Statistical Thermodynamic model gave better results in terms of the trends in the predicted results but the fit to experimental data was bad in most cases. Work done previously, using molecular sieves, where any of the above models have been used successfully, has been carried out at low fractional saturation (24, 25).

Under such circumstances inter-adsorbate forces are negligible and the adsorbed phase can be treated as an ideal mixture. The simplest form of the Polanyi Adsorption Potential Theory cannot be used to describe the binary equilibrium data in this work as it assumes a liquid-like adsorbate under circumstances where adsorption is taking place in two modes.

All of the models discussed in this section assume ideal adsorbed phase behaviour in the binary state. One may therefore conclude that, under conditions of high fractional saturation, where both modes of adsorption exist within a molecular sieve cavity, the adsorbed phase does not behave as an ideal mixture and that its density and free energy cannot be calculated in terms of a 'liquid' adsorbed state.

There is no simple 'a posteriori' method for predicting the binary adsorption equilibrium found in these experiments, using the models investigated, based on the single component isotherm coefficients.

As can be seen from Figures 19, 20 and 21, the binary adsorption equilibrium of methane and ethane at high fractional saturation on a 5A molecular sieve, is a function not only of the gas phase concentration of the interfering species but also the mole fraction of the adsorbate under consideration. Such dependence would be difficult to express in terms of modified forms of the models already discussed and would probably produce mathematical expressions requiring a large amount of calculation. This would render the mathematical modelling of fixed bed breakthrough prohibitively lengthy.

#### 4.5 Modified Coefficient Single Component Empirical Langmuir Model.

In order to be able to express the experimental single and binary adsorption equilibrium data in a simple mathematical model suitable for the computer modelling of fixed bed breakthrough, it was decided to express the isotherm for each component in every mixture as a single component empirical Langmuir model. Table 12 lists the results of a least squares fit of such a model to experimental data. It was found possible to express the single component empirical Langmuir model coefficients as a function of the gas phase mole fraction of that component in the total adsorbate.

As would be expected, the value of  $A_1$  decreased with increasing gas phase adsorbate mole fraction of ethane, as the amount of molecular sieve cavity available for the adsorption of methane was reduced by the increasing relative amount of ethane present. Similarly  $A_2$  decreased with increasing adsorbate gas phase mole fraction of methane. It was also assumed that:

$$1) \text{ when } y_1 = 0; \quad A_1 = 0$$

$$2) \text{ when } y_2 = 0; \quad A_2 = 0$$

$$\text{where } y_1 = \frac{c_1}{c_1 + c_2} \quad \dots \quad 4.3 \quad \text{and } y_2 = \frac{c_2}{c_1 + c_2} \quad \dots \quad 4.4$$

The model that gave the best representation of the coefficients  $A_1$  and  $A_2$  as a function of  $y_1$  and  $y_2$  respectively was a Langmuir type equation of the form:

$$A_1 = \frac{A^*_1 \times y_1}{1 + B^*_1 \times y_1} \quad \dots \quad 4.5$$

and

$$A_2 = \frac{A^*_2 \times y_2}{1 + B^*_1 \times y_2} \quad \dots \quad 4.6$$

A very good fit was obtained, as can be seen in Figures 23 and 24.

An expression relating  $B_1$  and  $B_2$  to  $y_1$  and  $y_2$  respectively presented a more difficult problem. For the case of  $B_1$  expressed as a function of  $y_1$  polynomial expressions up to 4th order were tried but were no improvement on the least squares straight line fit shown in Figure 23. Good results were obtained in the mathematical modelling of the breakthrough of methane in all the adsorption and desorption experiments. However, when a similar model was used to express  $B_2$  as a function of  $y_2$  significant 'tailing' in the computed breakthrough data occurred at values of  $y_2$  less than 0.1. It was therefore necessary to obtain a value for  $B_2$  at a value of  $y_2$  as close to zero as possible. As has been explained earlier (Chapter 2.5) it was impossible to carry out binary adsorption isotherm experiments in this region. However, as can be seen in Figure 21 the two component Statistical Thermodynamic model gave good results for ethane at a low mole fraction of that component. A value for  $B_2$  of  $124.1 \times 10^4 \text{ cm}^3/\text{gmol}$ . with  $y_2 = 0.01$  was therefore obtained from a least squares fit of the single component empirical Langmuir isotherm model to the ethane results obtained from the two component Statistical Thermodynamic model using  $y_2 = 0.01$  over the range of binary adsorption total adsorbate concentrations used in the binary isotherm experiments (Tables 8, 9 and 10). The value for  $A_2$  obtained at the same time ( $0.4 \times 10^{-4} \text{ gmol/gm}$ ) was in good agreement with the model used for  $A_2$  as a function of  $y_2$  shown in Figure 24. A Langmuir type equation was then used to express  $B_2$  as a function of  $y_2$ . A reasonable fit was

obtained, as can be seen in Figure 24 and good results were obtained in the mathematical modelling of the breakthrough of ethane in all the adsorption and desorption experiments.

A comparison between the experimental binary adsorption equilibrium data and the modified coefficient single component empirical Langmuir model is given in Figure 25. As can be seen a good fit is obtained between the model and experimental data over the range of gas phase adsorbate concentrations investigated. The isotherm equations derived were as follows:

$$q_1 = \frac{A_1 \times B_1 \times c_1}{1 + B_1 \times c_1} \quad \dots \quad 4.7$$

where

$$A_1 = \frac{0.00035 \times y_1}{1.0 - 0.8801 \times y_1} \quad \dots \quad 4.8$$

and

$$B_1 = 46970.0 - 42600.0 \times y_1 \quad \dots \quad 4.9$$

Similarly:

$$q_2 = \frac{A_2 \times B_2 \times c_2}{1 + B_2 \times c_2} \quad \dots \quad 4.10$$

where

$$A_2 = \frac{0.02951 \times y_2}{1.0 + 10.6 \times y_2} \quad \dots \quad 4.11$$

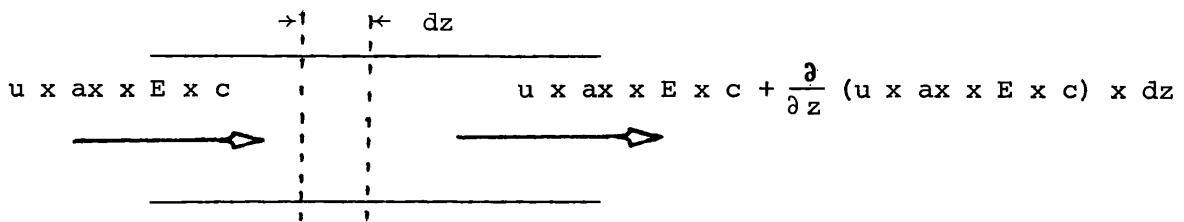
$$B_2 = 124.1 \times 10^4 - \frac{y_2 \times 4532.0 \times 10^4}{(1 + y_2 \times 44.52)} \quad \dots \quad 4.12$$

CHAPTER FIVE

MATHEMATICAL MODELLING OF FIXED-BED BREAKTHROUGH

5.1.1 Derivation of Equations

Assuming plug flow, no axial diffusion and a constant bed voidage and cross-sectional area, a mass balance across an element of the bed gives:



Generally:

$$\text{INPUT} - \text{OUTPUT} = \text{ACCUMULATION} + \text{LOSS BY SORPTION} \quad \dots \quad 5.1$$

Considering the fluid and solid phases together:

$$\text{INPUT} - \text{OUTPUT} = - \frac{\partial}{\partial z} (u \times a \times E \times c) \times dz \quad \dots \quad 5.2$$

$$\text{ACCUMULATION} = \frac{\partial}{\partial t} (\rho_{\text{BED}} \times q) \times a \times dz + \frac{\partial}{\partial t} (E \times a \times c) \times dz \quad 5.3$$

$$\text{LOSS BY SORPTION} = 0 \quad \dots \quad 5.4$$

Combining equations 5.2, 5.3 and 5.4 in the form of equation 5.1 gives:

$$\frac{\partial}{\partial z} (u \times c) \Big|_t + \frac{\partial c}{\partial t} \Big|_z = - \frac{\rho_{\text{BED}}}{E} \times \frac{\partial q}{\partial t} \Big|_z \quad \dots \quad 5.5$$

As has been discussed in Chapter 1.1, it had been decided to attempt to model fixed-bed breakthrough in cases where the amount of adsorbate was a considerable proportion of the total flow. It was therefore inappropriate to assume that the linear flowrate along the adsorbent bed axis was constant. Equation 5.5 was therefore expanded thus:

$$u \times \frac{\partial c}{\partial z} \Big|_t + c \times \frac{\partial u}{\partial z} \Big|_t + \frac{\partial c}{\partial t} \Big|_z = - \frac{\rho_{BED}}{E} \times \frac{\partial q}{\partial t} \Big|_z \dots 5.6$$

### 5.1.2 Mass Transfer Rate Controlling Mechanism.

As the experimental breakthrough of both adsorbates was rapid (Figures 31 to 41 incl.), it appeared reasonable to assume that there was negligible resistance to mass transfer, either from gas to solid phase or within the adsorbent particle. In order to justify this assumption breakthrough data was generated assuming various forms of the mass transfer rate controlling mechanism, using the experimental conditions of experiment No.5 (Table 6) for ethane on 5A molecular sieve.

#### 5.1.2a Micro-pore Diffusion Control.

At low gas phase concentrations of ethane, ( $5 \times 10^{-7}$  gmol/cm<sup>3</sup>), adsorption into a 5A molecular sieve has been shown to be controlled by the rate of diffusion of the gas phase adsorbate through the adsorbent micro-pores (12). In this case:

$$\frac{\partial q}{\partial t} \Big|_z = \frac{D_m}{\rho_{BED} \times r^2} \times \frac{\partial}{\partial r} (r^2 \times \frac{\partial c}{\partial r}) \dots 5.7$$

where  $D_m$  is the micro-pore diffusivity. Rosen (49) has solved equation 5.5 with a mass transfer mechanism given by equation 5.7 assuming a linear isotherm with spherical adsorbent particles and a concentration independent diffusion coefficient. By the following change of variables in equation 5.5,  $t - z/u$  for  $t$  and  $z \times (1-E)/u \times E$  for  $z$ , Rosen (50) was able to simplify the equations describing fixed bed breakthrough for intra-particle diffusion mass transfer with or without an external gas-solid mass transfer resistance. Lengthy mathematical manipulation yielded a series of breakthrough curves with  $\mu$ ,  $\theta$  and  $\tau$  as parameters, where;

$$\mu \text{ (bedlength parameter)} = 3 \times D_{m/s} \times (1-E) \times A \times B \times \ell / E \times U \times v^2.$$

$$\theta \text{ (film resistance parameter)} = E \times u / \ell \times h_{ga} \times (1-E) \quad \text{and}$$

$$\tau \text{ (time parameter)} = 2 \times E \times ( (u \times t / \ell) - 1 ) / 3 \times (1-E) \times A \times B$$

Breakthrough data, using the experimental conditions of experiment 5 (Table 6) were generated from Rosen's work, modified for a non-linear isotherm and non-spherical adsorbent particle geometry (12). The same literature source was used to obtain a value for  $\frac{D_m}{r^2}$ ;  $5.0 \times 10^{-4} \text{ s}^{-1}$  at  $20^\circ\text{C}$ . The results are given in Figure 27 using a value of  $\mu = 3.0$  (Figure 26) calculated from the experimental conditions of experiment 5 (Table 6), where  $\theta = 0$ .

#### 5.1.2b Surface Diffusion Control

The mass transfer rate from gas to solid phase can be limited by the rate at which adsorbed molecules move from the external surface of an adsorbent to its interior structure. This process is described mathematically by an equation similar to equation 5.7:

$$\left. \frac{\partial q}{\partial t} \right|_z = \frac{D_s}{r^2} \times \frac{\partial}{\partial r} \left( r^2 \times \frac{\partial q}{\partial r} \right) \quad \dots \quad 5.8$$

where  $D_s$  is the surface diffusion coefficient. No values for the surface diffusion coefficient of ethane on 5A molecular sieve were found in the literature but it would appear (51) that a surface diffusion coefficient is approximately one order of magnitude larger than the relevant micro-pore diffusion coefficient. A value of  $\frac{D_s}{r^2} = 5.0 \times 10^{-3} \text{ s}^{-1}$  was therefore used to generate breakthrough data for the experimental conditions of experiment No. 5 (Table 6) assuming surface diffusion control. Again, the results are shown in Figure 27, using a value of  $\mu = 30$  (Figure 26) and  $\theta = 0$ .

#### 5.1.2c Gas Phase Mass Transfer Control

In this case the overall rate of adsorption is limited by the transfer of adsorbate between the bulk of the fluid phase and the outer surfaces of the adsorbent particles. The rate of mass transfer is given in the classical form involving a driving force between the bulk fluid and the adsorbent particle surface,

therefore:

$$\left. \frac{\partial q}{\partial t} \right|_z = h g x (c_{z-1}^* - c_{z-1}) \quad \dots \quad 5.9$$

where  $c^*$  is the gas phase adsorbate concentration existing at the adsorbent surface in equilibrium with the pellet average adsorbate concentration.

A mass transfer film resistance,  $k_g a$ , was calculated (52) from the conditions obtaining in experiment 5 (Table 6), assuming laminar flow, using a gas phase diffusion coefficient calculated by the method of Wilke and Lee (53). The modified Reynolds Number ( $\frac{2ruE}{v}$ ) for experiment 5 was 0.21, well in the laminar region (54). The value of  $k_g a$  obtained was  $45.045 \text{ s}^{-1}$ , which gave a value of  $\theta = 0.0028$  for the Rosen Film Resistance parameter.

#### 5.1.2d Conclusions

The results obtained for micro-pore and surface diffusion control, using Rosen's model (49), modified for non-linear equilibrium and non-spherical adsorbent particle geometry gave slower breakthrough of ethane than the experimental result, (Figure 27). This indicates that the experimental rate of diffusion was much faster than that obtained from the literature at a lower gas phase concentration of ethane. A strong positive dependence of the rate of diffusion on adsorbate concentration has been reported for ethane and other hydrocarbons on type A zeolites, although some evidence to the contrary also exists (11, 12, 13, 55). It would therefore appear that a very fast rate of micro-pore and/or surface diffusion obtained under the experimental conditions of this work.

A comparison of the breakthrough curves calculated by Rosen, given in Figure 26, for constant values of the bed length parameter  $\mu$ , shows the very small influence that gas phase mass transfer resistance has on the breakthrough, even at the high value of  $\mu$  that would be required to duplicate the experimental results, for the value of  $\theta = 0.0028$ , calculated for the conditions of experiment No.5. It was therefore concluded that the resistance to mass transfer in the gas phase could be ignored throughout this work.



It was impossible to show conclusively that micro-pore and/or surface diffusion did not control the rate of adsorption in experiment No.5. However, as the experimental rate of diffusion was very high and an equilibrium control model gave good results under all the experimental conditions it was thought reasonable to assume that there was no resistance to mass transfer within the adsorbent pellet and hence that equilibrium control existed under all the experimental conditions.

### 5.1.3 Finite Difference Approximations

The following approximations to the partial derivatives in equation 5.6 were obtained using finite difference techniques. A central difference approximation to the axial linear flowrate gradient was used for maximum accuracy. Backward difference approximations were used for the rates of change of gas phase adsorbate concentration with axial position and time so that a simple explicit solution for  $c_z^t$  could be obtained and the previously calculated value of  $c_{z-1}^t$  could be included for maximum accuracy. A backward difference in both time and axial position was used to approximate to the rate of change of adsorbent adsorbate concentration with time so as to avoid the use of  $c_z^t$  which would produce a quadratic expression in  $c_z^t$  to be solved at each bed position. Also, for reasons given in the next section (5.1.4) the following approximation was made:

$$u_z^t \approx u_z^{t-\Delta t} \quad \dots \quad 5.10$$

therefore:

$$u \times \frac{\partial c}{\partial t} \Big|_t \approx \frac{u_z^{t-\Delta t} \times (c_z^t - c_{z-\Delta z}^t)}{\Delta z} \quad \dots \quad 5.11$$

$$c \times \frac{\partial u}{\partial z} \Big|_t \approx \frac{c_z^t \times (u_{z+\Delta z}^{t-\Delta t} - u_{z-\Delta z}^{t-\Delta t})}{2 \times \Delta z} \quad \dots \quad 5.12$$

$$\frac{\partial c}{\partial t} \Big|_z \approx \frac{c_z^t - c_z^{t-\Delta t}}{\Delta t} \quad \dots \quad 5.13$$

and

$$\left. \frac{\partial q}{\partial t} \right|_z \approx \frac{q_{z-\Delta z}^t - q_z^{t-\Delta t}}{\Delta t} \quad \dots \quad 5.14$$

for equilibrium control.

#### 5.1.4 Boundary Conditions

Inlet adsorbate gas phase concentrations  $c_{1I}^t$  and  $c_{2I}^t$  were obtained from the experimental conditions and were available for all  $t$ . The effect of a non-step change in inlet adsorbate gas phase concentration is discussed in section 5 of this chapter. The adsorbate bed outlet molar flowrate,  $F_{O\text{INITIAL}}$ , was set initially with pure carrier gas passing through the bed. The change in outlet molar flowrate and therefore the linear axial flowrate was modelled using equation 2.1, which in finite difference form gives:

$$\frac{u_o^t - u_o^{t=0}}{u_o^{t=0}} = 0.35 \times \frac{Y_T}{2} \times \left( \frac{1c_o^t}{1I} + \frac{2c_o^t}{2I} \right) \dots \quad 5.15$$

where:

$$Y_T = \frac{1c_I^t + 2c_I^t}{c_T} \quad \dots \quad 5.16$$

The inlet adsorbate gas phase molar flowrate after each time step was calculated using the same method as used in the Adsorption Data Analysis Program via equations 3.11, 3.12 and 3.5 where:

$$1Y_I = \frac{1c_I^t}{c_T} \quad \dots \quad 5.17$$

and

$$1Y_o = \frac{1c_o^t}{c_T} \quad \dots \quad 5.18$$

with similar expressions for  $c_2$ . Therefore  $F_I$  was calculated and converted to the linear interstitial velocity thus:

$$u_I = \frac{F_o}{c_T \times E \times ax} \quad \dots \quad 5.19$$

where  $a_x$  is the adsorption cell cross sectional area given by

$$a_x = \frac{\pi d^2}{4} \dots 5.20$$

However, as outlet gas phase adsorbate concentrations were only available at  $t - \Delta t$ ,  $u_o$  calculated by equation 5.19 is  $u_I^{t-\Delta t}$ . Similarly  $u_o$ , calculated by equations 5.15 and 5.16 is also at time  $t - \Delta t$ . At sufficiently small values of  $\Delta t$  this approximation was thought to be sufficient for an accurate solution to the finite difference equations.

### 5.1.5 Bed Axial Flow Profile

Having obtained values for the inlet and outlet linear interstitial flowrate boundary conditions, at each time step, it was necessary to find an expression for the change with bed axial position.

As the pressure drop across the bed had been shown to be small, then the change in linear interstitial axial flowrate must have been due to adsorption. Therefore, one could assume that the flowrate would remain constant when the gas phase adsorbate concentration was constant along the bed axis. Similarly, the gas phase adsorbate concentration and flowrate must change at the same fractional rate in the adsorption zones.

Figure 26 shows the equal fractional axial adsorbate concentration and flowrate given by equations 5.21, 5.22 and 5.23 which follow.

For one or two components, putting

$$DC = \frac{1}{2} \frac{dc_I^t}{c_I^t} + \frac{1}{2} \frac{dc_I^t}{c_I^t} - \frac{1}{2} \frac{dc_O^t}{c_O^t} - \frac{1}{2} \frac{dc_O^t}{c_O^t} \dots 5.21$$

and 
$$DU = \frac{1}{2} \frac{du_I^t}{u_I^t} - \frac{1}{2} \frac{du_O^t}{u_O^t} \dots 5.22$$

then

$$\frac{du_z^t}{u_z^t} \approx \frac{du_o^t}{u_o^t} + \frac{DU}{DC} \times \left( \frac{1}{2} \frac{dc_z^t}{c_z^t} + \frac{1}{2} \frac{dc_z^t}{c_z^t} - \frac{1}{2} \frac{dc_o^t}{c_o^t} - \frac{1}{2} \frac{dc_o^t}{c_o^t} \right) \dots 5.23$$

Hence a bed axial interstitial flowrate profile was calculated for all  $z$  before the calculation of the adsorbate axial concentration profile.

Therefore by substitution equations 5.11 to 5.14 in equation 5.6 and using the axial interstitial flow profile calculated by equations 5.21, 5.22 and

5.23 and finally rearranging, an explicit solution for either  $c_z^t$  or  $c_z^{t-\Delta t}$  was obtained thus; at  $t = t + \Delta t$ ,

$$c_z^t = \frac{c_z^{t-\Delta t} + \frac{\Delta t}{\Delta z} \times u_z^{t-\Delta t} \times c_{z-\Delta z}^t - q_z^t \times \frac{\rho_{BED}}{E}}{\frac{\Delta t}{\Delta z} \times (u_z^{t-\Delta t} + \frac{(u_{z-\Delta z}^{t-\Delta t} - u_{z-\Delta z}^{t-\Delta t})}{2}) + 1} \dots \quad 5.24$$

where

$$\Delta q_z^t = q_{z-\Delta z}^t - q_z^{t-\Delta t} \dots \quad 5.25$$

assuming equilibrium control.

Also,

$$q_{z-\Delta z}^t = \frac{A \times B \times c_{z-\Delta z}^t}{1 + B \times c_{z-\Delta z}^t} \dots \quad 5.26$$

and

$$q_z^{t-\Delta t} = \frac{A \times B \times c_z^{t-\Delta t}}{1 + B \times c_z^{t-\Delta t}} \dots \quad 5.27$$

The Langmuir coefficients A and B were calculated using the modified coefficient single component Langmuir model given in equations 4.8, 4.9, 4.11 and 4.12.

A computer program was written to solve the above set of equations to generate fixed bed breakthrough data for single component or binary adsorption. A fully annotated program listing, flowsheet and typical results for binary adsorption are given in Appendix 3.

### 5.1.6 Calculation Sequence.

The experimental breakthrough chromatogram peak areas and katherometer response checks were read in together with the other necessary data. Adsorbate gas phase inlet mole fractions, concentrations and outlet initial molar flowrate were calculated assuming ideal gas behaviour, the maximum adsorbate gas phase partial pressure in all the breakthrough experiments was 1.5 atmospheres.

The adsorbent bed intergranular voidage  $E_{IG}$  was calculated from the measured bulk density and the pellet density thus:

$$\frac{E_{IG}}{\rho_{PELLET}} = 1.0 - \frac{\rho_{BULK}}{\rho_{PELLET}} \quad \dots \quad 5.28$$

where  $\rho_{PELLET}$  for 5A molecular sieve = 1.14 gm/cm<sup>3</sup> (12). The pellet density for the activated carbon adsorbent was calculated from equation 5.28, using the value of  $\rho_{BULK}$  obtained by experiment, and assuming that  $E_{IG}$  for the activated carbon was equal to that for 5A molecular sieve, as the particle size and shape were similar (Chapter 2.8). As has been discussed in Chapter 3.2 the total bed voidage  $E$  was to include the macro-pore voidage obtained from the mercury porosimeter experiments.

Therefore:

$$E = E_{IG} + \frac{E_{MACRO}}{\rho_{BED}} \quad \dots \quad 5.29$$

The adsorbent bed length was calculated from the weight of adsorbent used, the bulk density and the adsorption cell dimensions, thus:

$$l = \frac{WT}{\rho_{BULK} \times \frac{\pi \times d^2}{4}} \quad \dots \quad 5.30$$

The change in dead time with the weight of adsorbent was taken into account (equation 3.2a). The apparatus dead time was corrected for flowrates other than that at which the dead time was calculated (equation 3.2b).

## 5.2 Single Component Breakthrough

The single component breakthrough from the first pressure steps in the isotherm experiments No.1 - 6 were studied. For experimental conditions see Tables 2 - 7.

The finite difference equations were solved in the following sequence:

- a) Set  $t = t + \Delta t$
- b) Set  $z = 2$  ( $z = 1$  contained the boundary conditions)
- c) Calculate  $u^{t-dt}$   
O and I

- d) Calculate  $u_z^{t-dt}$  for  $Z = 2$  to bed exit ( $Z=NZ$ ).
- e) Calculate  $\Delta q_z^t$
- f) Calculate  $\epsilon_z^t$
- g) Set  $Z = Z+1$
- h) Return to e) until the solution reaches the bed exit ( $Z=NZ$ ).
- i) Return to a) until complete breakthrough.

For the first time step a linear axial interstitial flow profile was used, given by:

$$u_z^{t-\Delta t} = u_o^{t-\Delta t} + \frac{DU}{DC} \times \frac{NZ + 1 - Z}{NZ} \dots \quad 5.31$$

Figure 28 shows how this linear profile differs from the equal axial concentration and flowrate profile.

Considerable difficulty was encountered when solving the above sequence of equations and a total lack of stability was found at what appeared to be appropriate values for  $\Delta Z$  and  $\Delta t$ .

5.2.1 Stability and Convergence.

In the following sections a stable solution is taken as being one which makes physical sense, i.e. a positive gas phase adsorbate concentration of a maximum value of the same order as the maximum experimental value.

Convergence is used with its normal meaning. It has been shown previously (55, 56) that, for stability, in its strict sense, the speed of calculation of a hyperbolic partial differential equation, of the type derived for fixed bed adsorption, expressed as  $\Delta Z/\Delta t$  must be greater than the speed of the calculated or experimental breakthrough. The solution will converge as  $\Delta Z/\Delta t$  is further increased.

5.2.1a Equilibrium Control Model.

The speed of the solution for the experimental results was obtained from the breakthrough data as,

$$V_s = \frac{1}{t_{0.5}} \dots \quad 5.32$$

where  $t_{0.5}$  is the time for 50% breakthrough.

The experimental data from experiment No.2 (Table 3) was used for the work on stability and convergence, including a ramp input gas phase adsorbate concentration change (see section 5.5 of this chapter).

In this case:

$$l = 42.3 \text{ cm.} \qquad t_{0.5} = 7.25 \text{ min.}$$

This gives a solution velocity of 0.0973 cm/s.

To ensure an accurate calculation 1,000 length intervals were used,

therefore:  $\Delta Z = 0.0423 \text{ cm.}$

hence;  $\Delta t \leq \frac{0.0423}{0.0973} = 0.435$

However, with values of  $\Delta t$  of 0.25, 0.5 and 1.0 seconds the calculated breakthrough data were very unstable, often being large and negative.

A stable solution, which was in very good agreement with the experimental data (Figure 32), was obtained at  $\Delta t = 2.0\text{s}$ , which diverged slowly as  $\Delta t$  was increased to 10 s. It was therefore obvious that, in the case of an equilibrium control model, the usual stability criterion was inappropriate. A criterion for obtaining a stable, converged calculated solution, in terms of the ratio  $\Delta t/\Delta z$  was obtained from equation 5.24, as follows.

For the solution, at any axial position Z, to make physical sense,

$$c_z^t \geq 0 \qquad \dots \qquad 5.33$$

For all but the most extraordinary circumstances the denominator of equation 5.24 is always positive. Therefore, applying the criterion of equation 5.33 to the numerator of equation 5.24 yields

$$c_z^{t-\Delta t} + \frac{\Delta t}{\Delta z} \times u_z^{t-\Delta t} \times c_{z-\Delta z}^t \geq \Delta q_z^t \times \frac{\rho_{\text{BULK}}}{E} \qquad \dots \qquad 5.34$$

For the worst case, i.e. a maximum value of  $\Delta q_z^t$ , from equation 5.25.

$$q_z^{t-\Delta t} \ll q_{z-\Delta z}^t \quad \dots \quad 5.35$$

therefore

$$\Delta q_z^t = q_{z-\Delta z}^t \quad \dots \quad 5.36$$

which, from equation 5.25 becomes

$$\Delta q_z^t = \frac{A \times B \times c_{z-\Delta z}^t}{1 + B \times c_{z-\Delta z}^t} \quad \dots \quad 5.37$$

The criterion in equation 5.33 is most likely to be broken when  $C_z^t \rightarrow 0$ .

In which case,

$$B \times c_{z-\Delta z}^t \ll 1 \quad \dots \quad 5.38$$

Therefore equation 5.37 becomes:

$$\Delta q_z^t = A \times B \times c_{z-\Delta z}^t \quad \dots \quad 5.39$$

Also, for a stable, converged solution

$$c_z^t \approx c_{z-\Delta z}^t \approx c_z^{t-\Delta t} \quad \dots \quad 5.40$$

Therefore, substituting equation 5.39 in equation 5.34 and using equation 5.40,

$$1 + \frac{\Delta t}{\Delta z} \times u_z^{t-\Delta t} \geq A \times B \times a \frac{\rho_{BULK}}{E} \quad \dots \quad 5.41$$

which, on rearranging, yields,

$$\frac{\Delta z}{\Delta t} \leq \frac{u_z^{t-\Delta t}}{A \times B \times \rho_{BULK} - 1} \quad \dots \quad 5.42$$

In the case of methane or ethane on either absorbent,

$$A \times B \times \frac{\rho_{BULK}}{E} \gg 1 \quad \dots \quad 5.43$$

Therefore

$$\frac{\Delta z}{\Delta t} \leq \frac{u_z^{t-\Delta t}}{A \times B \times \frac{\rho_{BULK}}{E}} \quad \dots \quad 5.44$$



Again, for the worst case, i.e. the minimum value of  $\frac{\Delta z}{\Delta t}$ ,

$$u_z^{t-\Delta t} = \frac{F_{O\text{INITIAL}}}{a x \times E \times c_T} \quad \dots \quad 5.45$$

Therefore, substituting equation 5.45 in equation 5.44, gives:

$$\frac{\Delta z}{\Delta t} \leq \frac{F_{O\text{INITIAL}}}{A \times B \times \rho_{\text{BULK}} \times E \times a x \times c_T} \quad \dots \quad 5.46$$

which leaves:

$$\frac{\Delta z}{\Delta t} \leq \frac{F_{O\text{INITIAL}}}{A \times B \times \rho_{\text{BULK}} \times a x \times c_T} \quad \dots \quad 5.47$$

This gives a criterion for  $\Delta z/\Delta t$  based on measurable quantities.

In the case of methane (experiment No. 2):

$$\frac{F_{O\text{INITIAL}}}{a x \times c_T} = 0.591$$

Also:

$$\begin{aligned} \rho_{\text{BED}} &= 0.732 \text{ gm/cm}^3 \\ E &= 0.588 \\ A_1 &= 2.963 \times 10^{-3} \text{ gmol/gm} \\ B_1 &= 7.125 \times 10^3 \text{ cm}^3/\text{g mol} \end{aligned}$$

Substituting these values in equation 5.44 gives:

$$\frac{\Delta z}{\Delta t} \leq \frac{0.591}{2.962 \times 7.125 \times 0.732}$$

$$\therefore \frac{\Delta z}{\Delta t} \leq 0.0205 \text{ cm/s.} \quad \dots \quad 5.48$$

This is approximately one fifth of the experimental solution velocity of 0.0973 cm/s. Hence, for a value of  $\Delta z = 0.0423$  cm,

$$\Delta t \geq \frac{0.0423}{0.0205} = 2.085 \text{ s}$$

This is in good agreement with the value of  $\Delta t$ , found by trial and error, that gave a stable, converged solution, i.e. unstable at  $\Delta t = 1$  s but stable at  $\Delta t = 2$  s. As the criterion given in equation 5.47 gives a value of  $\Delta t$  greater than a given value, then the most accurate solution

should be found, for a given  $\Delta z$ , with  $\Delta t$  just greater than this value. Otherwise, having found the critical ratio  $\Delta z/\Delta t$ , the values of  $\Delta z$  and  $\Delta t$  should be reduced, maintaining the ratio until the solution converges.

The criterion was applied to all the single component fixed bed experimental breakthrough data obtained from the first pressure steps in experiments 1 - 6 and was found to give a stable, convergent solution in all cases. The value for  $\Delta z/\Delta t$  found from the experimental solution velocity was always higher than that derived above and always produced instability.

5.2.1b Linear Lumped Parameter Model.

Similar reasoning to that used in the previous section (5.2.1a) was employed to determine a stability criterion when the rate of mass transfer from gas to solid phase could be described by a linear lumped parameter model.

In this case:

$$\Delta q_z^t = \frac{h}{\Delta t} \times (q_z^t - q_{z-\Delta z}^{t-\Delta t}) \quad \dots \quad 5.49$$

therefore:

$$\frac{\Delta t}{\Delta z} \leq \frac{F_o \text{ INITIAL}}{h \times A \times B \times \rho_{\text{BED}} \times a \times e_T} \quad \dots \quad 5.50$$

Again, the results from experiment No. 2 were used, with a value of  $h = 0.1$ , which was found by trial and error to give results in good agreement with the experimental data.

Hence:

$$\Delta z \leq \frac{0.591}{0.1 \times 2.963 \times 2.125 \times 0.732} = 0.427 \text{ cm}$$

Good agreement was found between this criterion and a trial and error solution. With  $\Delta t = 0.5$  s:

stability was found with  $\Delta z = 0.2$  cm, and instability found when  $\Delta z = 0.4$  cm. The solution was found to converge with a value of  $\Delta t = 2.0$ s, giving a calculated approximate solution velocity of  $\frac{0.2}{2.0} = 0.1$  cm/s. This is in good agreement with the criterion of Courant, Friedrichs and Levy (55, 56) when compared with the experimentally derived velocity of 0.0973 cm/s.

### 5.2.2 The Effect of Various Bed Axial Flow Profiles and the Mole Fraction of Adsorbate in the Total Gas Phase.

The first pressure step of Experiments 1, 4 and 5 were used in the following comparisons, assuming equilibrium gas-solid mass transfer control, and using a ramp input gas phase adsorbate concentration change at the bed inlet.

#### 5.2.2a No Axial Flow Profile.

The linear interstitial flowrate along the adsorbent bed axis was taken as the initial outlet velocity. Such an assumption, at a high mole fraction of adsorbate in the total flow (0.537) led to serious errors in the calculated breakthrough data, as can be seen in Figure 31. This effect decreased with decreasing mole fraction of adsorbate in the total flow, as is shown in Figures 31, 34 and 35.

#### 5.2.2b Linear Axial Flow Profile.

This assumption gave better results than using no axial flow profile but significant errors occurred at the completion of breakthrough, leading to a more unstable solution as the mole fraction of adsorbate in the total flow increased (Figures 31, 34 and 35).

### 5.2.2c Equal Fractional Axial Concentration and Flow Profiles.

This model gave the best results (Figures 31, 34, 35) and was subsequently used, with success, over a wide range of adsorbate mole fractions of the total flow for both single component and binary adsorption.

### 5.2.3 The Effect of the Change in Outlet Flowrate with Gas Phase Composition.

As has been discussed in Chapter 2.13 the outlet gas flowrate changed with gas phase composition and was modelled as shown in Figure 14 and equation 2.1.

### 5.2.3a Equilibrium Model.

As the breakthrough of the adsorbate lasted typically only 60 s, with this model for gas-solid mass transfer, the effect of the change in outlet flowrate with gas phase composition made no significant difference to the solution of the fixed bed breakthrough equations over the range of gas phase compositions studied.

### 5.2.3b Linear Lumped Parameter Model

The use of this model with  $h = 0.01$  in equation 5.46 produced adsorbate breakthrough which lasted over a period of approximately 15 minutes when used with the experimental conditions of the first pressure step of experiment No. 1. Consequently the change in outlet flowrate with gas phase composition made a difference to the mathematical model solution for fixed bed breakthrough. Figure 29 shows the results obtained with and without the effect of the change in outlet flowrate included in the mathematical model.

Therefore, in cases when the outlet flowrate changes with outlet gas phase concentration and the breakthrough curve is diffuse, a model for the change in outlet flowrate with gas phase concentration should be included in any mathematical model of fixed bed breakthrough. Failure to do so would result in erroneous values for any parameter in the model of

gas-solid mass transfer obtained by fitting experimental data to a mathematical model.

#### 5.2.4 The Effect of a Non-step Change in Inlet Adsorbate Concentration.

As can be seen from Figure 7 the change in adsorbate gas phase concentration, when gas samples were switched at VII, lasted 90 s at the sample point, with the adsorption cell packed with glass beads. It was thought that this spending of the inlet adsorbate concentration step change was due to the vena contracta formed when gas flowed through the small bore of VII into the larger connecting pipe work. Axial diffusion was not thought to play a significant part in this phenomenon as the adsorbate breakthrough in all of the first pressure steps in experiments 1 - 9 was very sharp, being consistent with equilibrium gas-solid mass transfer control. The adsorbent bed inlet would therefore experience a change in gas phase adsorbate concentration similar in shape to that shown in Figure 7. A number of computer simulations were run, using the data of the first pressure step of experiment No. 1 assuming equilibrium control. A finite difference approximation to a ramp input was used where the inlet adsorbate gas phase concentration was increased from zero to the final value in a series of equal steps. Figure 30 shows the results obtained for a ramp input lasting for various periods of time. Although the ramp input lasting 90 s produced only a small change in the mathematical model, it was included in all the computer simulations of single and binary adsorption. Where flowrates other than that at which the 90 s ramp input was altered in inverse proportion to the flowrate.

#### 5.3 Results.

Computer simulations were run, employing the finite difference techniques discussed earlier in this chapter, for single component breakthrough for the first pressure steps in experiments 1 - 6, with methane and ethane on 5A molecular sieve and the activated carbon. A 90 s ramp

change in gas phase inlet concentration, equal fractional axial gas phase adsorbate concentration and flowrate profiles and a model for the change in outlet flowrate with bed exit gas phase composition were included. Equilibrium control of the gas-solid mass transfer rate was assumed. Figures 31 - 36 show the good agreement between the model and experimental results. For the sake of clarity, in all the figures showing fixed bed breakthrough experimental data, some data points have been omitted in the region of constant composition. The region of constant composition is between the breakthrough of the two species for binary adsorption or after complete breakthrough in the case of single component adsorption.

#### 5.4 Conclusions

With negligible pressure drop across the adsorbent bed, the axial flowrate profile, for cases where the adsorbate was a significant fraction of the total flow, is well represented by assuming identical axial fractional gas phase adsorbate concentration and flow profiles.

The equilibrium control model provided a good model for the gas-solid mass transfer under the experimental conditions employed.

Care should be taken when assuming a step change in inlet gas phase concentration and a suitable model employed in the cases where non-step changes occur. Any change in outlet flowrate with gas phase composition will have a more pronounced effect the more diffuse the breakthrough of the adsorbed species. In the case of equilibrium control, the classical stability criterion for the choice of  $\Delta z/\Delta t$  for the numerical solution of the finite difference equations involved in fixed bed adsorption is inappropriate.

A criterion for predicting a suitable  $\Delta z/\Delta t$  ratio was obtained, by considering the physical reality of the calculated gas phase adsorbate concentration, which provided stable, converged solutions in all cases.

When considering a linear lumped parameter mass transfer model, the classical criterion for  $\Delta z/\Delta t$  gives good results. However, by similar

reasoning as was used in the case of equilibrium control, values for  $\Delta z$  and hence  $\Delta t$  were successfully obtained.

### 5.5 Binary Adsorption Breakthrough

From the shape of the experimental breakthrough data for binary adsorption on a 5A molecular sieve, it was decided to use an equilibrium gas-solid mass transfer model. A problem arose, however, inasmuch as the use of equation 5.44 to predict a value for  $\Delta z/\Delta t$  gave different results for each component. This is because the expression contains the empirical Langmuir coefficients A and B. For the case of methane and ethane on a 5A molecular sieve:

$$\frac{\Delta t_2}{\Delta t_1} = \frac{A_2 \times B_2}{A_1 \times B_1} \approx 18 \quad \dots 5.51$$

using a constant value for  $\Delta z$ .

It was thought more economical (in computer time) to use a constant  $\Delta z$  and two separate values for  $\Delta t$ .  $\Delta z/\Delta t$ , was chosen, using equation 5.44 with a value for  $\Delta z$  which gave a converged solution for methane as a single component. Equation 5.51 was then used to calculate  $\Delta t_2$  as:

$$\Delta t_2 = 18 \times \Delta t_1 \quad \dots 5.52$$

The same finite difference mathematical model was used as had been used successfully for single component adsorption, but with the following alteration in procedure (required to accommodate the differing values of  $\Delta t_1$  and  $\Delta t_2$ ). The finite difference equations were solved for methane, along the whole bed-length, for 18 time steps, each of value  $\Delta t_1$ , followed by a single time step for ethane, of value  $\Delta t_2$  along the whole bed length. The mutual interference of the adsorbates with their solid surface equilibrium concentrations was calculated, using the most recent value of the gas phase concentration of each species at each bed axial position, substituted in the modified coefficient single component empirical Langmuir model (Equations 4.7 to 4.12). The bed axial flow profile was calculated before each methane time step.

The values of  $\Delta t_1$  and  $\Delta t_2$  were calculated using the values for the Langmuir coefficients **A** and **B** for both methane and ethane, assuming that they were single components. One might expect, therefore, that the solution could have become unstable as **A** and **B** varied as the relative gas phase concentrations of each component changed (see equations 4.8, 4.9, 4.11 and 4.12). There was, however, no evidence of such instability. This was thought to be due to the fact that, for either component, as **A** decreased so **B** increased and therefore the product **A** x **B** remained within a range of values that gave a stable solution.

## 5.6 Results

The first pressure steps in experiments 7 - 9 were modelled. The comparisons between the experimental and computer model results are shown in Figures 37, 38 and 39, covering a range of mole fractions of ethane in the adsorbate and mole fractions of the total adsorbate in the total flow. Experiments 10 - 13 were modelled, covering two flowrates at two values of the total adsorbate concentration. The experimental conditions are given in Tables 13 - 16 and the results are shown in Figures 40 and 41.

## 5.7 Conclusions

An equilibrium gas-solid mass transfer model gave a good representation of binary adsorption on 5A molecular sieve over the range of experimental conditions studied. The modified coefficient single component empirical Langmuir model gave a good representation of the mutual interference of the adsorbed species on 5A molecular sieve.

The use of two different time steps can be successfully accommodated in a finite difference mathematical model of binary adsorption with equilibrium control.



CHAPTER SIX

THE DESORPTION SEPARATION OF BINARY MIXTURES ON 5A MOLECULAR SIEVE

6.1 Introduction

Table 17 shows the mole fraction of methane in the adsorbed phase on a 5A molecular sieve for various mole fractions of methane in the gas phase, at a constant gas phase concentration of ethane. The same gas phase concentration of ethane was used as that employed in the series of experiments reported in section 6.3 of this chapter. The adsorbed phase concentrations were calculated using the modified coefficient single component empirical Langmuir model developed for the adsorption of methane-ethane mixtures on 5A molecular sieve (Chapter 4, Section 5). As can be seen from Table 17, the mole fraction of methane in the adsorbed phase increases with an increase in gas phase mole fraction of methane. At high gas phase mole fractions of methane its adsorbed phase mole fraction becomes large compared with that of ethane. For a gas feed similar in composition to a British natural gas (3% v/v ethane) the adsorbed phase mole fraction of methane is 0.31. The simple desorption of a bed of 5A molecular sieve in equilibrium with such a feed would produce an effluent gas that may require further enrichment to produce an ethane feed suitable for subsequent processing. It was therefore decided to undertake a preliminary investigation of the desorption kinetics of methane-ethane mixtures from a 5A molecular sieve with a view to effecting a further separation. As with the adsorption experiments, those concerned with desorption were performed under isothermal conditions.

As explained earlier (Chapter 2) it was impracticable to perform binary adsorption experiments at gas phase mole fractions of ethane less than 0.1. It was therefore decided to perform experiments at equal gas phase mole fractions of methane and ethane in order to determine their desorption kinetics and to run computer simulations over a range of gas phase compositions using the kinetic data thus acquired.

No reference could be found in the literature to the desorption kinetics of methane from any adsorbent. Studies have been made of the desorption of ethane from 4A molecular sieves under conditions where micro-pore diffusion mass transfer control obtains (13, 57, 58). The desorption rate of ethane from a 4A molecular sieve was found to be the same as for adsorption (57) for a small change in adsorbate concentration. For larger changes in ethane concentration, desorption has been found to be slower than adsorption on a 4A molecular sieve (13). There is also conflicting evidence concerning the concentration dependence of diffusivity for adsorption of other low molecular weight hydrocarbons on this type of zeolite (11, 57, 58, 13, 12). Crank (59) has shown that it is possible to have adsorption and desorption processes occurring at different rates when the diffusion coefficient is a function of concentration.

No work has been reported on the change in surface or micro-pore diffusivity with changes in the relative concentrations of adsorbates in binary fixed bed adsorption or desorption.

## 6.2 Experimental

Three experiments were performed under identical conditions (Table 18), with the exception that the helium carrier gas was reconnected to the bed inlet after 5, 10 and 15 minutes respectively.

## 6.3 Results

The results are shown in Figures 42, 43 and 44. The increase in gas phase bed outlet fractional response immediately after the start of desorption in experiment No.16 (Figure 44) was due to an initial mis-match of pressures which was immediately rectified. In all cases the rate of desorption was slower than the rate of adsorption for both ethane and methane. The rate of desorption of methane was much faster than the rate of desorption of ethane.

#### 6.4.1 Mathematical Modelling of the Experimental Adsorption-Desorption Cycles.

The adsorption of both components was modelled using the same techniques and computer program (Appendix 3) as described through Chapter 5, using an equilibrium mass transfer model. As it had already been demonstrated (Chapter 5, Section 1.2c) that gas-solid mass transfer was not the rate limiting step under the experimental conditions used in this work (and an equilibrium control model gave a very poor fit to the experimental data) it was decided to describe the desorption kinetics of both adsorbates in terms of a linear lumped parameter model (Chapter 5, Section 2.1b). It was hoped that this model would provide a simple but sufficiently accurate description of the effects of surface and/or micro-pore diffusion representing a considerable saving in computing effort when compared with the analytical solutions (Chapter 5, Section 1.2a and b).

The computer program for adsorption (Appendix 3) was modified for use in the modelling of fixed-bed desorption in the following ways:

- a) after a given period of time, or complete breakthrough of both species, a ramp decrease in inlet gas phase concentration was applied at the bed inlet, (the reverse of the initial adsorption ramp (Chapter 5, Section 2.4), until the gas phase inlet concentration reached a constant zero level.
- b) Adsorption or desorption kinetics were applied depending whether the change in solid phase adsorbate concentration was positive or negative.
- c) the program was halted when the bed outlet gas phase fractional response had fallen below  $10^{-2}$ .

Time and axial bed length increments used in the desorption section were chosen according to the criterion developed in Chapter 5, Section 2.1b.

#### 6.4.2 Results

A least squares fit of the experimental results to model data for the desorption section of the complete adsorption-desorption cycle (Figure 43) gave the following values for the linear lumped parameters used in the

subsequent mathematical modelling of desorption kinetics; to an accuracy of 1 significant figure:

$$h_1 = 0.5 \text{ s}^{-1}$$
$$h_2 = 0.005 \text{ s}^{-1}$$

Further accuracy was not thought to be warranted as the model was relatively insensitive to the value of the parameter  $h$  and this preliminary investigation was limited to 3 experiments.

The values of  $h$  obtained from experiment No. 16 (Figure 44), were used to model the experiments carried out at shorter adsorption times (Figures 42 and 43). As the adsorption time decreased so the solid phase ethane concentration over the majority of the desorption period was less than that at which  $h_2$  had been calculated and the fit of the mathematical model to experimental data became worse.

#### 6.4.3 Conclusions

A linear lumped parameter approximation to the desorption kinetics of methane from a 5A molecular sieve gave good agreement between a mathematical model and experimental results over the range of experimental conditions used. In the case of the desorption of ethane from a 5A molecular sieve the rate of desorption was dependent on the adsorbate concentration. A linear lumped parameter model, with a constant value of  $h$ , only gave an accurate desorption of the desorption kinetics of ethane for the experimental conditions under which it was determined.

#### 6.5.1 The Computer Simulations of Adsorption-Desorption Cycles

Computer simulations were run using the four values of the gas phase mole fraction of methane given in Table 17. As it had been shown that the desorption rate of ethane depended on the solid phase concentration of ethane (Chapter 6, Section 4.3) it was decided to use an inlet gas phase concentration of ethane equal to that used in experiment No.16 from which the kinetic parameter  $h_2$  had been calculated. As the rate of desorption

of methane was very fast it was thought that the kinetic parameter,  $h_1$ , could be used over a wide range of conditions without serious error. The conditions used in the computer simulations are given in Tables 19-22 inclusive. Adsorption was stopped and desorption initiated by pure carrier gas at a time found by subtracting  $1.5 \times$  (the breakthrough time for methane) from the breakthrough time for ethane.

### 6.5.2 Results

The results of the four computer simulations are shown in Figures 45 to 48 inclusive.

### 6.5.3 Conclusions

In all cases the very fast rate of desorption of methane allowed a complete separation of the methane and ethane adsorbed on the 5A molecular sieve under conditions of equilibrium mass transfer control of adsorption and isothermal operation. The decrease in ethane capacity was approximately 10-15% of the equilibrium value.

There are therefore three strategies for the operation of an adsorber to separate or enrich ethane-methane mixtures on 5A molecular sieves assuming that a fuller study of the desorption kinetics and the complete adsorption-desorption cycle under non-isothermal conditions confirms the results of this preliminary investigation.

- 1) Simple adsorption - desorption.
- 2) Adsorption followed by desorption during the initial period in which the bed effluent containing methane is discarded.
- 3) Adsorption followed by desorption initiated at a time when all the methane is desorbed before the breakthrough of ethane.

The method chosen will depend on the composition of the feed, the ethane purity required and overall plant cost optimisation.

Although, in the above adsorption-desorption cycles, desorption has been carried out by elution with an inert carrier gas, similar results, but with a faster desorption of the ethane could be obtained using pressure and/or temperature swing desorption after the methane has been swept out by the inert carrier. It might be possible to affect the complete separation of methane and ethane using pressure and/or temperature swing desorption only.

#### SUGGESTIONS FOR FURTHER WORK

- 1) The addition of computer control to the existing data acquisition program.
- 2) The development of an analytical technique that could provide more data points and hence improve the accuracy of the Simpsons Rule method for integration. A more rapid method would also be required when species are used that have a large retention volume when analysed by gas chromatography.
- 3) The adaptation of the method developed for permanent gases to include the vapours of liquids.
- 4) The extension of the modified coefficient single component empirical Langmuir model to tertiary and higher mixtures and to non-isothermal data.
- 5) A study of the non-isothermal adsorption-desorption separation of methane-ethane mixtures on 5A molecular sieves and a process optimisation study.
- 6) The development of mathematical models for pressure swing desorption and sorption in large beds with appreciable pressure drop, using the technique developed for calculating the inlet flowrate boundary condition.

NOMENCLATURE

A	=	coefficient in empirical Langmuir Equation gmol/gm.
A*	=	coefficient in modified coefficient empirical Langmuir equation gmol/gm.
a	=	particle surface area cm <sup>2</sup> .
ax	=	cross-sectional area of flow cell cm <sup>2</sup> .
B	=	coefficient in empirical Langmuir equation cm <sup>3</sup> /gmol.
B*	=	coefficient in modified coefficient empirical Langmuir equation cm <sup>3</sup> /gmol.
B <sub>e</sub>	=	empirical coefficient in extended empirical Langmuir equation cm <sup>3</sup> /gmol.
c	=	gas phase concentration gmol/cm <sup>3</sup> .
D	=	correlating divisor in Polanyi Adsorption Potential Theory.
D <sub>m</sub>	=	Micro-pore diffusion coefficient cm <sup>2</sup> /s.
D <sub>s</sub>	=	Surface diffusion coefficient cm <sup>2</sup> /s.
DT	=	Time interval between bed exit gas sample analyses s.
d	=	diameter of flow cell cm.
E <sub>IG</sub>	=	Intergranular voidage.
E <sub>MACRO</sub>	=	Adsorbent macro-pore voidage.
E	=	total bed voidage.
F	=	molar flowrate gmol/min.
f	=	gas phase fugacity atm.
f <sup>o</sup>	=	fugacity of adsorbed 'liquid' at adsorption temperature atm.
h	=	kinetic parameter in linear lumped parameter model s <sup>-1</sup> .
hg	=	kinetic parameter in gas phase mass transfer model s <sup>-1</sup> gm/cm <sup>3</sup> .
I	=	Polanyi Adsorption Potential gmol °K/cm <sup>3</sup> .
K <sub>o</sub>	=	Henry's Law Constant molecules/cavity torr
K	=	Henry's Law Constant molecules/cavity torr
kga	=	Mass transfer film resistance s <sup>-1</sup> .
ℓ	=	adsorbent bed length cm.

P	=	adsorbate partial pressure torr
p	=	pressure in adsorption cell psig.
Q	=	molecular sieve adsorbate concentration molecules/cavity
q	=	solid phase adsorbate concentration gmol/gm
R	=	gas law constant
r	=	5A molecular sieve crystal equivalent radius cm
T	=	temperature °K
t	=	time s
$t_{0.5}$	=	time for $\frac{C_0}{C_I} = 0.5$ s
u	=	linear interstitial fluid velocity cm/s
v	=	adsorbate volume cm <sup>3</sup> /gm.
WT	=	weight of adsorbent gm
X	=	instantaneous rate of sorption gmol/min
wx	=	adsorbed phase mole fraction
Y	=	mole fraction of adsorbate in total gas phase
y	=	gas phase mole fraction of component in total adsorbate
$\beta$	=	effective molecular volume cm <sup>3</sup>
$\gamma$	=	effective volume of molecular sieve cavity cm <sup>3</sup>
$\theta$	=	film resistance parameter (Rosen) dimensionless $E \times U/\ell \times kga$ $\times (1 - E)$
$\mu$	=	bed length parameter (Rosen) dimensionless $D_{m/s} \times 3 \times (1 - E)$ $\times A \times B \times \ell/E \times u \times r^2$
$\tau$	=	time parameter (Rosen) dimensionless $2 \times E \times ( u \times t/\ell  - 1)$ $/3 \times (1 - E) \times A \times B$
$\Delta t$	=	time step in finite difference approximation s
$\Delta z$	=	bed length step in finite difference approximation cm
$\pi$	=	surface potential or spreading pressure dynes/cm



$\rho_{\text{BULK}}$  = bulk density of adsorbent bed gm/cm<sup>3</sup>  
 $\rho_{\text{PELLET}}$  = adsorbent pellet density gm/cm<sup>3</sup>  
 $\nu$  = kinematic viscosity cm<sup>2</sup>/s

SUBSCRIPTS

1 = methane  
2 = ethane  
T = methane + ethane  
TG = methane + ethane + carrier gas  
I = adsorbent bed inlet  
O = adsorbent bed inlet.

REFERENCES

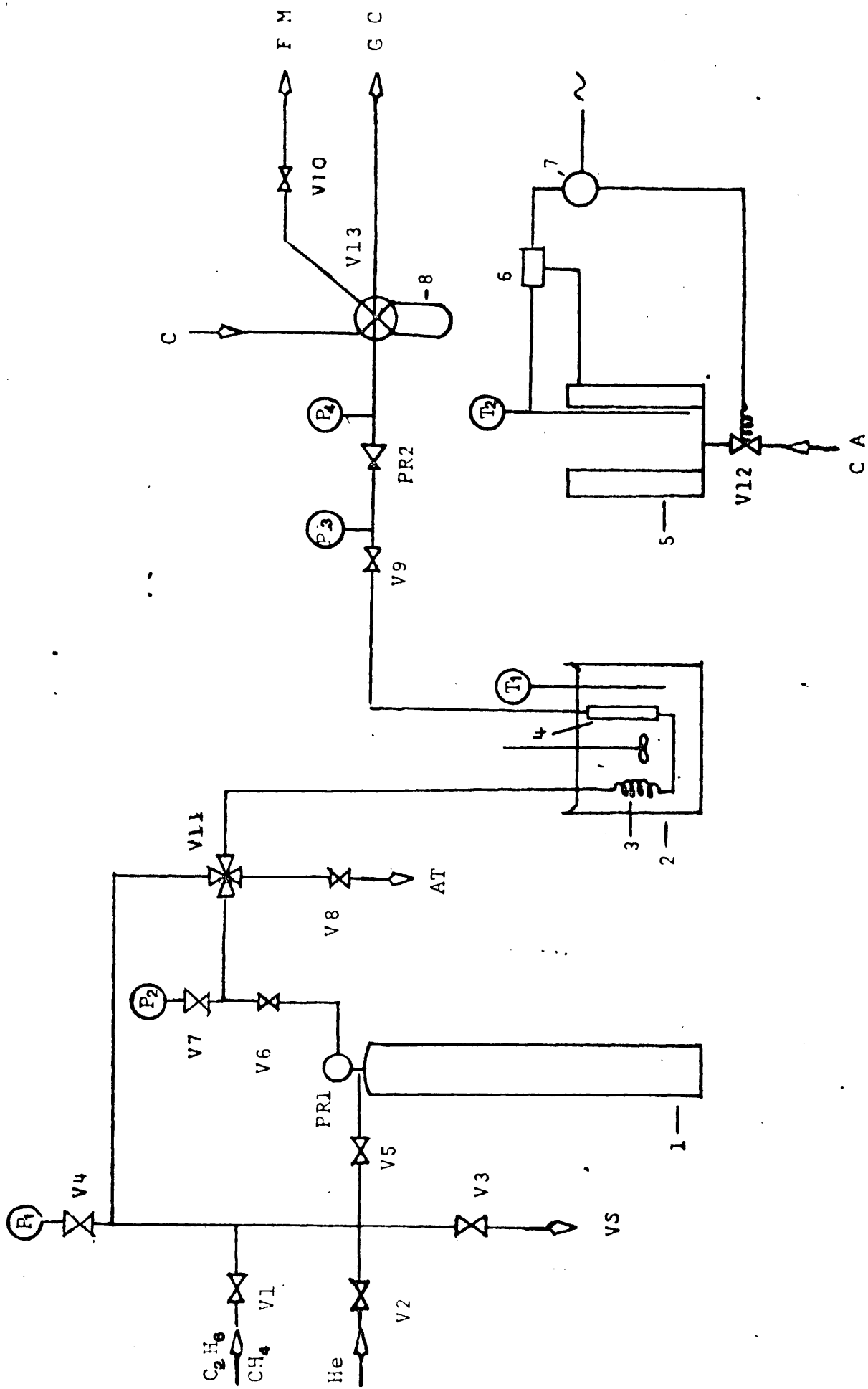
1. Cooperburg, D., Inst. Chem. Eng. Symp. Series, No.44, 5-90, (1976).
2. The Properties of British Natural Gas, Pub. The Gas Council, (Nov. 1971).
3. Anderson, R. A. and Springett, H. S., Inst. Chem. Eng. Symp. Series, No.44, 1 - 10, (1976).
4. Siemens, H. J., Inst. Chem. Eng. Symp. Series, No.44, 1 - 29, (1976).
5. Leavitt, F. W., Chem. Eng. Prog., Vol. 58, No. 8, 54, (August, 1962).
6. Augood, D. R., Trans. Inst. Chem. Eng., 35, 394, (1957).
7. Dunbar, C. L., Proceedings of the Symposium on the Less Common Means of Separation, Birmingham, (April, 1963).
8. Chemical Engineering Vol. 3, Chapter 7, Ed. Richardson, J. F. and Peacock, D. G., Pub. Pergamon Press, (1971).
9. Hoori, S. E. and Pransnitz, J. M., Chem. Eng. Prog. Symp. Series, Vol. 63, No. 74, 3 - 9, (1967).
10. Thomas, W. J. and Lombardi, J. L., Trans. Inst. Chem. Eng., Vol. 49, 240 - 250, (1971).
11. Habgood, H. W., Can. J. Chem., Vol. 36, 1384 - 1397, (1958).
12. Antonson, C. R. and Dranoff, J. S., Chem. Eng. Prog. Symp. Series, Vol. 65, No. 96, 27 - 33, (1969).
13. Kondis, E. F. and Dranoff, J. S., A.I. Ch. E. Symp. Series, Vol. 67, No. 117, 25 - 34, (1971).
14. Ruthven, D. M. and Loughlin, K. F., J. Chem. Soc. Faraday Trans., 68, 696, (1972).
15. Lewis, W. K., Gilliland, B., Chertow, B. and Cadogan, W. P., Ind. Eng. Chem., 42, 1326, (1950).
16. Hasz, J. W. and Barraire, C. A., Chem. Eng. Prog. Symp. Series, Vol. 65, No. 96, 48, (1969).

17. Grant, R. J., Manes, M. and Smith, S. B., A.I.Ch. E. Journal, Vol. 8, No. 3, 403, (1962).
18. Grant, R. J. and Manes, M., Ind. Eng. Chem. Found., Vol. 5, No. 4, 490, (1966).
19. Lewis, W. K., Gilliland, B., Chertow, B. and Cadogan, W. P., Ind. Eng. Chem., Vol. 42, No. 1, 1319 (1950).
20. Myers, A. L. and Prausnitz, J. M., A.I.Ch.E. Journal, Vol. 11, No. 1, 121, (1965).
21. Friederick, R. O. and Mullins, J. C., Ind. Eng. Chem. Fund., Vol. 11, No. 4, 457, (1972).
22. Fernbacher, J. M. and Wenzel, L. A., Chem. Eng. Prog. Symp. Series, Vol. 65, No. 96, 457, (1969).
23. Glessner, A. J. and Myers, A. L., Chem. Eng. Prog. Symp. Series, Vol. 65, No. 96, 73, (1969).
24. Kidnay, A. J. and Myers, A. L., A.I.Ch.E. Journal, Vol. 12, No. 5, 981, (1966).
25. Ruthven, D. M., Loughlin, K. F. and Holborrow, K. A., Chem. Eng. Sci., Vol. 28, 701, (1973).
26. Masamune, S. and Smith, J. M., A.I.Ch.E. Journal, Vol. 11, No. 1, 34, (1965).
27. McGreavy, C., Nussey, C. and Creswell, D. L., Inst. Chem. Eng. Symp. Series, No. 23, 111, (1967).
28. Cooney, D. O. and Lightfoot, E. N., Ind. Eng. Chem. Fund, Vol. 4, No. 2, 233, (1965).
29. Hall, K. R., Engleton, L. C., Acrivos, A., and Vermeulen, T., Ind. Eng. Chem. Fund., Vol. 5, No. 2, 212 (1966).

30. Cooney, D. O. and Lightfoot, E. N., *Ind. Eng. Chem. Proc. Dev.*, Vol. 5, No. 1, 25, (1966).
31. Cooney, D. O. and Paolo Strusi, F., *Ind. Eng. Chem. Fund.*, Vol. 11, No. 1, 123, (1972).
32. Garg, D. R. and Ruthven, D. M., *A.I.Ch.E. Journal*, Vol. 19, No.4, 852, (1973).
33. Shen, J. and Smith, J. M., *Ind. Eng. Chem. Fund*, Vol. 7, No.1, 100, (1968).
34. Chi. C. W. and Lew, H., *Chem. Eng. Prog. Symp. Series*, Vol. 65, No. 69, 65, (1969).
35. Rootave, H. M. and Spencer, J., *Powder Technol.* Vol. 6, 17, (1972).
36. *Chemical Engineers Handbook*, 4th Ed., 5-8, Eds. Perry et al., Pub. McGraw-Hill.
37. *Chemical Engineering*, Vol. 1, 123, Eds. Coulson, J. M. and Richardson, J. F., Pub. Pergamon Press (1966).
38. *Chemical Engineering*, Vol. 1, 443, Eds. Coulson, J. M. and Richardson, J. F., Pub. Pergamon Press (1966).
39. *Elements of Physical Chemistry*, 29, Glasstone, S. and Lewis, D., Pub. Macmillan (1960).
40. Benedict M., Webb, G. B. and Rubin, L. C., *Chem. Eng. Prog.*, Vol. 47, No. 8, 419, (1951).
41. *A.P.I. Handbook*, Pub. American Petroleum Institute, (1974).
42. Cook, W. H. and Basmadjian, D., *Can. J. Chem. Eng.*, Vol. 42, 146, (1964).
43. *Chemical Process Principales*, Part II, Hougen, O. A., Watson, K. M., and Ragatz, R. A., Wiley, New York, (1959).
44. Private communication, Laporte Industries, Ltd., Catalyst Section, Widnes, Lancs.
45. *Applied Numerical Analysis*, 106, Gerald, C. F., Pub. Addison-Wesley Pub. Corp., London, Ontario, 1970.

46. Lederman, P. B. and Williams, B., A.I.Ch.E. Journal, Vol. 10, 30, (1964).
47. Szepesy, L. and Illés, V., Act. Chin. Hung. Vol. 35, 37, (1963).
48. Gáspary, R. L. and Zwiebel, I., A.I.Ch.E., Symp. Series, Vol. 67, No. 117, 17, (1971).
49. Rosen, J. B., Ind. Eng. Chem., Vol. 49, 1590, (1951).
50. Rosen, J. B., J. Chem. Phys., Vol. 20, 387, (1952).
51. Camp, D. T. and Canjar, L. N., A.I.Ch.E. Journal, Vol. 12, No. 2, 339, (1966).
52. Wilke, C. R. and Hanzen, O. A., Trans. Am. Inst. Chem. Engrs., Vol. 41, 445, (1945).
53. Wilke, C. R. and Lee, C. Y., Ind. Eng. Chem., Vol. 47, 1253, (1955).
54. Fluidisation, 49, Leva, P., Pub. McGraw-Hill, New York, (1959).
55. Courant, R., Friedrichs, K. O. and Levy, M., I.B.M. Journal, 215, (March 1967).
56. Computational Fluid Dynamics, 47, Roache, P. J., Pub. Hermosa, Albuquerque, New Mexico (1972).
57. Kondis, E. F., Ph.D. Thesis, Northwestern Univ., Evanston, Ill. (1969).
58. Allen, J. L., Ph.D. Thesis, Cookston College of Technology, Potsdam, New York (1964).
59. The Mathematics of Diffusion, Crank, J., Pub. Oxford Univ. Press, Oxford (1956).

FIGURES AND TABLES



ADSORPTION APPARATUS

FIG. 1

KEY

V1-8	High pressure/high vacuum shut-off valves	6	Pye-Ether Mini temperature controller
V9	High pressure flow control valve	7	Time switch
V10	Flow control valve	8	Sample loop
V11	High pressure/high vacuum 4-way valve	VS	Vacuum system
V12	Solenoid valve	CA	Laboratory compressed air supply
V13	Pye 6-way sampling valve	FM	Bubble flow meter
PR1	Cylinder head pressure regulator	GC	Gas chromatography unit (Pye 104)
PR2	Chromatography grade pressure regulator	AT	Vent to atmosphere
1	Sample cylinder	CH <sub>4</sub>	Methane
2	Lagged constant temperature water bath	C <sub>2</sub> H <sub>6</sub>	Ethane
3	Pre-heater coil	He	Helium
4	Adsorption tube	C	Gas chromatography carrier gas (Helium)
5	Regeneration furnace		



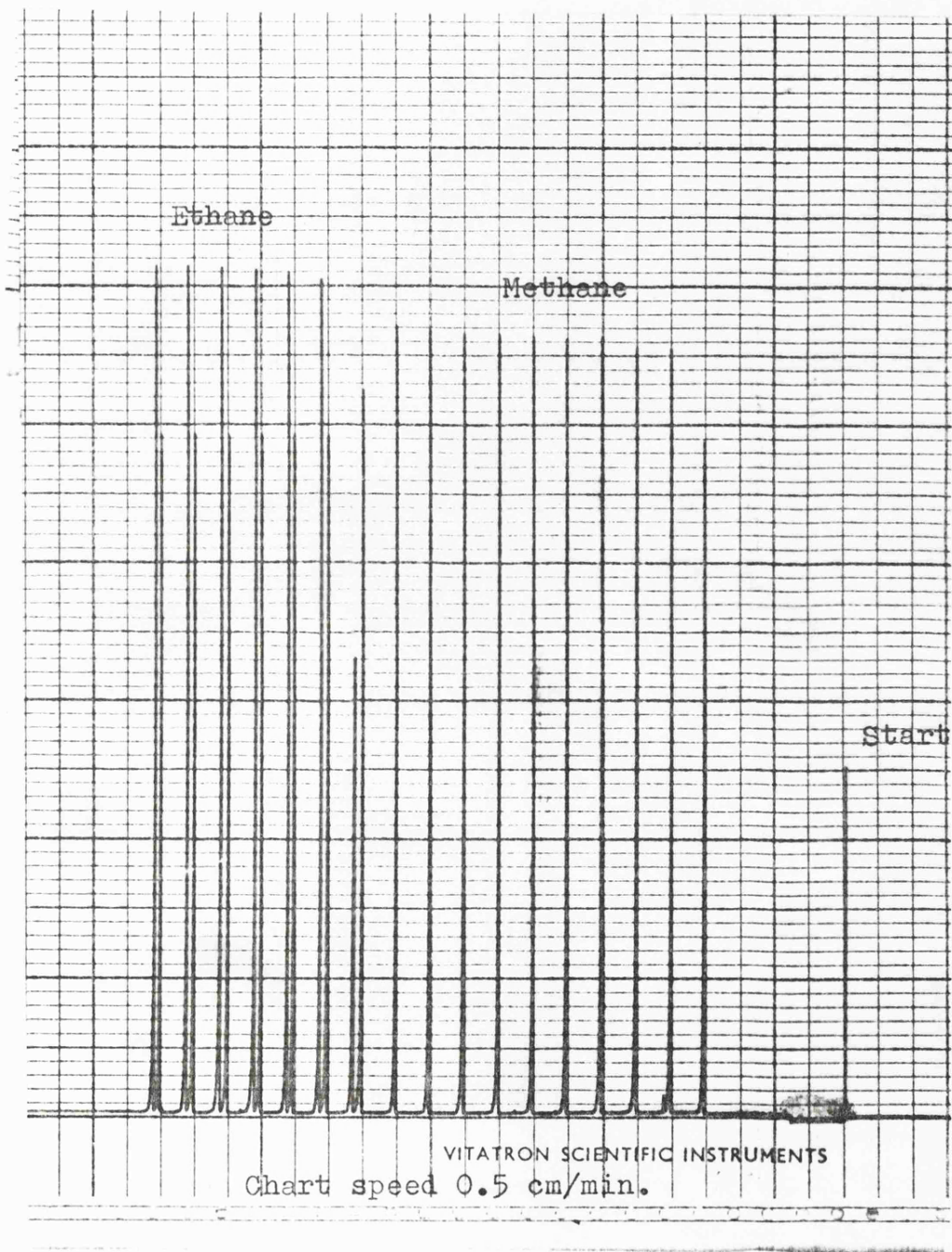


FIG. 2 TYPICAL GAS SAMPLE CHROMATOGRAM FOR BINARY  
ADSORPTION

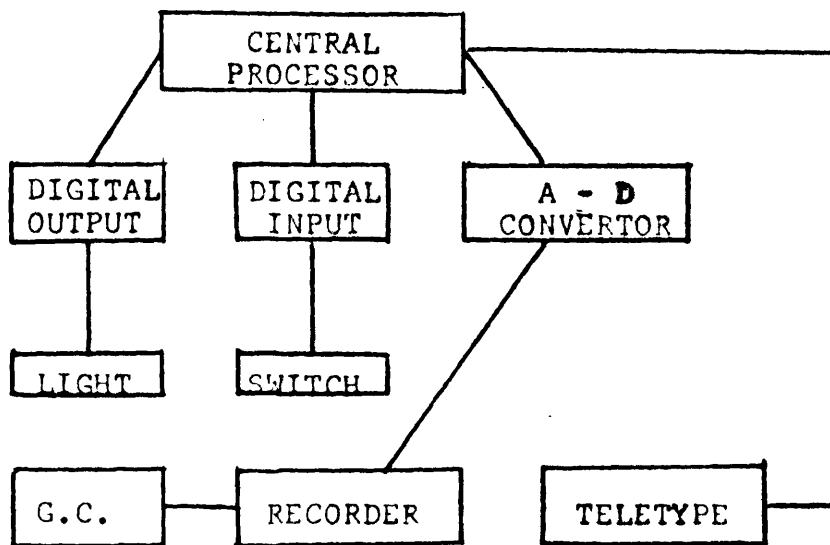
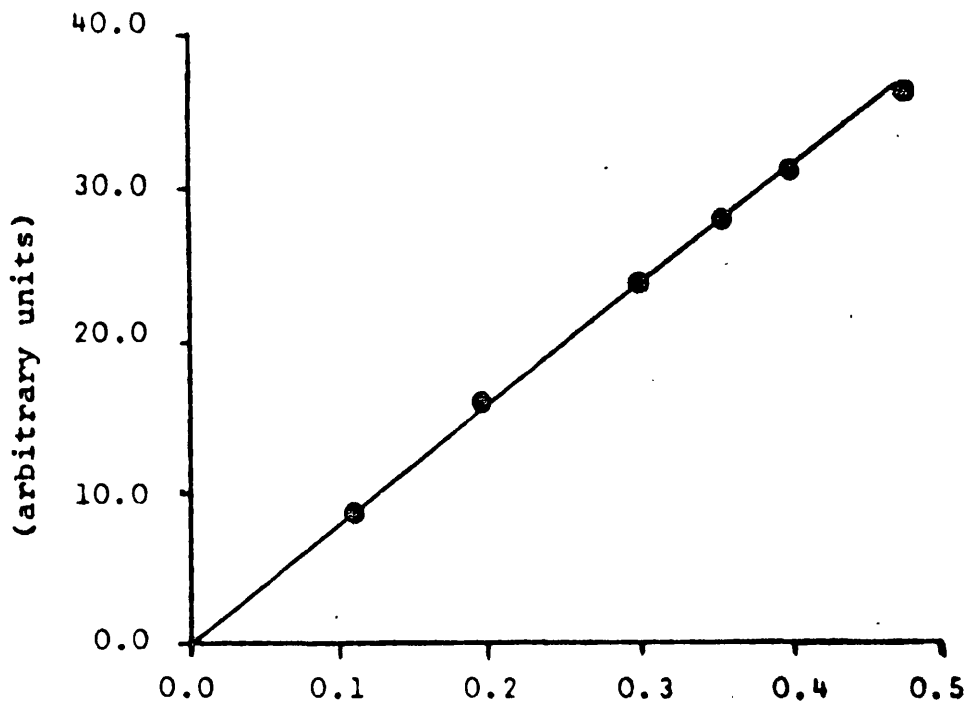


FIG. 3 BLOCK DIAGRAM OF ON-LINE COMPUTER LINK

---

PEAK AREA FROM ON-LINE COMPUTER INTEGRATION



PEAK AREA INTEGRATED FROM RECORDER CHART  
(arbitrary units)

FIG. 4 CORRELATION BETWEEN GRAPHICAL AND ON-LINE COMPUTER

INTEGRATION OF CHROMATOGRAMS

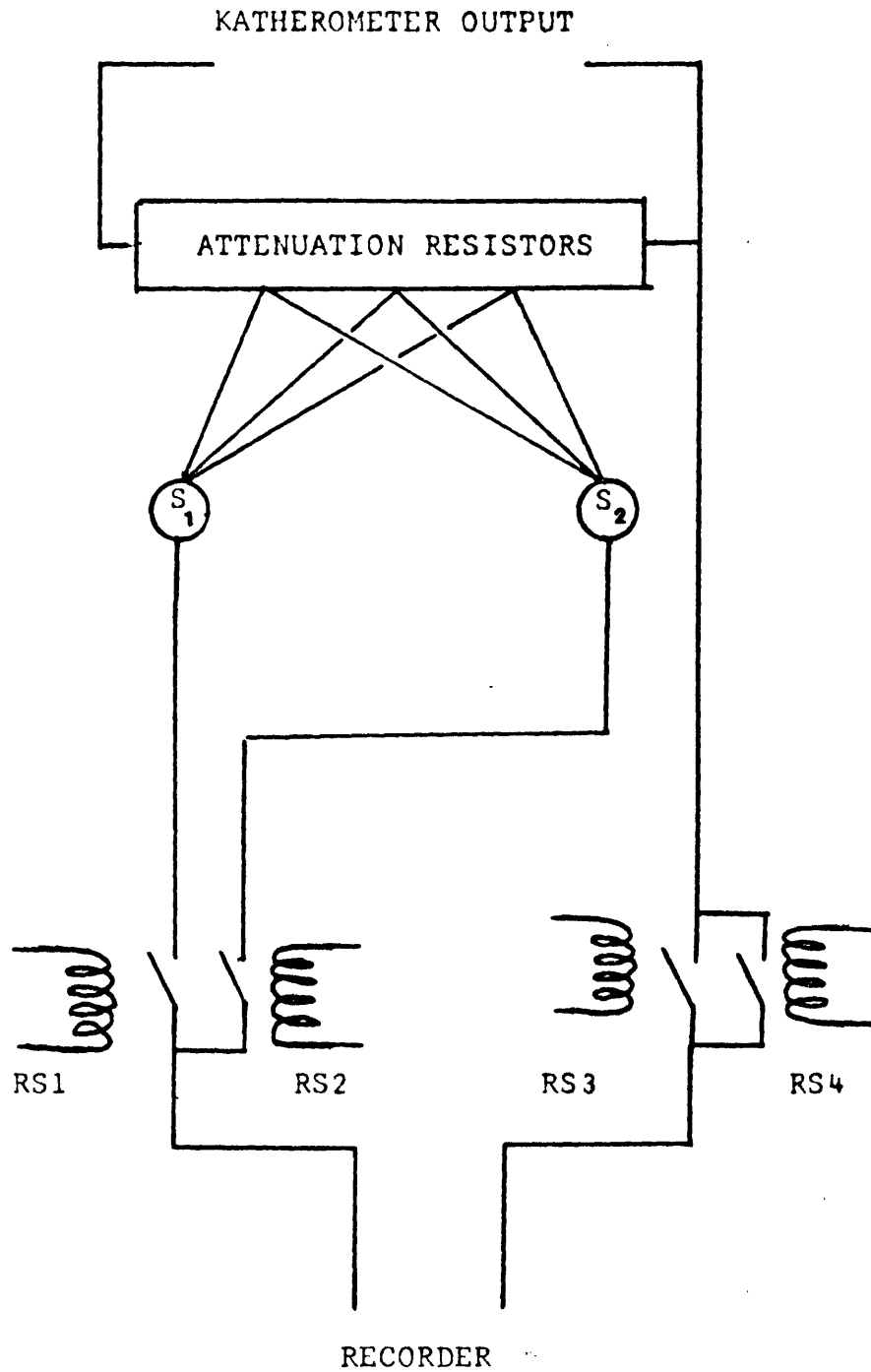


**FIG. 5**      BLOCK DIAGRAM OF ATTENUATION SWITCHING CIRCUIT

---

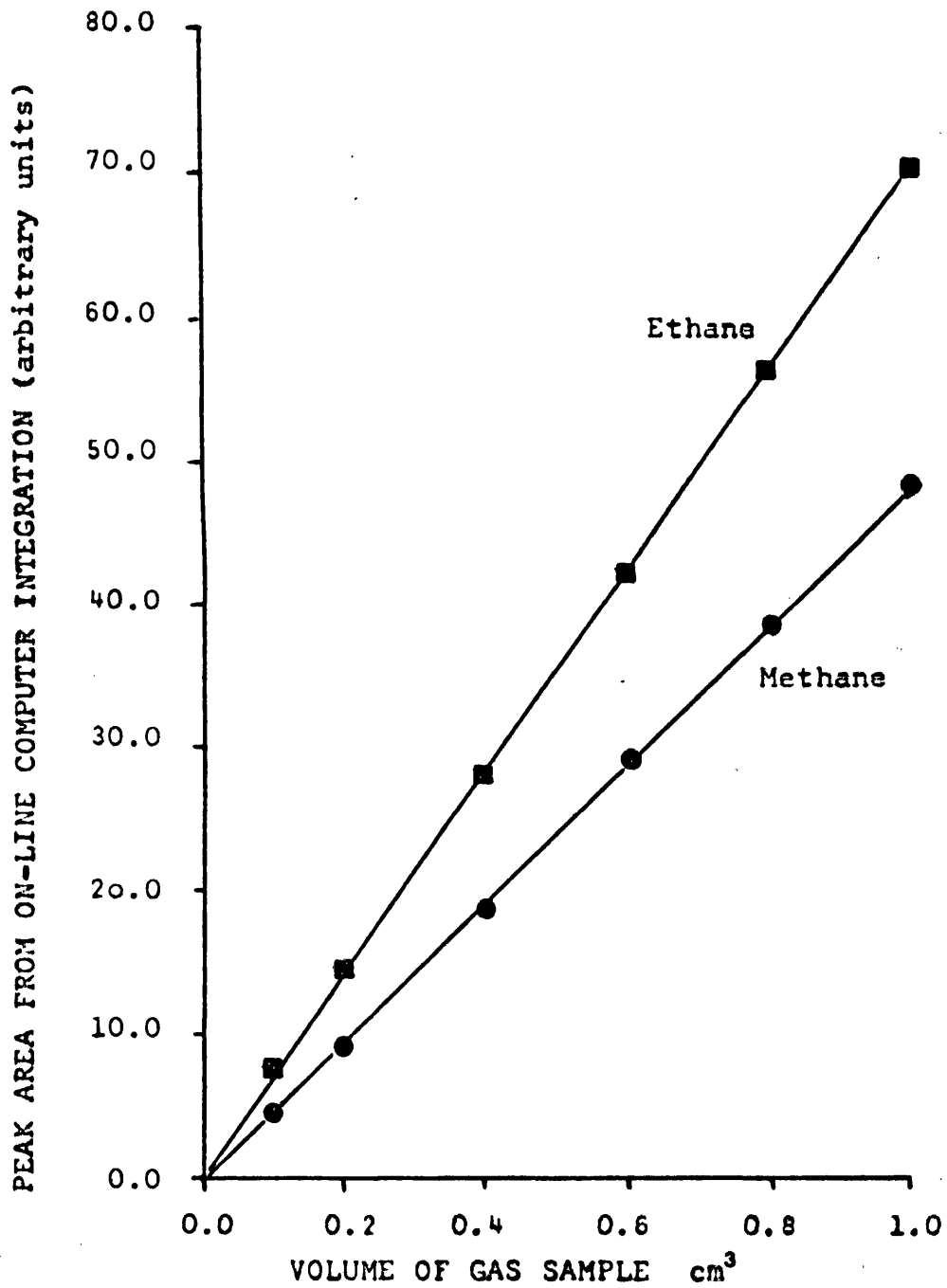


FIG. 6 CALIBRATION OF KATHEROMETER RESPONSE FOR  
METHANE AND ETHANE

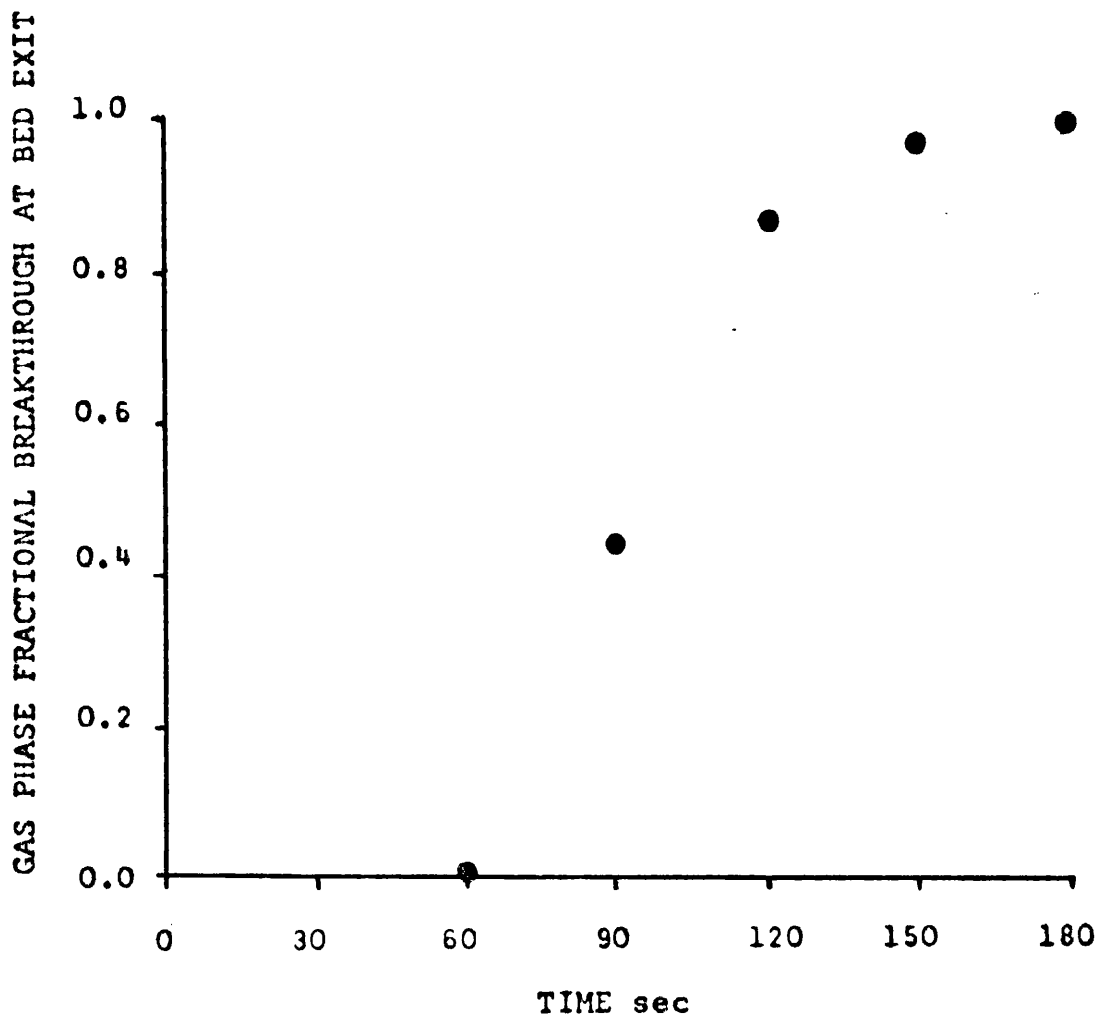


FIG. 7 DETERMINATION OF APPARATUS DEAD-TIME

1.00 gm 30-44 mesh; heat treated, 5A molecular sieve  
using 3mm diameter tube

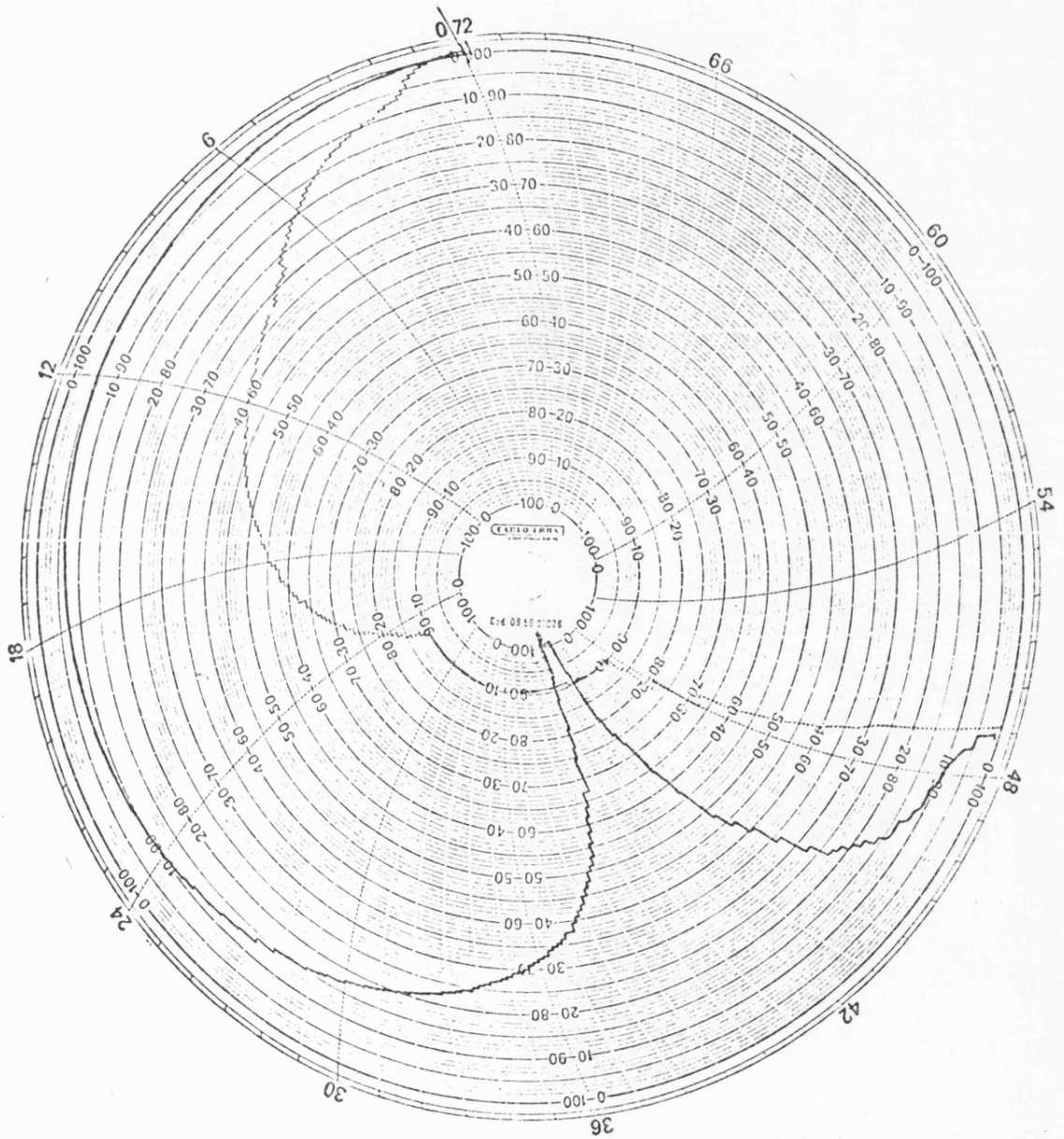


FIG. 8

POROSIMETER CHART

POROSIMETRY CALCULATIONS-PORE AREA-DISTRIBUTION  
 5-A MOLECULAR SIEVE (30-60MESH) HEATED 450 C. NO HE

PORE DIAMETER MICRONS	VOLUME PERCENT	AREA PERCENT
2.0000	5.04	0.10
1.5000	5.23	0.10
1.0000	7.67	0.24
0.6000	12.02	0.60
0.4000	16.42	1.13
0.2000	30.66	4.41
0.1000	59.38	16.30
0.0900	63.50	18.84
0.0800	64.09	19.33
0.0700	64.68	19.82
0.0600	65.27	20.31
0.0500	70.00	25.99
0.0400	77.47	35.59
0.0300	84.38	47.18
0.0200	92.06	65.39
0.0100	99.51	96.87
0.0000	100.00	100.00

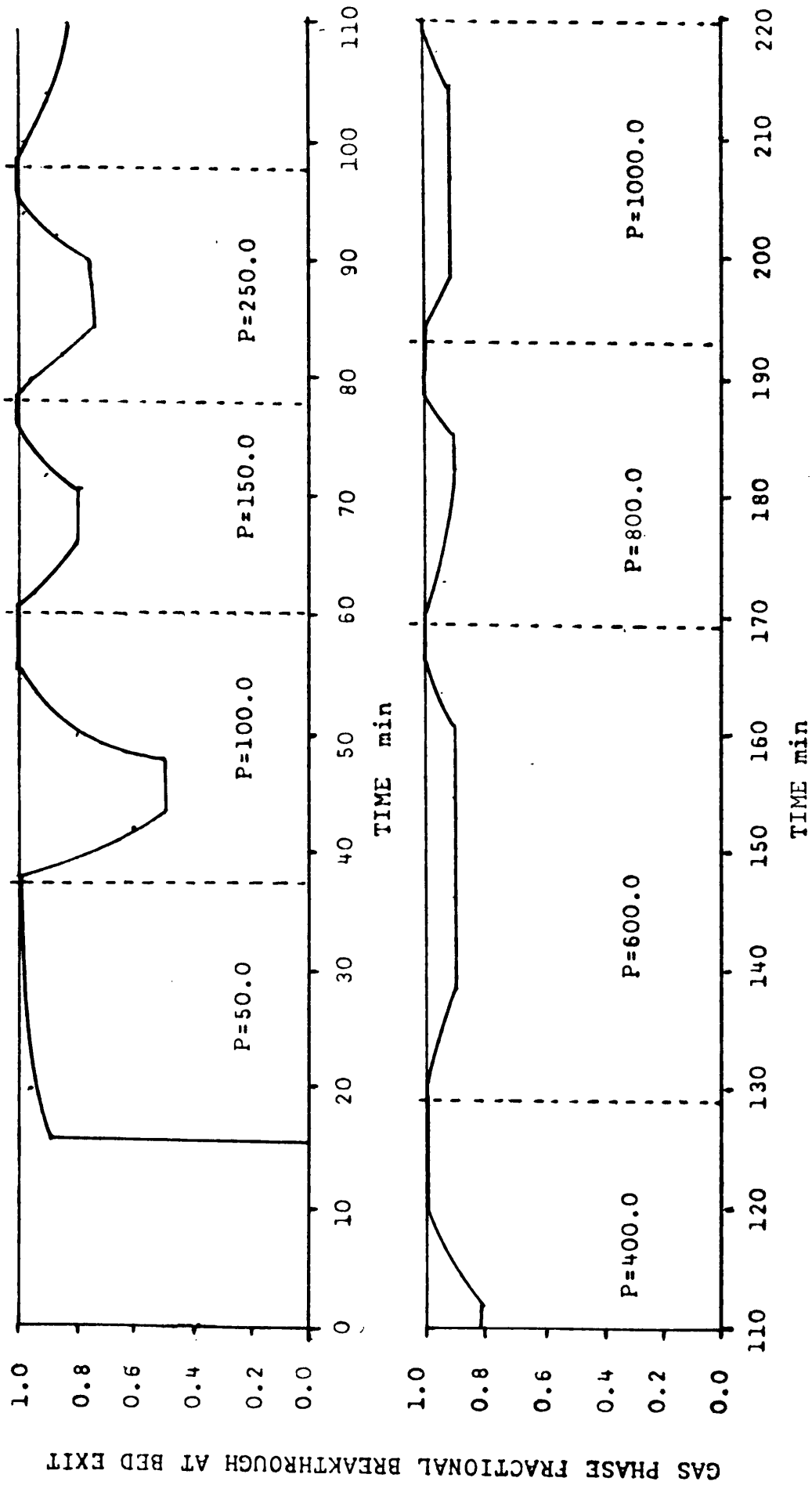
SUMMARY TABLE

1. MEDIAN PORE DIAMETER...	0.1327	MICRONS
2. TOTAL PORE VOLUME...	0.3238	CC/G
3. AVERAGE PORE DIAMETER (4V/A)...	0.0577	MICRONS
4. TOTAL PORE AREA...	22.439	M <sup>2</sup> /GM

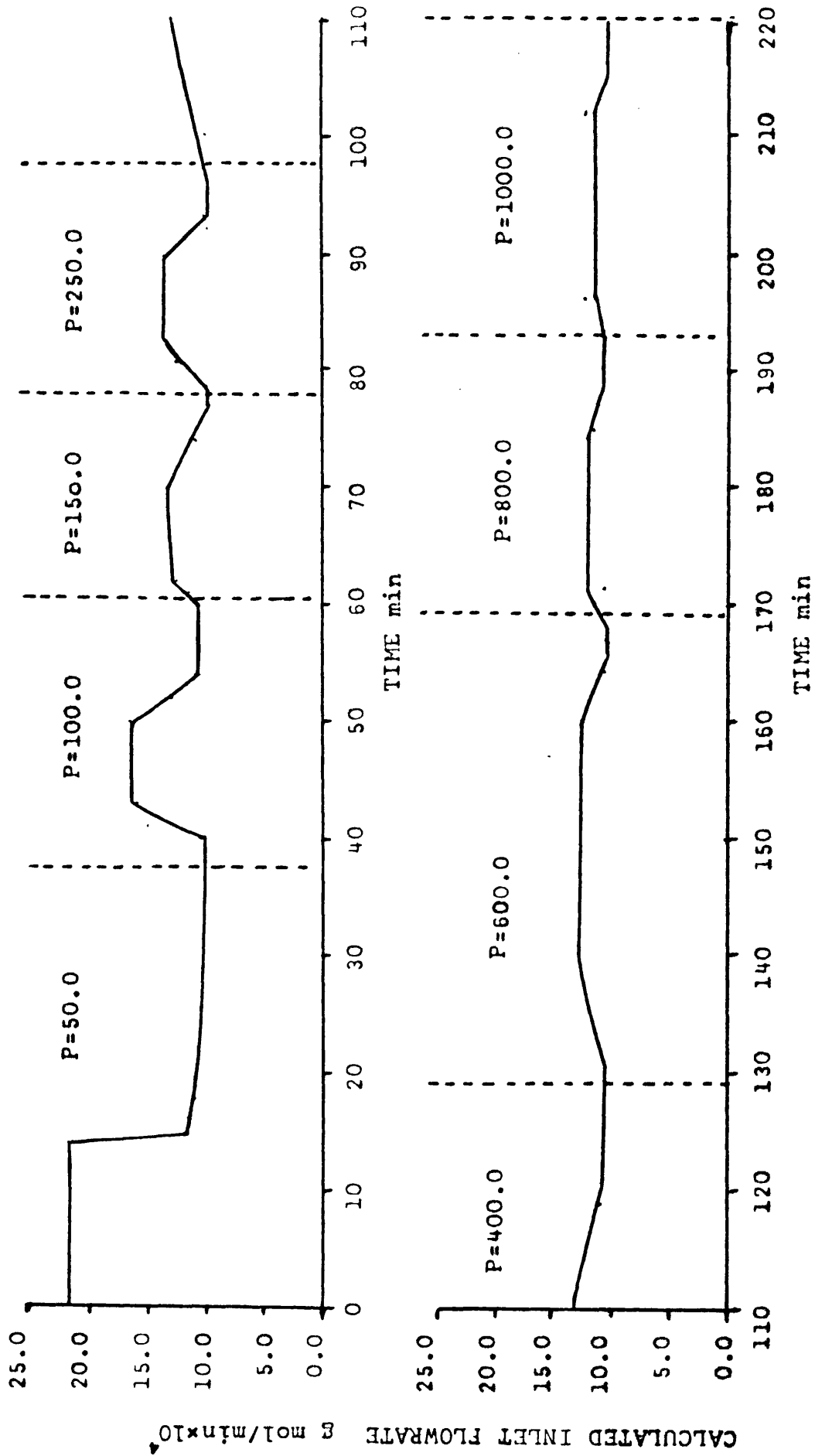
\*\*FORTRAN \*\* STOP

TABLE 1





**FIG. 9** SINGLE COMPONENT ISOTHERMAL BREAKTHROUGH DATA-EXPERIMENT NO. 2



**FIG.10** SINGLE COMPONENT ISOTHERMAL ADSORPTION-CALCULATED INLET FLOWRATE-EXPERIMENT NO. 2

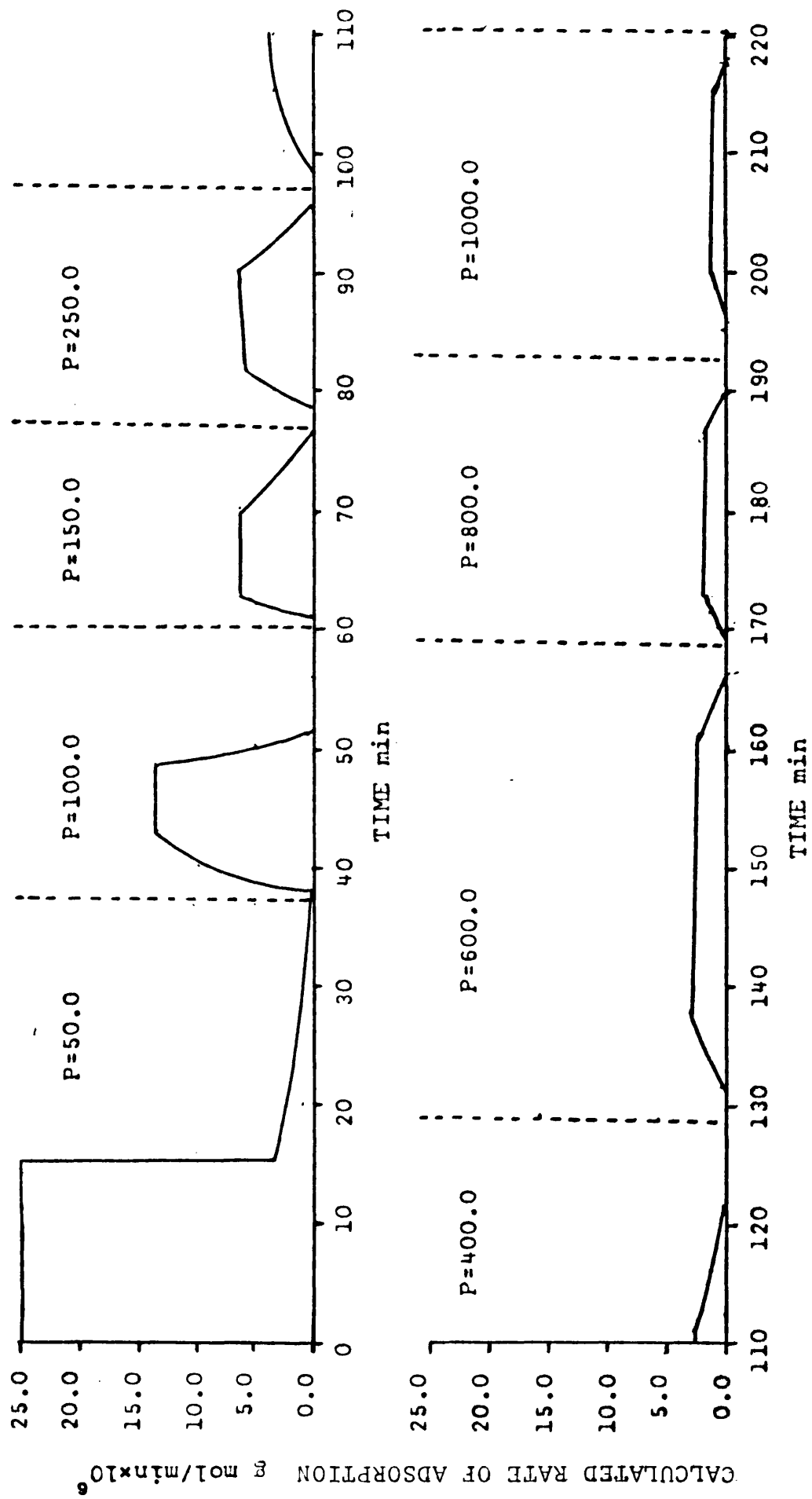


FIG.11 SINGLE COMPONENT ISOTHERMAL ADSORPTION-CALCULATED RATE OF ADSORPTION-EXPERIMENT NO. 2

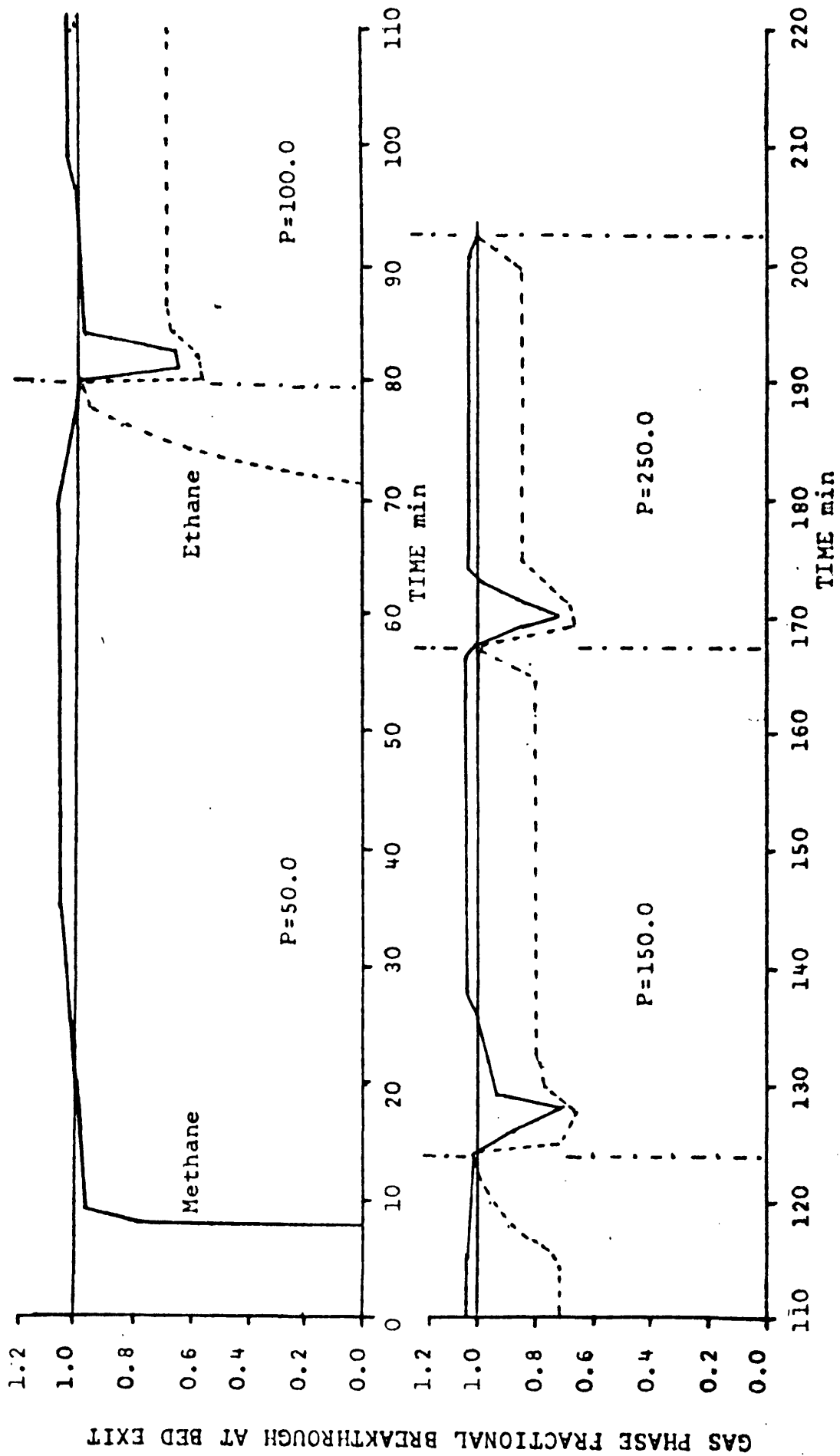
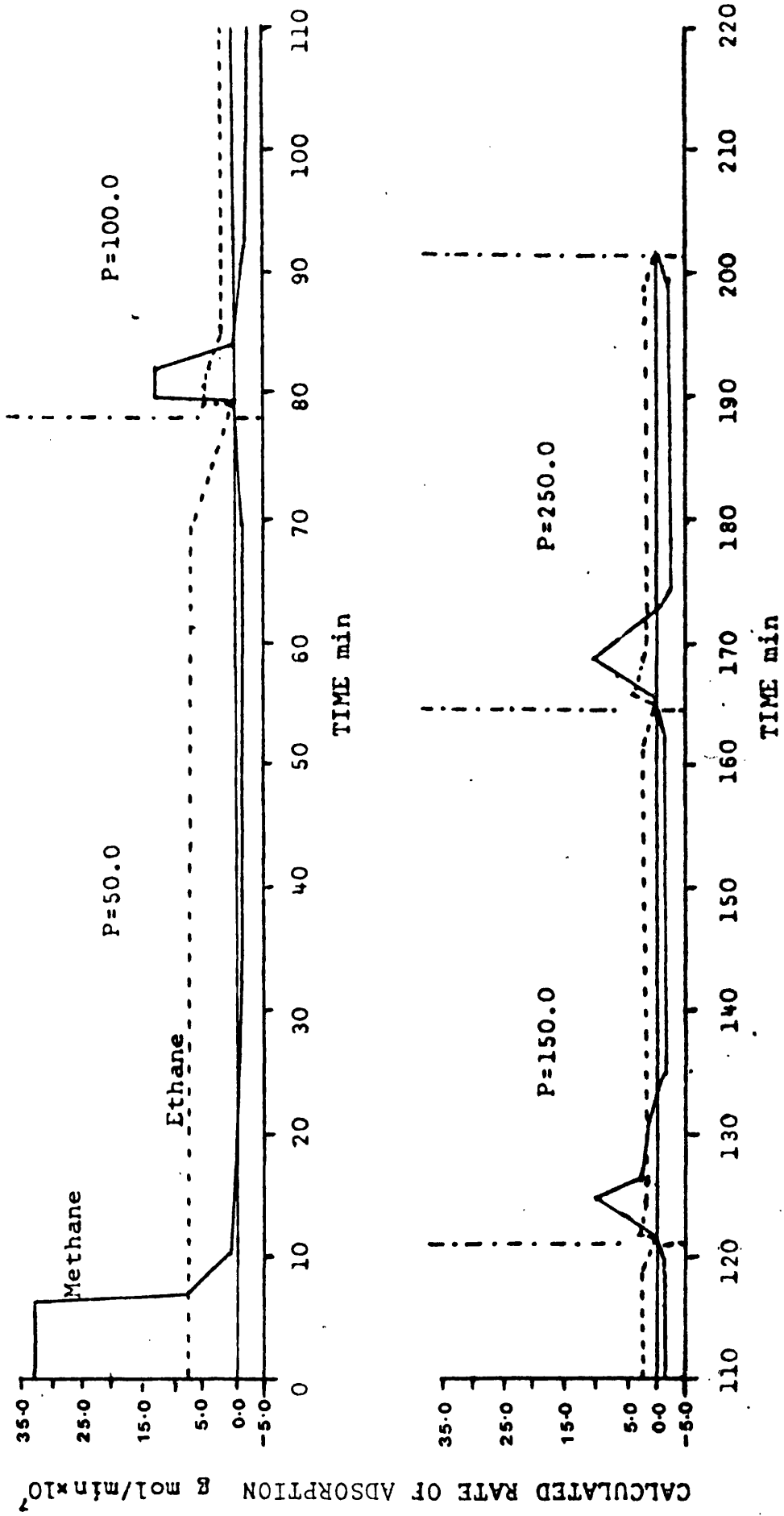


FIG. 12 TWO COMPONENT ISOTHERMAL BREAKTHROUGH DATA-EXPERIMENT NO. 7



**FIG. 13** TWO COMPONENT ISOTHERMAL ADSORPTION-CALCULATED RATE OF ADSORPTION-EXPERIMENT NO. 7

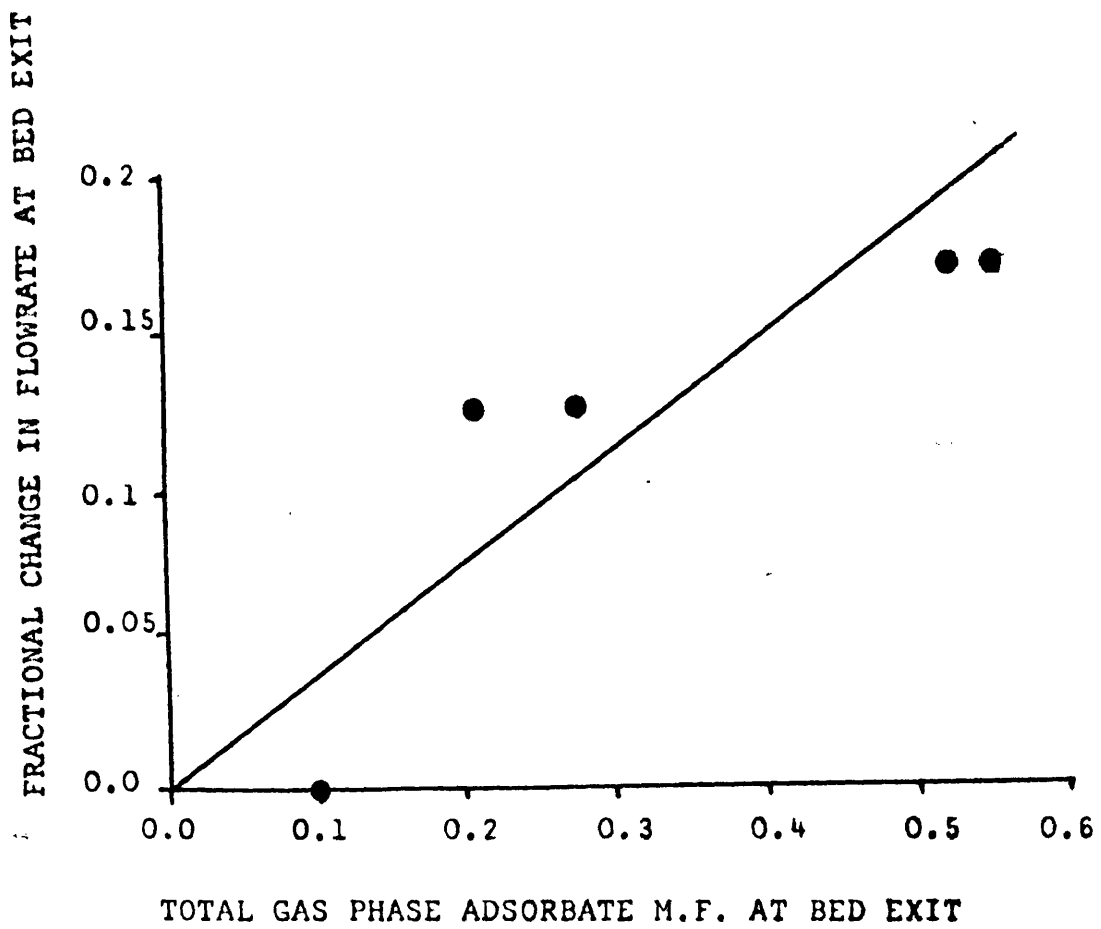


FIG.14 MODEL OF OUTLET FLOW CONTROL VALVE RELATING CHANGE  
IN FLOWRATE FROM THAT SET WITH PURE CARRIER GAS WITH  
TOTAL GAS PHASE M.F. OF ADSORBATE AT BED EXIT

EXPERIMENT NO. 1

SYSTEM: METHANE ON ACTIVATED CARBON

ADSORBATE M.F. IN TOTAL FLOW: 0.537

M.F. METHANE IN ADSORBATE: 1.0

ADSORPTION TEMPERATURE: 20.0°C

WEIGHT OF ADSORBENT: 3.707 gm

INITIAL OUTLET FLOWRATE: 23.5 cm<sup>3</sup>/min

FINAL OUTLET FLOWRATE: 27.5 cm<sup>3</sup>/min

P psig.	q <sub>1</sub> g mol/gm x 10 <sup>4</sup>	i <sub>1</sub> g mol/cm <sup>3</sup> x 10 <sup>5</sup>	v <sub>1</sub> cm <sup>3</sup> /gm x 10 <sup>2</sup>	I <sub>1</sub> g mol.°K /cm <sup>3</sup>
50.0	15.79	9.88	8.53	36.66
100.0	19.85	17.59	10.72	29.21
150.0	22.42	25.35	12.11	26.41
200.0	25.76	33.17	13.91	24.36
300.0	29.62	48.97	15.99	21.42
400.0	31.71	65.00	17.12	19.31
600.0	33.39	97.75	18.03	16.31
800.0	34.82	131.5	18.80	14.18
1000.0	36.28	166.1	19.59	12.53

TABLE. 2

EXPERIMENT NO. 2

SYSTEM: METHANE ON 5A MOLECULAR SIEVE

ADSORBATE M.F. IN TOTAL FLOW: 0.553

M.F. METHANE IN ADSORBATE: 1.0

ADSORPTION TEMPERATURE: 20.0 °C

WEIGHT OF ADSORBENT: 5.514 gm

INITIAL OUTLET FLOWRATE: 23.5 cm<sup>3</sup>/min

FINAL OUTLET FLOWRATE: 27.4 cm<sup>3</sup>/min

P psig.	$q_1$ g mol/gm x 10 <sup>4</sup>	$c_1$ g mol/cm <sup>3</sup> x 10 <sup>5</sup>	$v_1$ cm <sup>3</sup> /gm x 10 <sup>2</sup>	$I_1$ g mol. <sup>o</sup> K /cm <sup>3</sup>
50.0	11.08	10.18	5.98	33.43
100.0	17.00	18.12	9.18	28.98
150.0	19.23	26.14	10.38	26.18
250.0	22.18	44.28	11.98	22.52
400.0	24.61	66.98	13.29	19.09
600.0	26.07	100.8	14.08	16.09
800.0	26.95	135.6	14.55	13.96
1000.0	27.36	171.4	14.77	12.31

TABLE 3



EXPERIMENT NO. 3

SYSTEM: METHANE ON 5A MOLECULAR SIEVE

ADSORBATE M.F. IN TOTAL FLOW: 0.129

M.F. METHANE IN ADSORBATE: 1.0

ADSORPTION TEMPERATURE: 20.0°C

WEIGHT OF ADSORBENT: 5.514 gm

INITIAL OUTLET FLOWRATE: 23.5 cm<sup>3</sup>/min

FINAL OUTLET FLOWRATE: 23.5 cm<sup>3</sup>/min

P psig.	$q_1$ g mol/gm x 10 <sup>4</sup>	$I_1$ g mol/cm <sup>3</sup> x 10 <sup>5</sup>	$v_1$ cm <sup>3</sup> /gm x 10 <sup>2</sup>	$I_1$ g mol. <sup>o</sup> K /cm <sup>3</sup>
30.0	3.47	1.64	1.87	47.64
100.0	7.17	4.22	3.87	40.28
150.0	9.02	6.06	4.86	37.46
200.0	10.83	7.91	5.85	35.39
300.0	13.62	11.62	7.35	32.40
400.0	14.23	15.34	7.71	30.27

TABLE 4

EXPERIMENT NO. 4

SYSTEM: METHANE ON ACTIVATED CARBON

ADSORBATE M.F. IN TOTAL FLOW: 0.129

M.F. METHANE IN ADSORBATE: 1.0

ADSORPTION TEMPERATURE: 20.0°C

WEIGHT OF ADSORBENT: 2.524

INITIAL OUTLET FLOWRATE: 23.5 cm<sup>3</sup>/min

FINAL OUTLET FLOWRATE: 23.5 cm<sup>3</sup>/min

P psig.	$q_1$ g mol/gm x 10 <sup>4</sup>	$i_{C_1}$ g mol/cm <sup>3</sup> x 10 <sup>5</sup>	$v_1$ cm <sup>3</sup> /gm x 10 <sup>2</sup>	$T_1$ g mol.°K /cm <sup>3</sup>
50.0	7.54	2.37	4.07	44.75
100.0	10.07	4.22	5.44	40.28
150.0	12.34	6.06	6.66	37.18
200.0	13.99	7.91	7.54	35.25
300.0	16.04	11.62	8.86	32.40
400.0	18.04	15.34	9.74	30.27

TABLE 5

EXPERIMENT NO. 5

SYSTEM: ETHANE ON 5A MOLECULAR SIEVE

ADSORBATE M.F. IN TOTAL FLOW: 0.0988

M.F. METHANE IN ADSORBATE: 0.0

ADSORPTION TEMPERATURE: 20.0°C

WEIGHT OF ADSORBENT: 1.050 gm

INITIAL OUTLET FLOWRATE: 23.5 cm<sup>3</sup>/min

FINAL OUTLET FLOWRATE: 23.5 cm<sup>3</sup>/min

P psig.	$q_2$ g mol/gm x 10 <sup>4</sup>	$c_2$ g mol/cm <sup>3</sup> x 10 <sup>5</sup>	$v_2$ cm <sup>3</sup> /gm x 10 <sup>2</sup>	$I_2$ g mol. <sup>o</sup> K /cm <sup>3</sup>
50.0	18.00	1.81	9.90	20.86
100.0	20.49	3.21	11.28	17.83
150.0	21.54	4.65	11.52	15.91
200.0	22.27	6.08	12.13	14.51
258.0	23.00	7.75	12.76	13.25
303.0	23.27	9.05	13.05	12.45
400.0	23.78	11.88	13.62	11.06
500.0	24.05	14.83	14.01	9.94
600.0	24.29	17.82	14.35	9.02
800.0	24.54	23.91	14.87	7.58

TABLE 6

EXPERIMENT NO. 6

SYSTEM: ETHANE ON ACTIVATED CARBON

ADSORBATE M.F. IN TOTAL FLOW: 0.0988

M.F. METHANE IN ADSORBATE: 0.0

ADSORPTION TEMPERATURE: 20.0°C

WEIGHT OF ADSORBENT: 1.173 gm

INITIAL OUTLET FLOWRATE: 23.5 cm<sup>3</sup>/min

FINAL OUTLET FLOWRATE: 23.5 cm<sup>3</sup>/min

P psig.	$q_2$ g mol/gm x 10 <sup>4</sup>	$2C_{r3}$ g mol/cm <sup>3</sup> x 10 <sup>5</sup>	$v_2$ cm <sup>3</sup> /gm x 10 <sup>2</sup>	$I_2$ g mol.°K /cm <sup>3</sup>
50.0	27.95	1.81	15.38	20.86
100.0	31.51	3.21	17.34	17.83
150.0	33.73	4.65	18.03	15.91
200.0	35.31	6.08	19.24	14.51
250.0	36.51	7.75	20.25	13.25
300.0	37.64	9.05	21.11	12.45
400.0	39.13	11.88	22.40	11.06
600.0	40.96	17.82	24.20	9.02
800.0	42.45	23.91	25.68	7.58

TABLE 7

EXPERIMENT NO. 7

SYSTEM: METHANE-ETHANE ON 5A MOLECULAR SIEVE

ADSORBATE M.F. IN TOTAL FLOW: 0.205

M.F. METHANE IN ADSORBATE: 0.829

ADSORPTION TEMPERATURE: 20.0°C

WEIGHT OF ADSORBENT: 2.400 gm

INITIAL OUTLET FLOWRATE: 23.5 cm<sup>3</sup>/min

FINAL OUTLET FLOWRATE: 26.4 cm<sup>3</sup>/min

P psig.	q		c <sub>T</sub>		v <sub>T</sub> cm <sup>3</sup> /gm x 10 <sup>2</sup>	I <sub>T</sub> g mol.°K /cm <sup>3</sup>
	g mol/gm x 10 <sup>4</sup> 1	2	g mol/cm <sup>3</sup> x 10 <sup>5</sup> 1	2		
50.0	2.43	11.02	3.11	0.64	7.43	25.77
100.0	3.65	13.13	5.55	1.14	9.27	22.62
150.0	4.36	14.44	7.98	1.64	10.39	20.63
250.0	5.28	15.34	12.87	2.63	11.43	18.04
400.0	6.36	16.01	20.29	4.18	12.44	15.51

TABLE 8

EXPERIMENT NO. 8

SYSTEM: METHANE-ETHANE ON 5A MOLECULAR SIEVE

ADSORBATE M.F. IN TOTAL FLOW: 0.082

M.F. METHANE IN ADSORBATE: 0.597

ADSORPTION TEMPERATURE: 20.0 °C

WEIGHT OF ADSORBENT: 0.755 gm

INITIAL OUTLET FLOWRATE: 23.4 cm<sup>3</sup>/min

FINAL OUTLET FLOWRATE: 23.4 cm<sup>3</sup>/min

P psig.	q		c <sub>T</sub>		v <sub>T</sub> cm <sup>3</sup> /gm x 10 <sup>2</sup>	I <sub>T</sub> g mol. <sup>o</sup> K /cm <sup>3</sup>
	1	2	1	2		
50.0	1.12	13.42	0.89	0.61	8.01	26.48
100.0	1.39	16.82	1.59	1.07	10.05	23.42
150.0	1.59	18.60	2.29	1.54	11.13	21.47
250.0	2.11	21.25	3.67	2.48	12.89	18.93
500.0	3.17	24.05	7.23	4.87	14.71	15.35

TABLE 9

EXPERIMENT NO. 9

SYSTEM: METHANE-ETHANE ON 5A MOLECULAR SIEVE

ADSORBATE M.F. IN TOTAL FLOW: 0.270

M.F. METHANE IN ADSORBATE: 0.902

ADSORPTION TEMPERATURE: 20.0 °C

WEIGHT OF ADSORBENT: 0.738 gm

INITIAL OUTLET FLOWRATE: 23.4 cm<sup>3</sup>/min

FINAL OUTLET FLOWRATE: 26.4 cm<sup>3</sup>/min

P psig.	q		c <sub>I</sub>		v <sub>T</sub> cm <sup>3</sup> /gm x 10 <sup>2</sup>	I <sub>T</sub> g mol. <sup>o</sup> K /cm <sup>3</sup>
	g mol/gm x 10 <sup>4</sup> 1	g mol/gm x 10 <sup>4</sup> 2	g mol/cm <sup>3</sup> x 10 <sup>5</sup> 1	g mol/cm <sup>3</sup> x 10 <sup>5</sup> 2		
70.0	4.43	8.51	5.66	0.61	7.15	25.59
150.0	6.82	10.65	12.01	1.29	9.67	21.37
300.0	9.96	12.23	22.59	2.43	12.32	17.83
500.0	12.60	12.99	36.34	3.88	14.31	15.22

TABLE 10

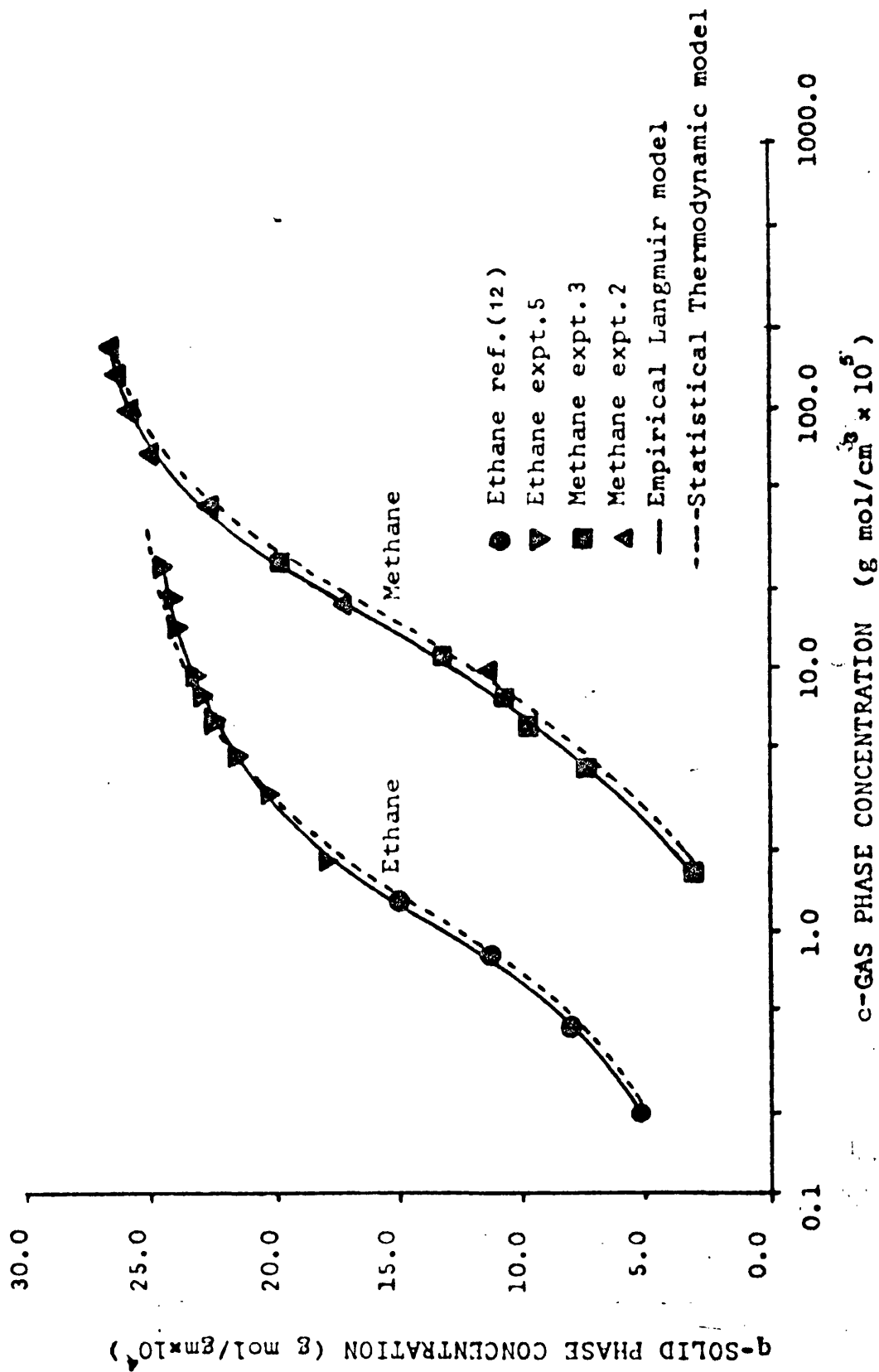


FIG. 15 SINGLE COMPONENT ISOTHERMAL ADSORPTION



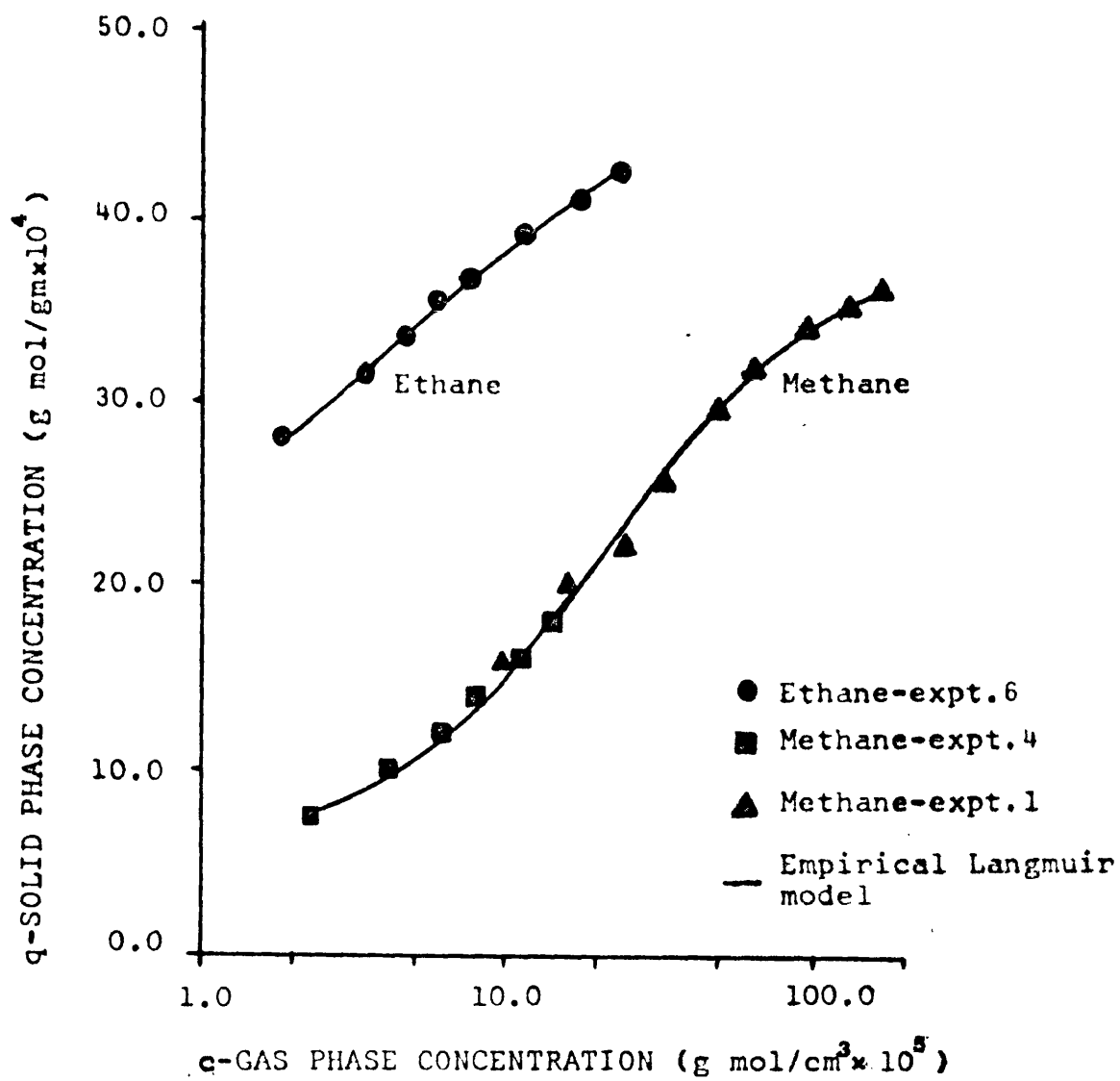
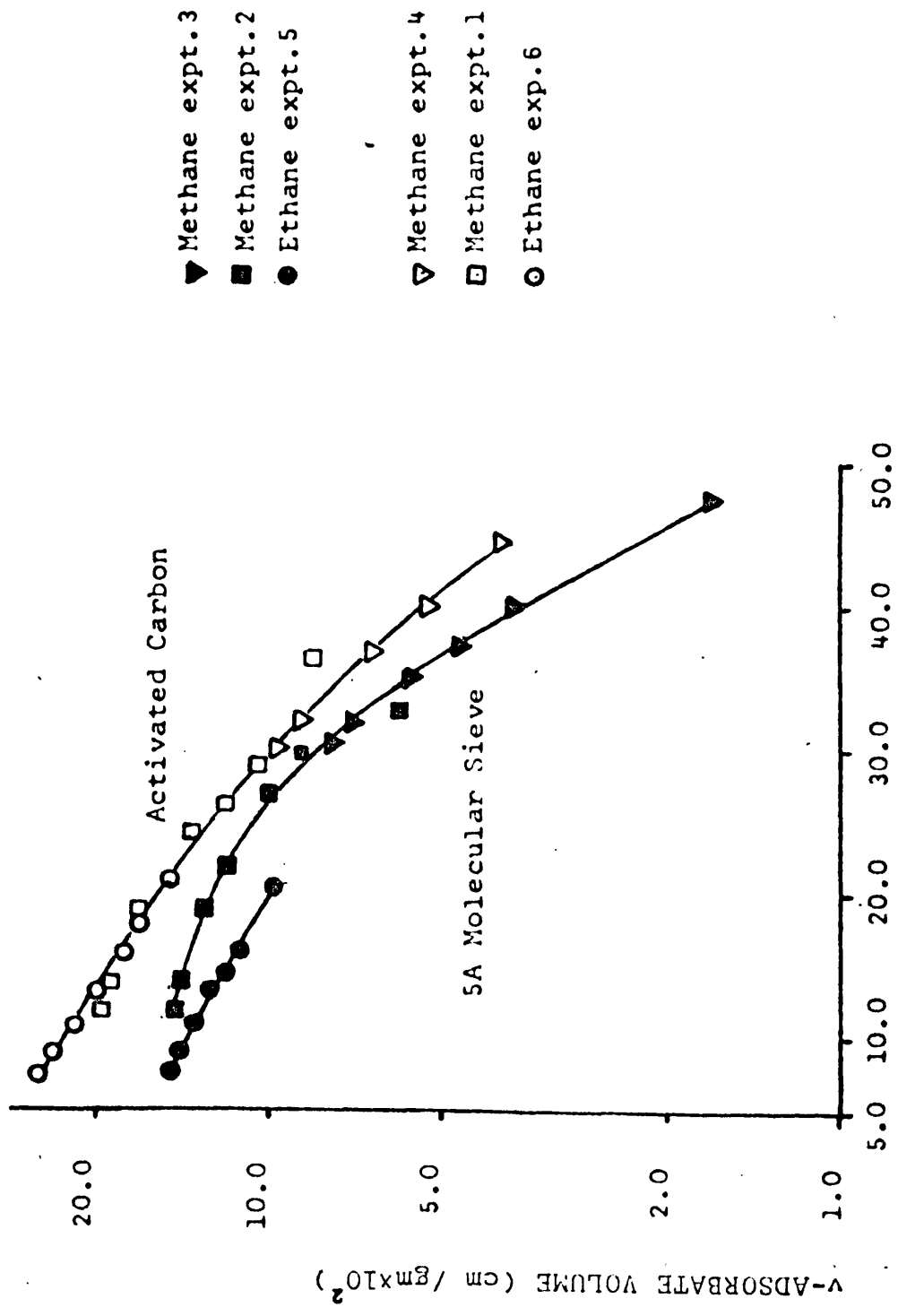


FIG. 16

SINGLE COMPONENT ISOTHERMS ON ACTIVATED CARBON



I-POLANYI ADSORPTION POTENTIAL (g mol<sup>-1</sup> K / cm<sup>3</sup>)

FIG. 17 SINGLE COMPONENT ISOTHERMAL ADSORPTION DATA CORRELATION WITH POLANYI

ADSORPTION POTENTIAL

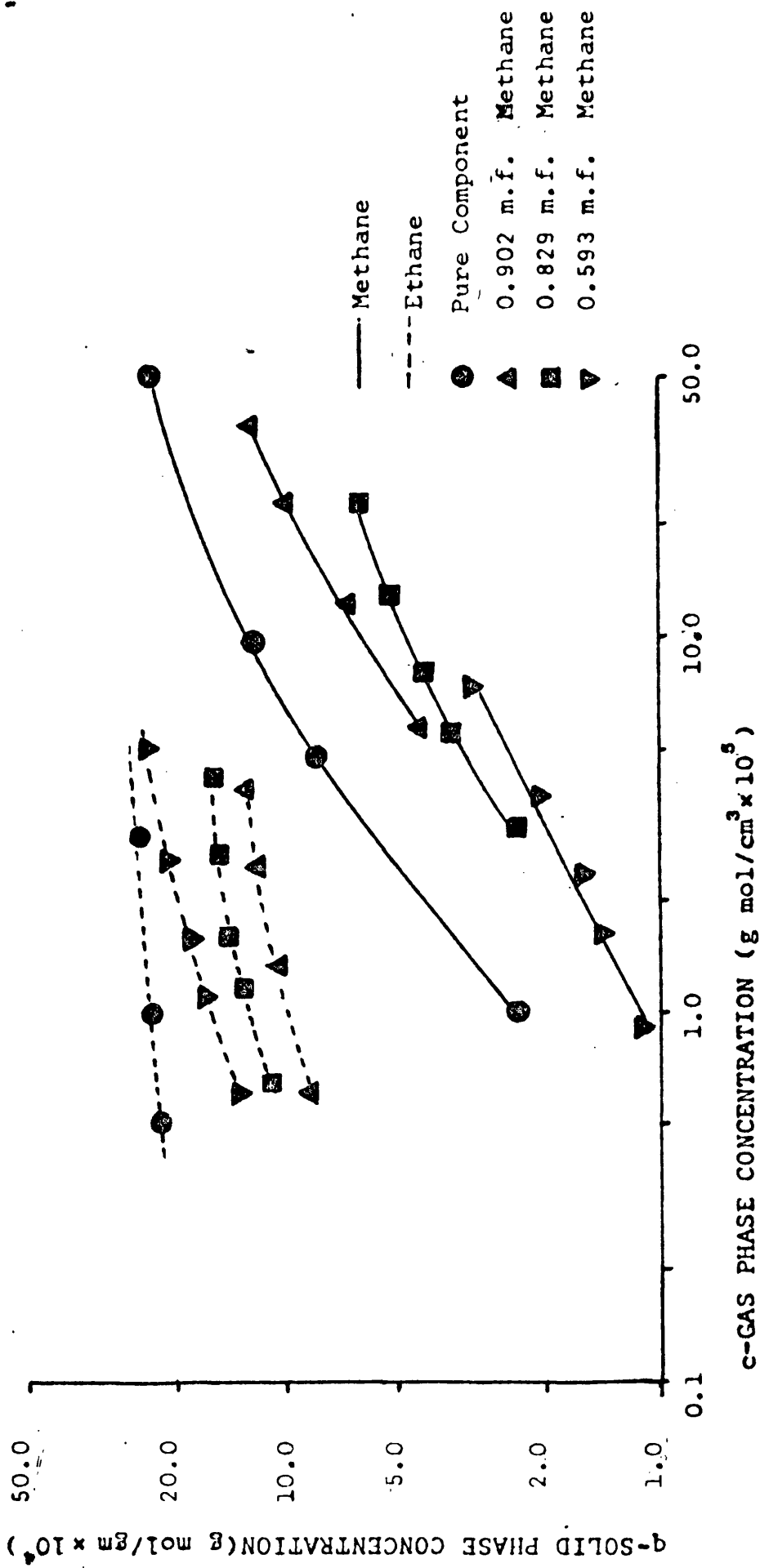


FIG. 18 BINARY AND SINGLE COMPONENT ISOTHERMAL DATA AND CORRELATION WITH SINGLE COMPONENT EMPIRICAL

LANGMUIR MODELS

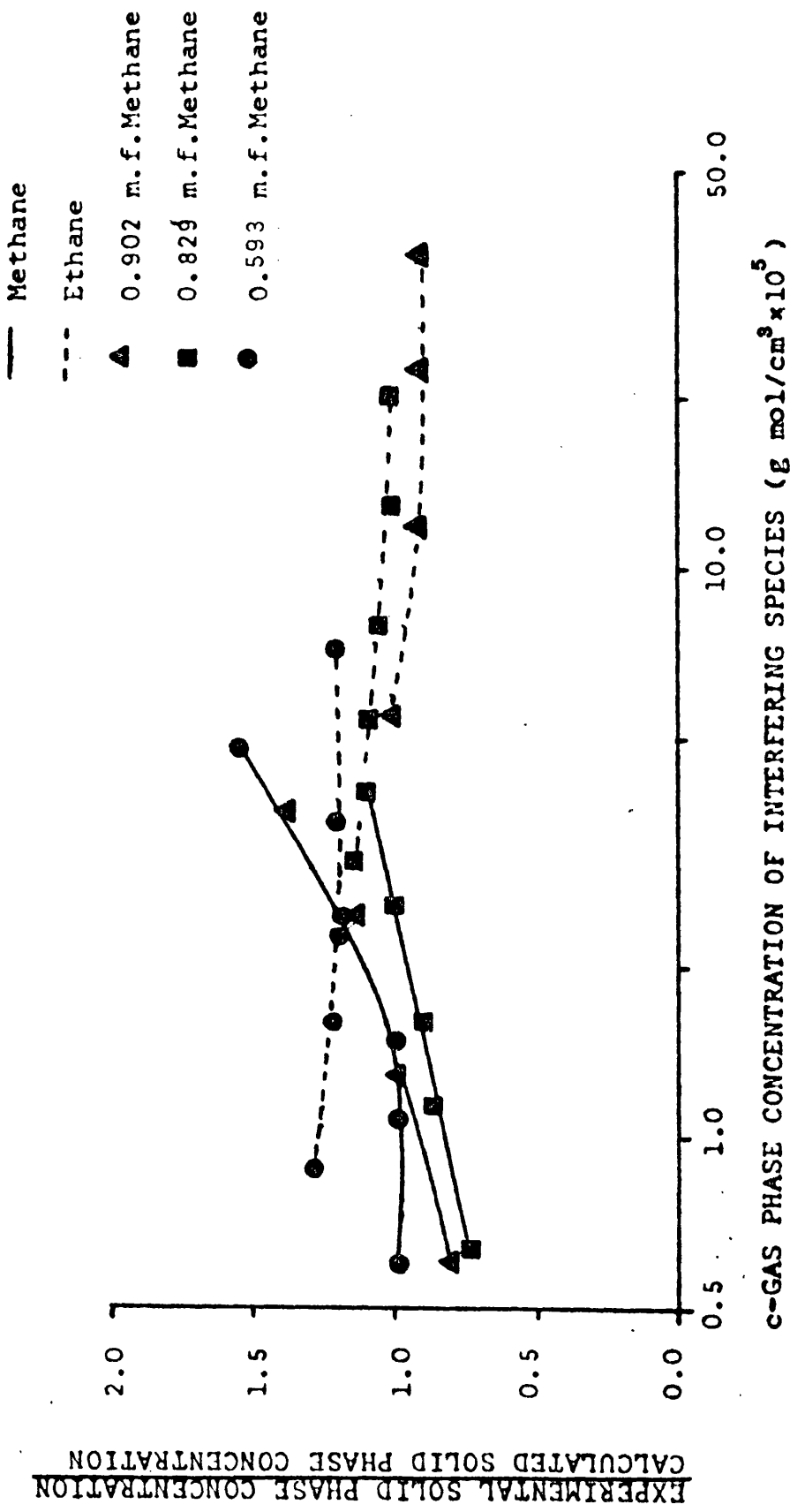


FIG. 19 BINARY ADSORPTION ISOTHERMAL DATA CORRELATION WITH EXTENDED EMPIRICAL LANGMUIR MODEL

EXPERIMENTAL SOLID PHASE CONCENTRATION  
CALCULATED SOLID PHASE CONCENTRATION

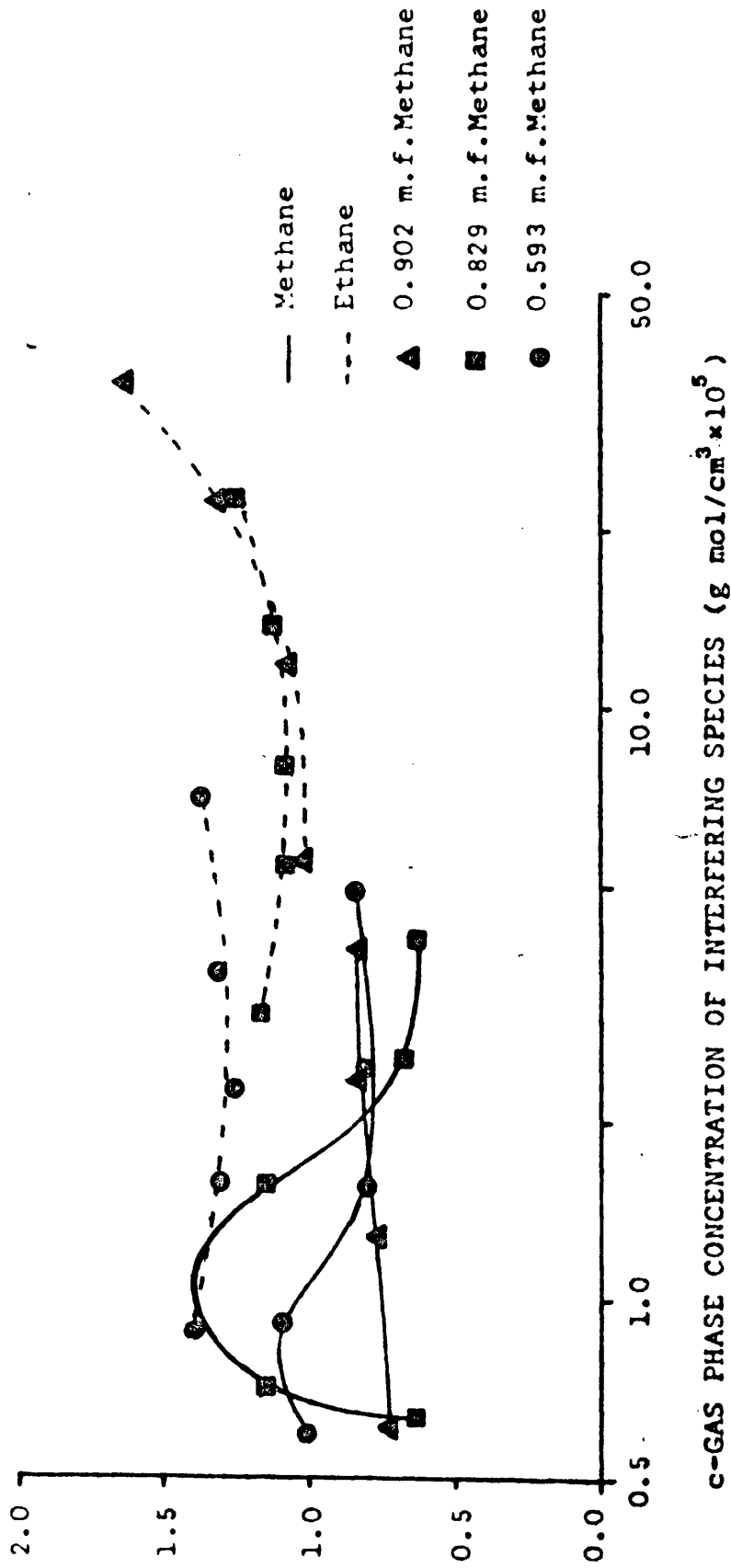


FIG. 20 BINARY ADSORPTION ISOTHERMAL DATA CORRELATION WITH KIDNAY-MEYERS MODEL

— Methane  
 - - - Ethane  
 ▼ 0.902 m. f. Methane  
 ■ 0.829 m. f. Methane  
 ▲ 0.593 m. f. Methane

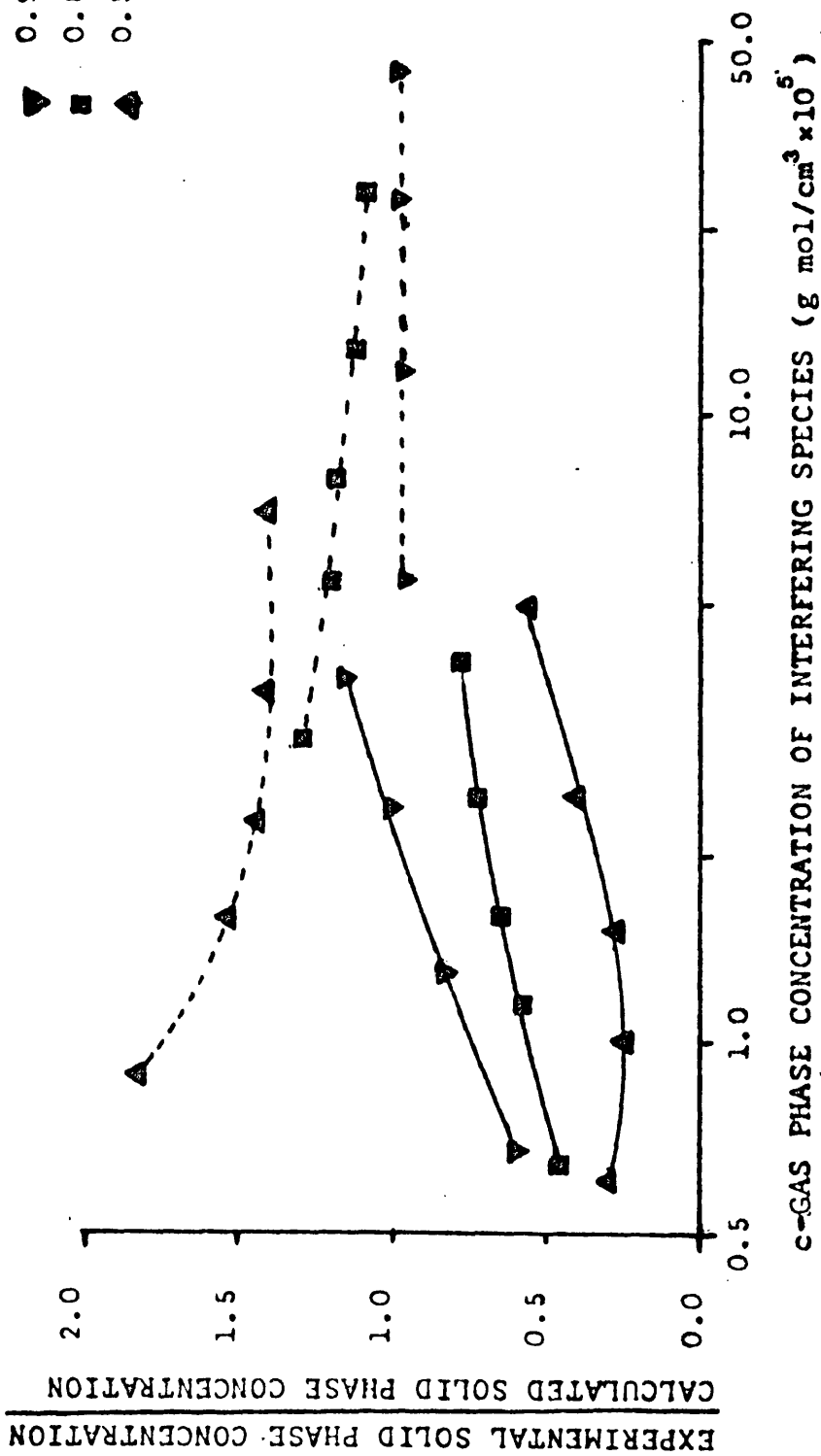
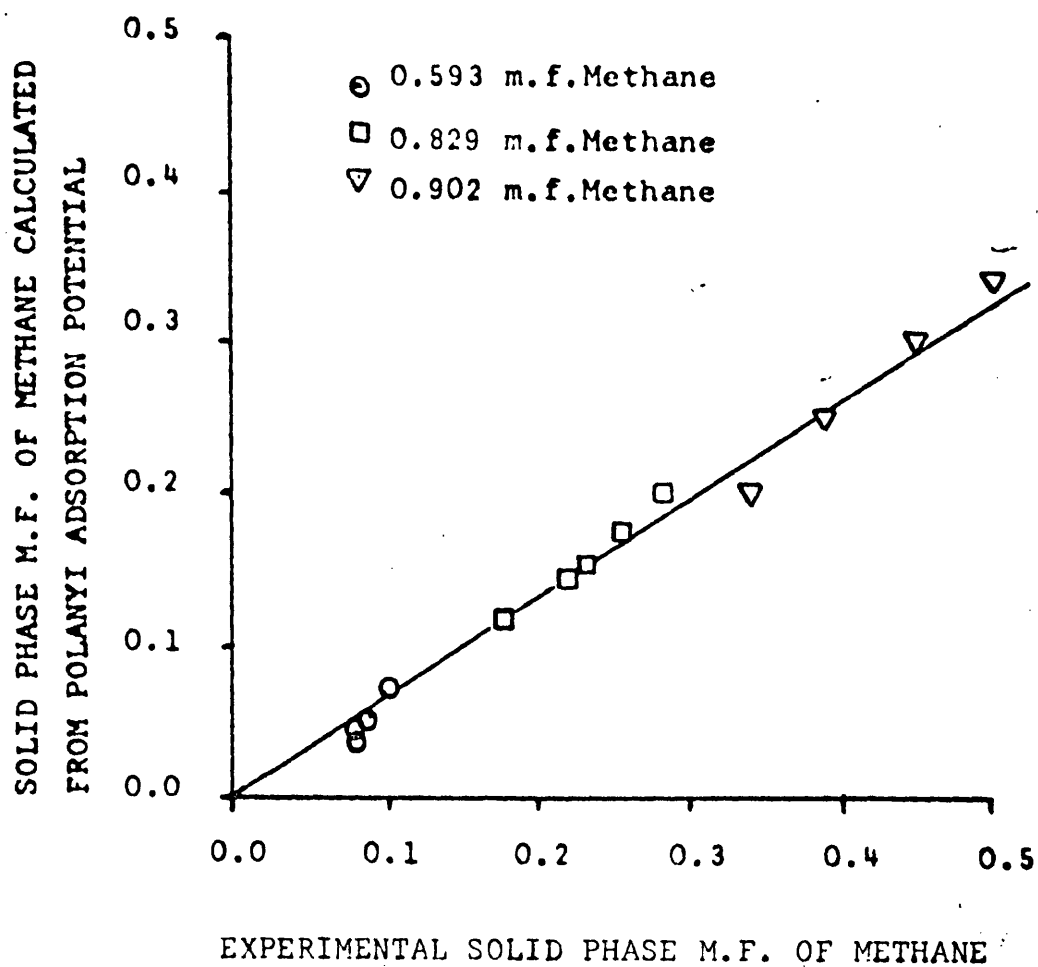


FIG.21 BINARY ADSORPTION ISOTHERMAL DATA CORRELATION WITH STATISTICAL THERMODYNAMIC MODEL



**FIG. 22** COMPARISON OF EXPERIMENTAL SOLID PHASE M.F. OF METHANE  
WITH THAT CALCULATED FROM THE POLANYI ADSORPTION POTENTIAL

STATISTICAL THERMODYNAMIC MODEL CONSTANTS

	METHANE	ETHANE	
$K_0$	$6.0 \times 10^{-7}$	$7.7 \times 10^{-7}$	molecule/cavity torr
$\Delta H_0$	5.1	6.6	kcal/g mol
$\beta$	77.0	90.0	$\text{\AA}^3$ /g mol

1 molecule/cavity=0.56mmol/gm anhydrous 5A  
molecular sieve crystal

Volume of a 5A molecular sieve cavity

$$\gamma = 776 \text{ \AA}^3$$

TABLE 11



SINGLE COMPONENT EMPIRICAL LANGMUIR MODEL CONSTANTS

on 5A sieve	A g. mol/gm $\times 10^4$	B cm <sup>3</sup> /g mol $\times 10^{-4}$
100% Methane	29.63	0.7415
90.2% Methane		
Methane	19.58	0.4773
Ethane	14.47	22.427
82.9% Methane		
Methane	8.84	1.221
Ethane	17.43	27.563
59.3% Methane		
Methane	4.57	2.754
Ethane	22.75	14.891
100% Ethane	25.39	12.400
on activated carbon		
100% Methane	39.00	6.287
100% Ethane	44.50	67.870

TABLE 12

SINGLE COMPONENT EMPIRICAL LANGMUIR COEFFICIENTS FOR METHANE

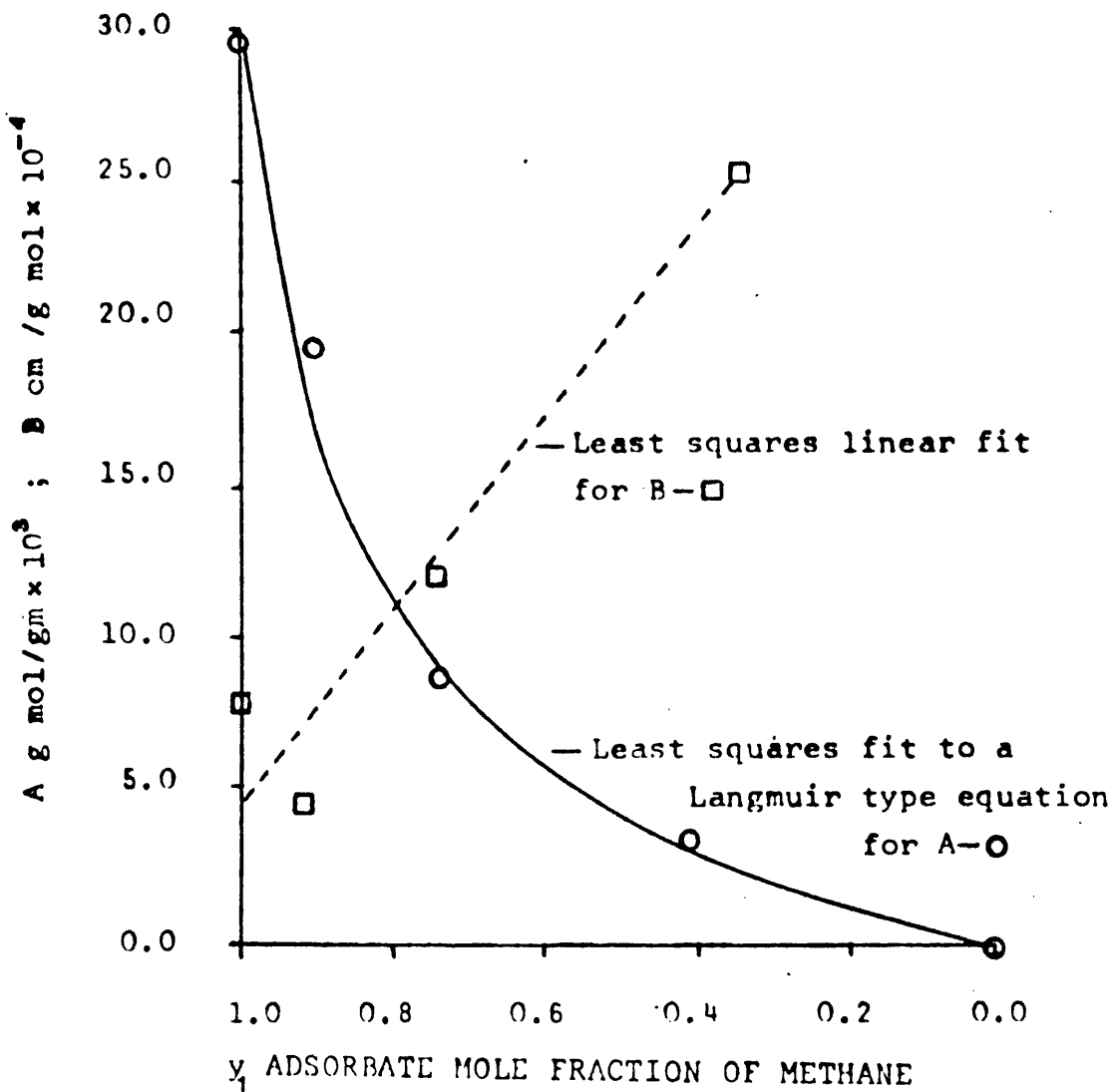


**FIG. 23** SINGLE COMPONENT EMPIRICAL LANGMUIR COEFFICIENTS  
FOR METHANE EXPRESSED AS A FUNCTION OF THE  
ADSORBATE MOLE FRACTION OF METHANE

SINGLE COMPONENT EMPIRICAL LANGMUIR COEFFICIENTS FOR ETHANE

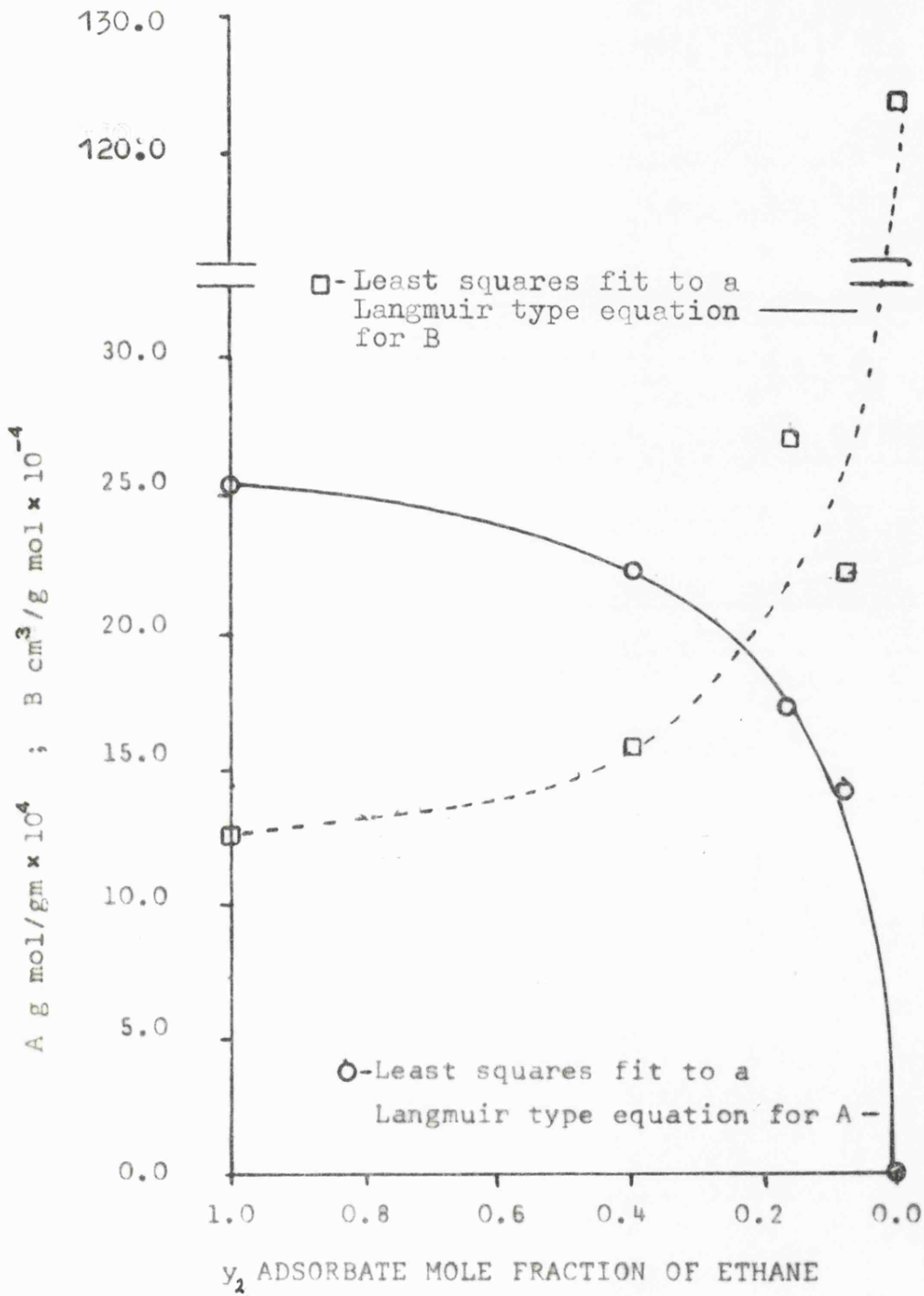


**FIG. 24** SINGLE COMPONENT EMPIRICAL LANGMUIR COEFFICIENTS  
FOR ETHANE EXPRESSED AS A FUNCTION OF THE  
ADSORBATE MOLE FRACTION OF ETHANE

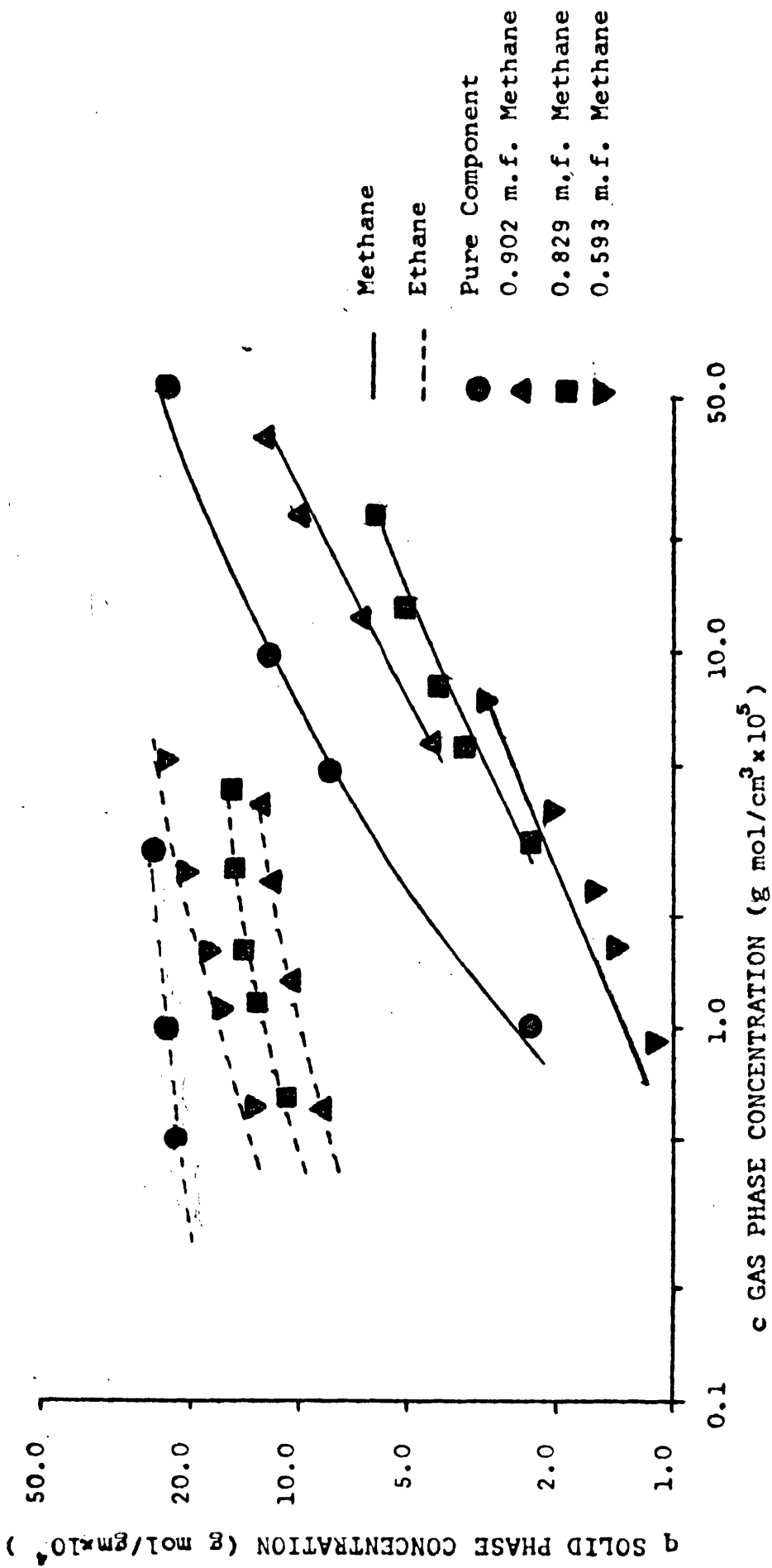
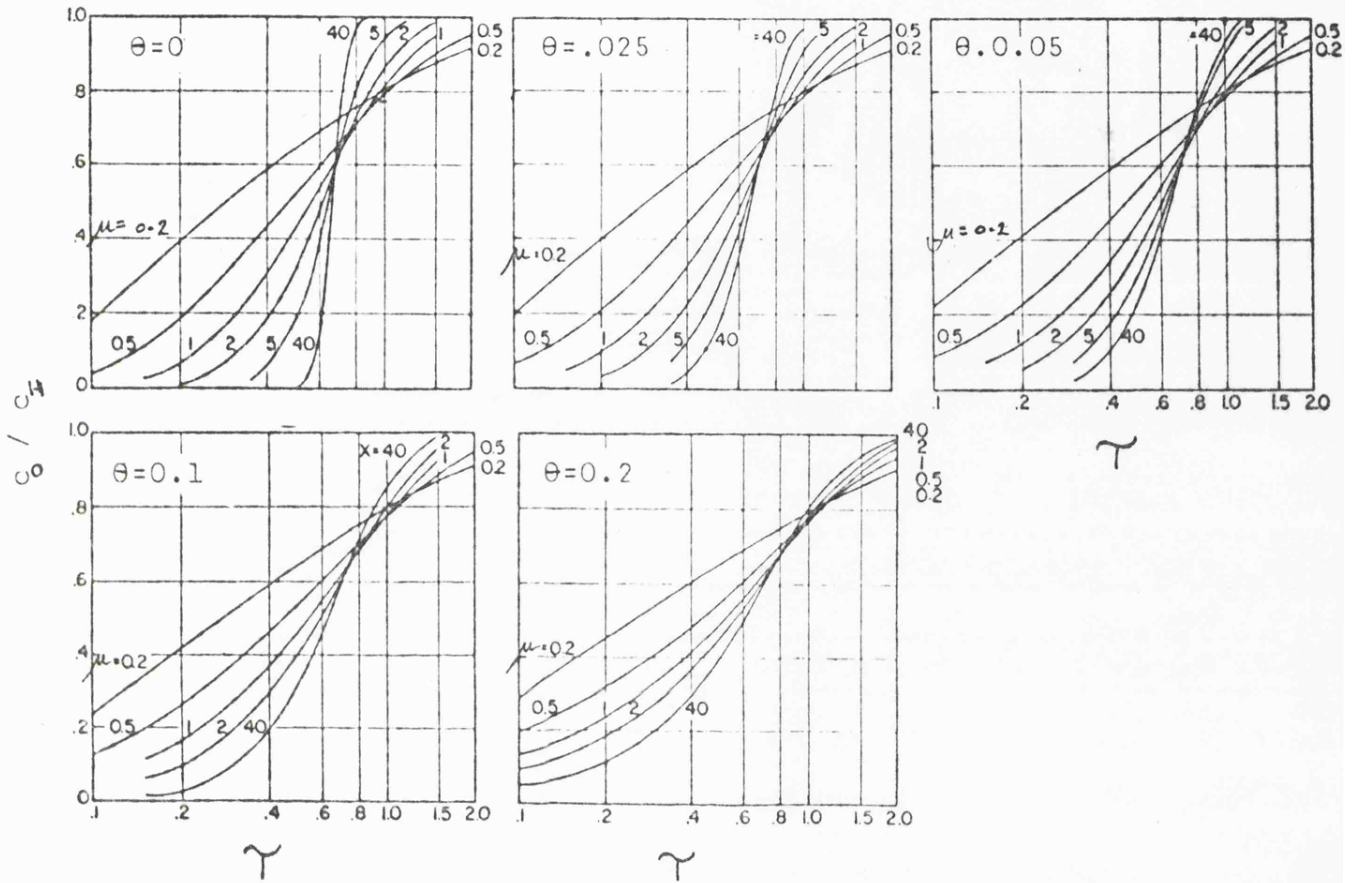


**FIG.25 BINARY AND SINGLE COMPONENT ISOTHERMAL DATA AND CORRELATION WITH MODIFIED COEFFICIENT**

SINGLE COMPONENT EMPIRICAL LANGMUIR MODEL



BED EFFLUENT FRACTIONAL RESPONSE VERSUS TIME PARAMETER  
FOR SELECTED VALUES OF BED LENGTH AND FILM RESISTANCE  
PARAMETERS (49)

FIG. 26

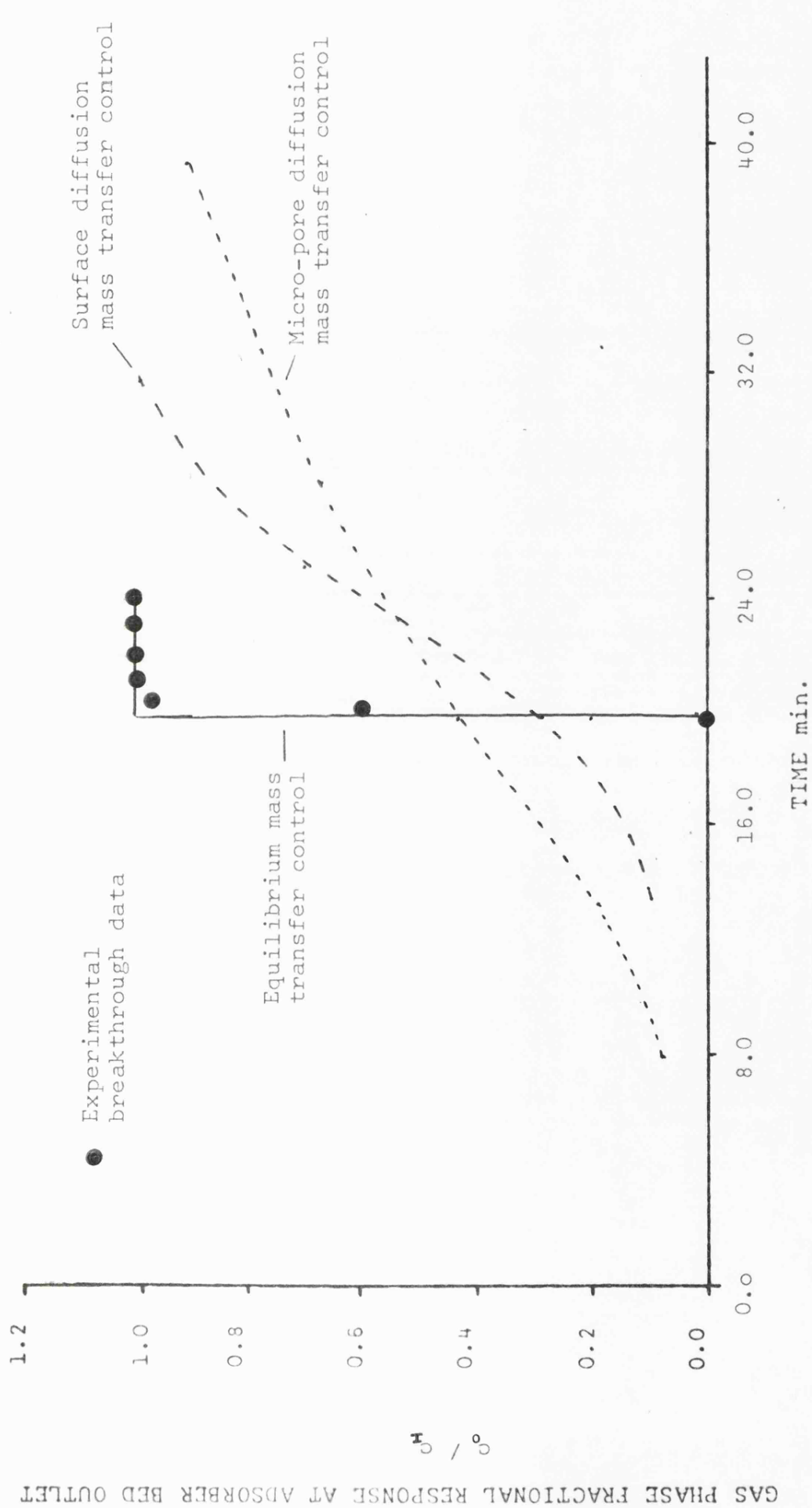


**FIG. 27** THE EFFECT OF MASS TRANSFER MECHANISM ON THE MODELLING OF FIXED BED BREAKTHROUGH  
 EXPERIMENT NO. 5 ETHANE ON SA MOLECULAR SIEVE,  $Y=0.0988$   $c = 1.18$  g mol/cm<sup>3</sup> × 10<sup>5</sup>

GAS PHASE FRACTIONAL RESPONSE AT ADSORBER BED OUTLET

$c/c_0$

TIME min.

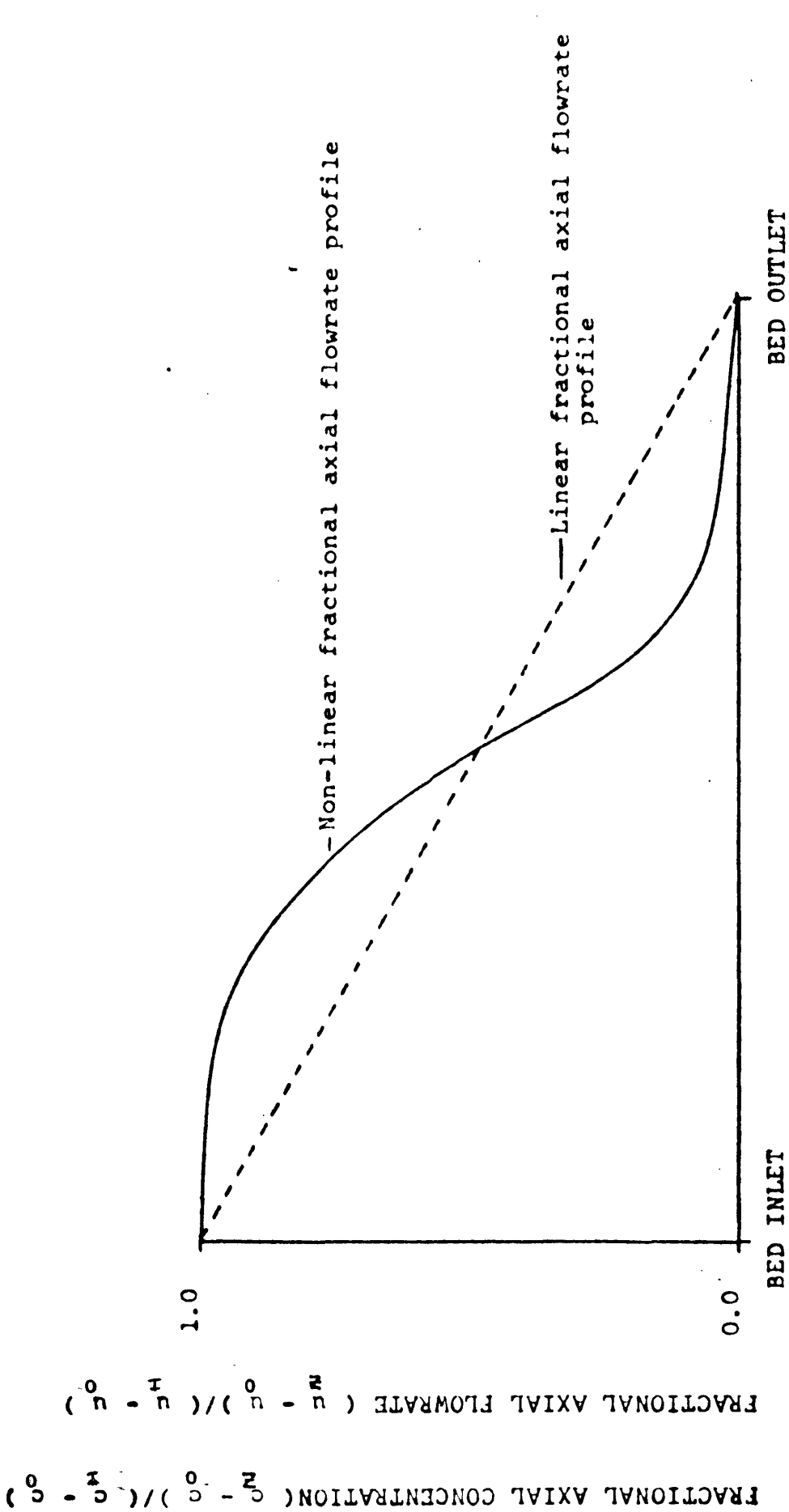


FIG. 28 ADSORBENT BED FRACTIONAL AXIAL FLOWRATE PROFILES

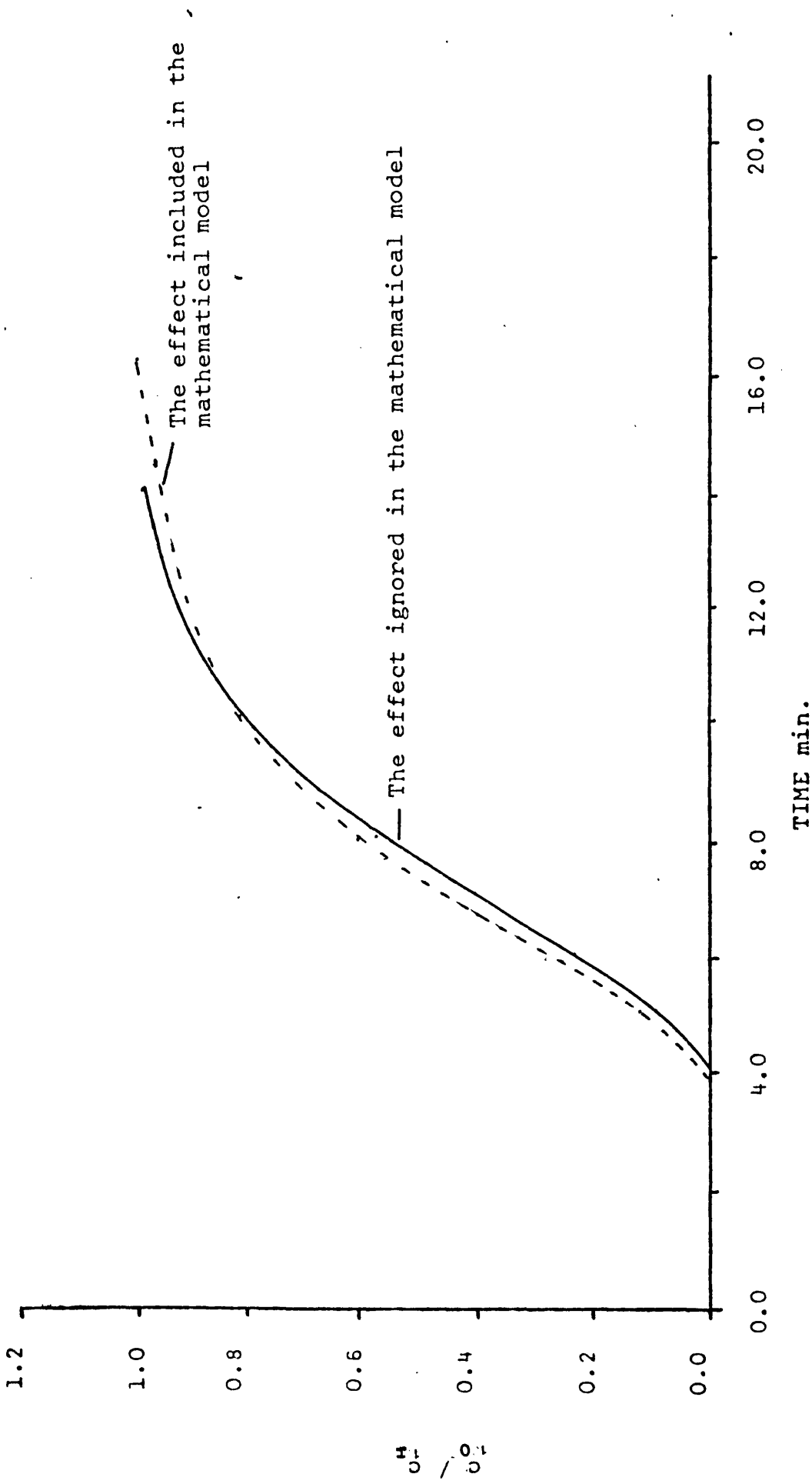


FIG. 29

THE EFFECT OF A CHANGE IN BED OUTLET FLOWRATE WITH OUTLET GAS PHASE COMPOSITION



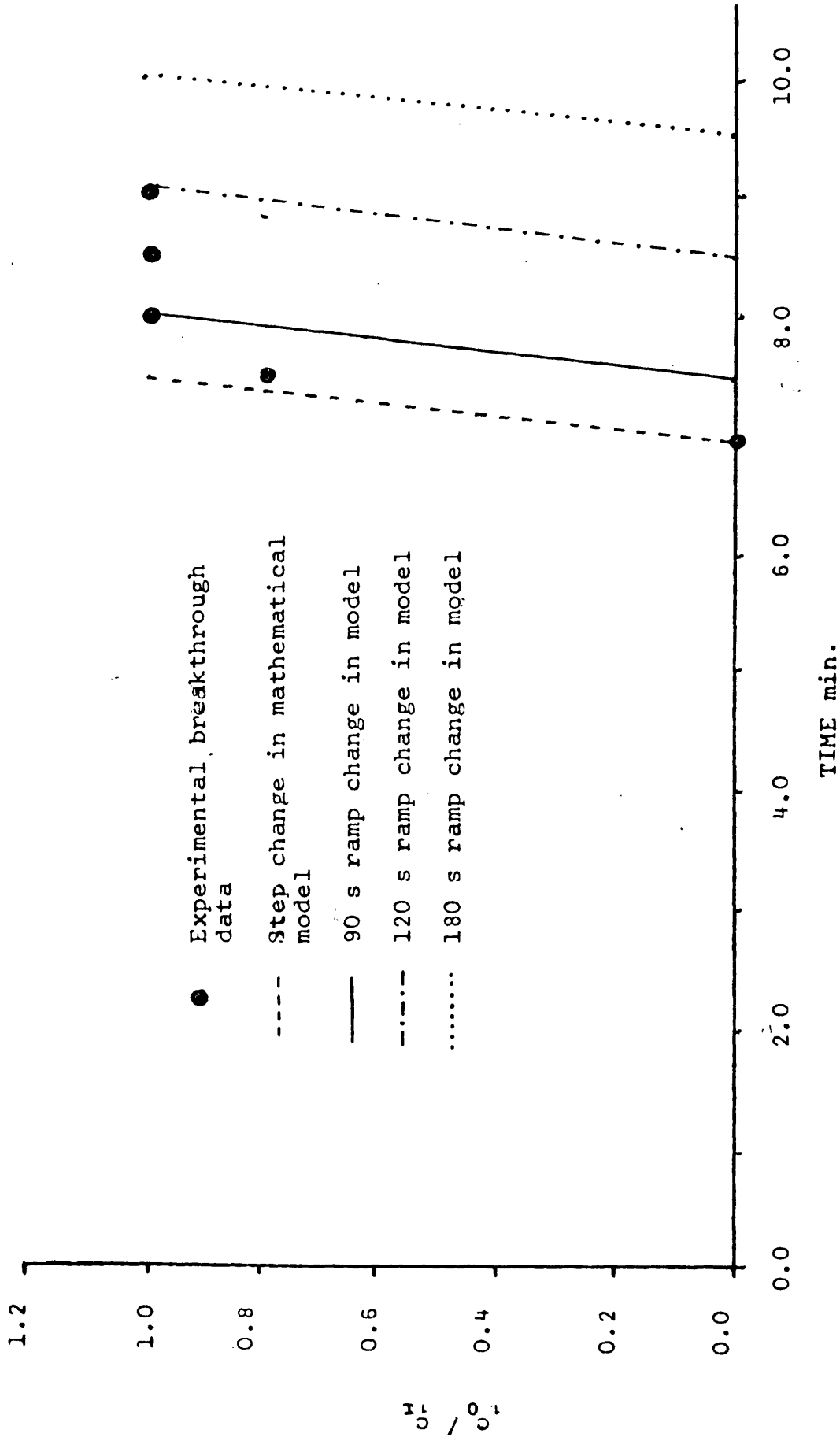


FIG.30

THE EFFECT OF A NON-STEP CHANGE IN BED INLET ADSORBATE CONCENTRATION, EXPT.NO.2

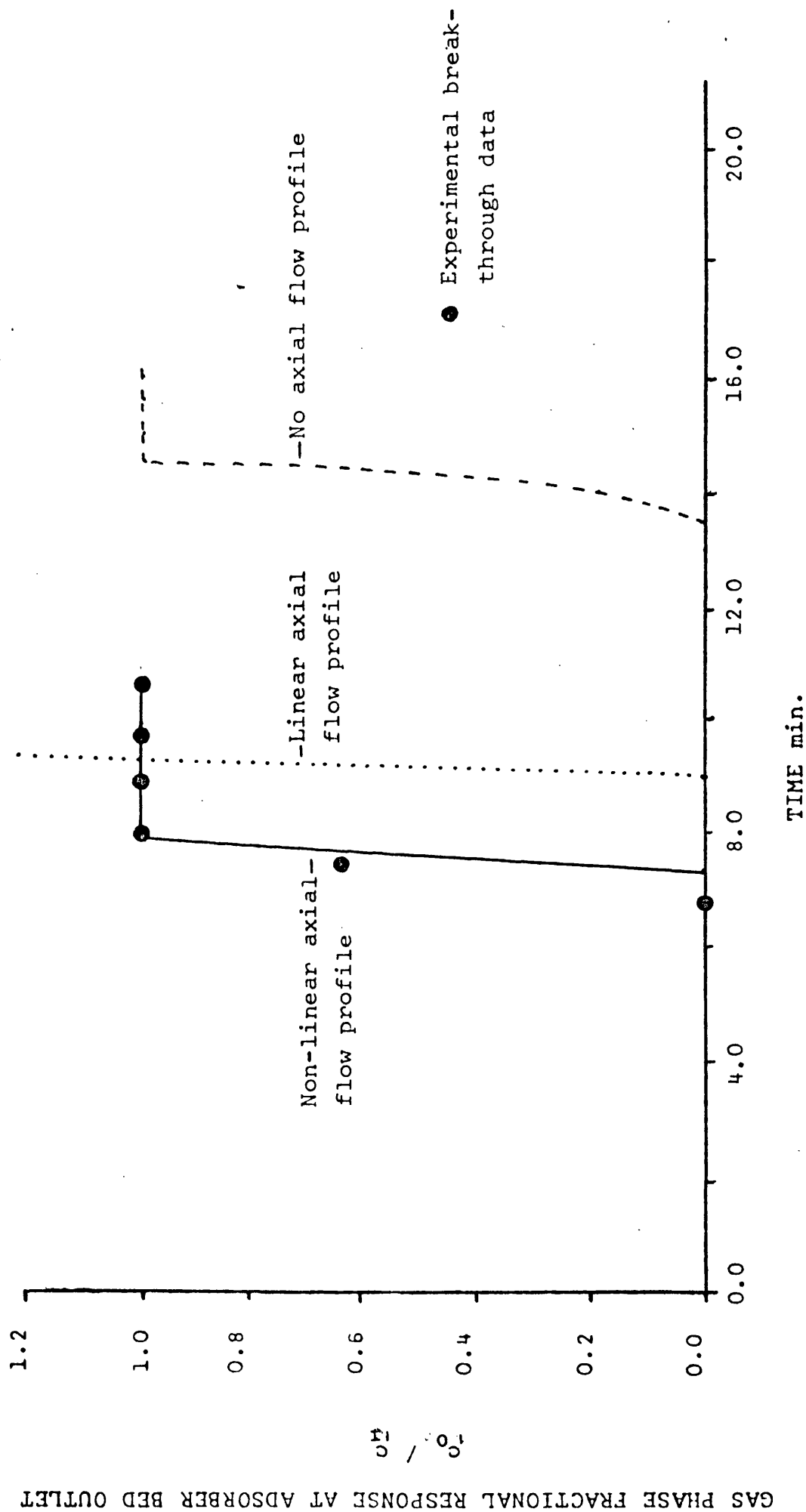


FIG. 31  
EXPERIMENT NO. 1 METHANE ON ACTIVATED CARBON,  $Y_1 = 0.537$ ,  $C_1 = 9.88 \text{ g mol/cm}^3 \times 10^5$

GAS PHASE FRACTIONAL RESPONSE AT ADSORBER BED OUTLET

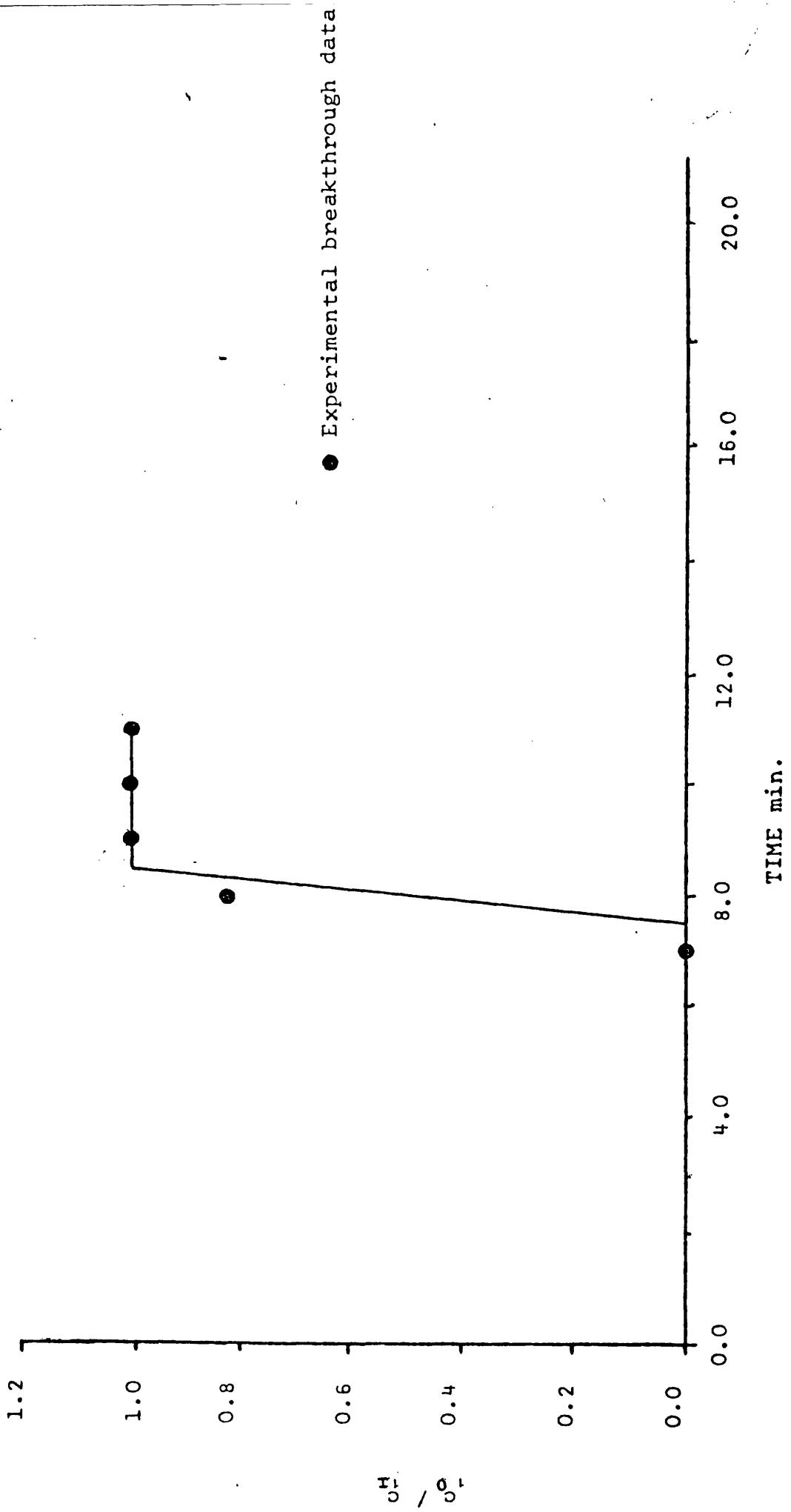


FIG.32

EXPERIMENT NO.2 METHANE ON 5A MOLECULAR SIEVE,  $\chi_1=0.553$ ,  $C_1=10.18 \text{ g mol/cm}^3 \times 10^5$

GAS PHASE FRACTIONAL RESPONSE AT ADSORBER BED OUTLET

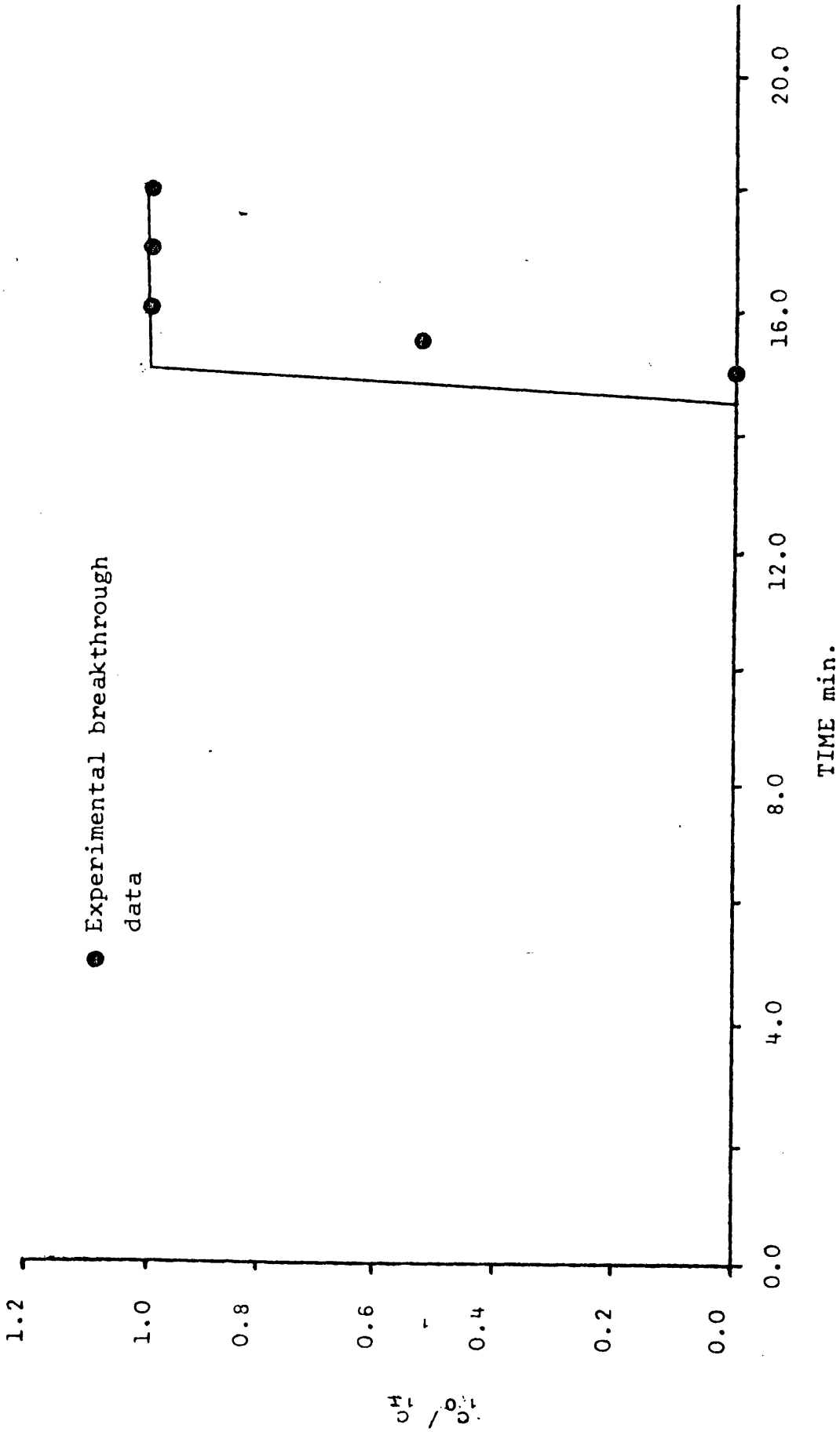


FIG. 33

EXPERIMENT NO. 3 METHANE ON 5A MOLECULAR SIEVE,  $Y_1=0.129$ ,  $C_1=1.64 \text{ g mol/cm}^3 \times 10^5$

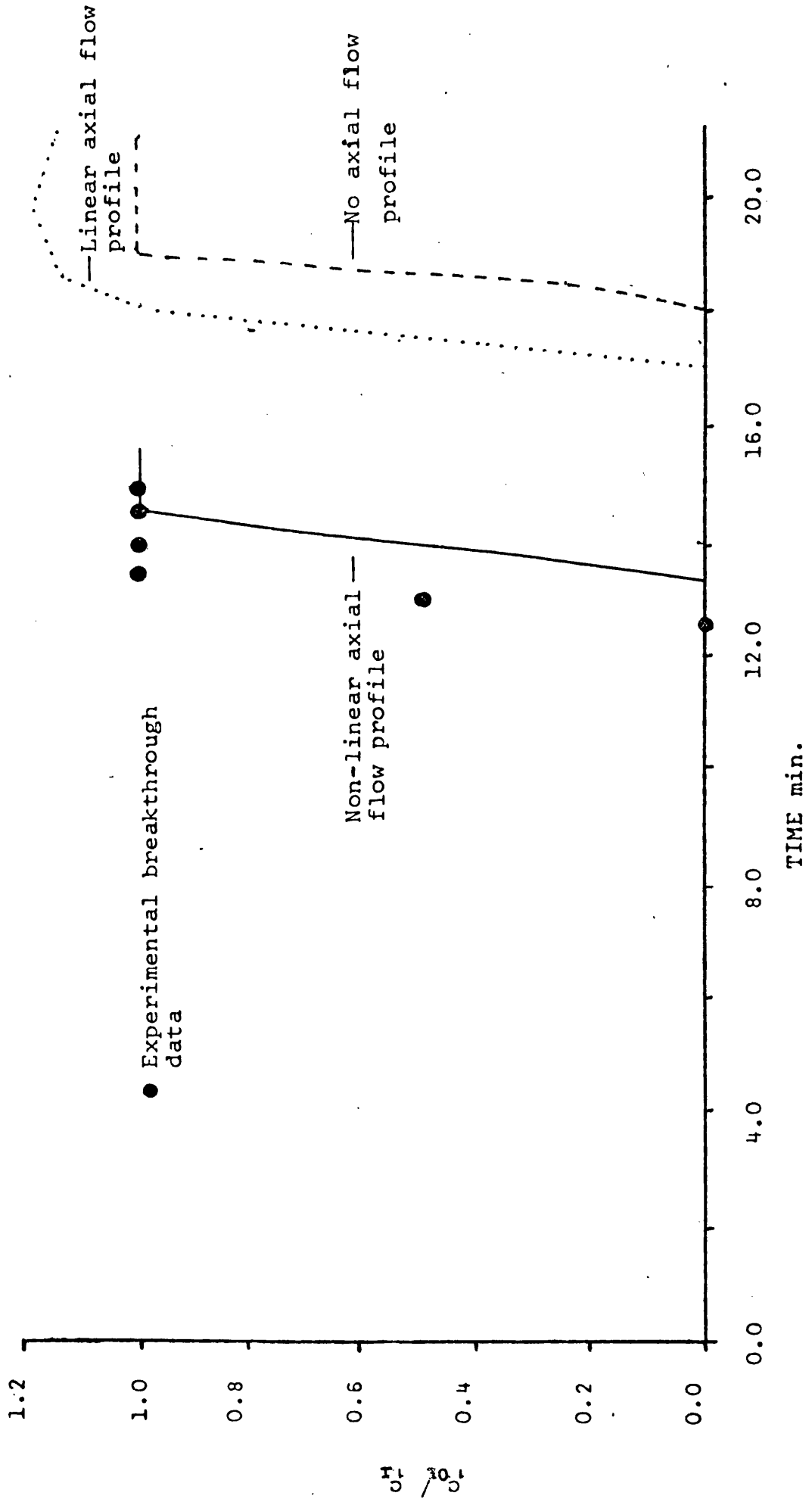


FIG.34 EXPERIMENT NO.4 METHANE ON ACTIVATED CARBON,  $Y_1=0.129$ ,  $C_s=2.37 \text{ g mol/cm}^3 \times 10^5$

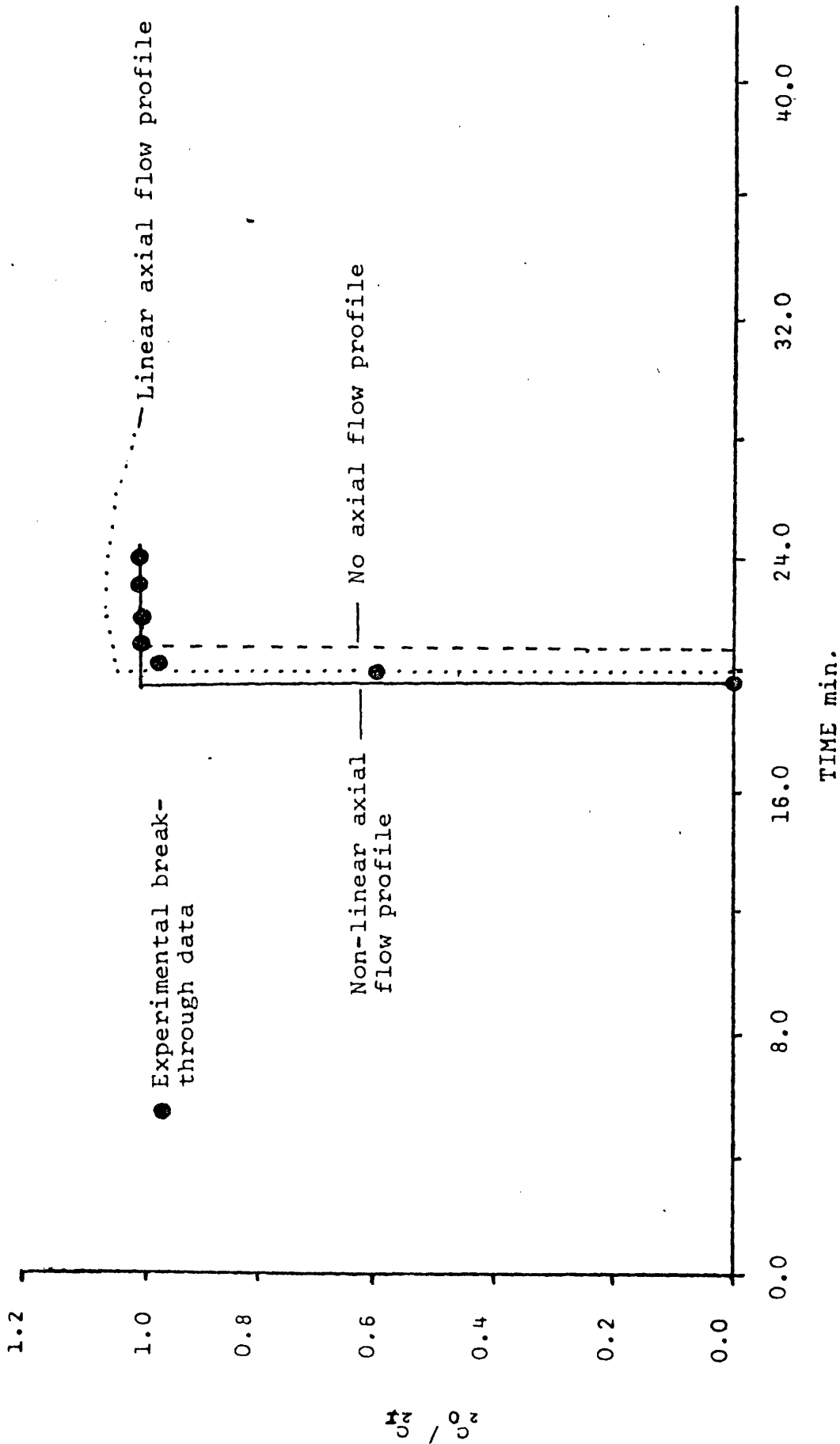


FIG.35 EXPERIMENT NO.5 ETHANE ON 5A MOLECULAR SIEVE,  $Y_2 = 0.0988$ ,  $C_2 = 1.18 \text{ g mol/cm}^3 \times 10^5$

GAS PHASE FRACTIONAL RESPONSE AT ADSORBER BED OUTLET

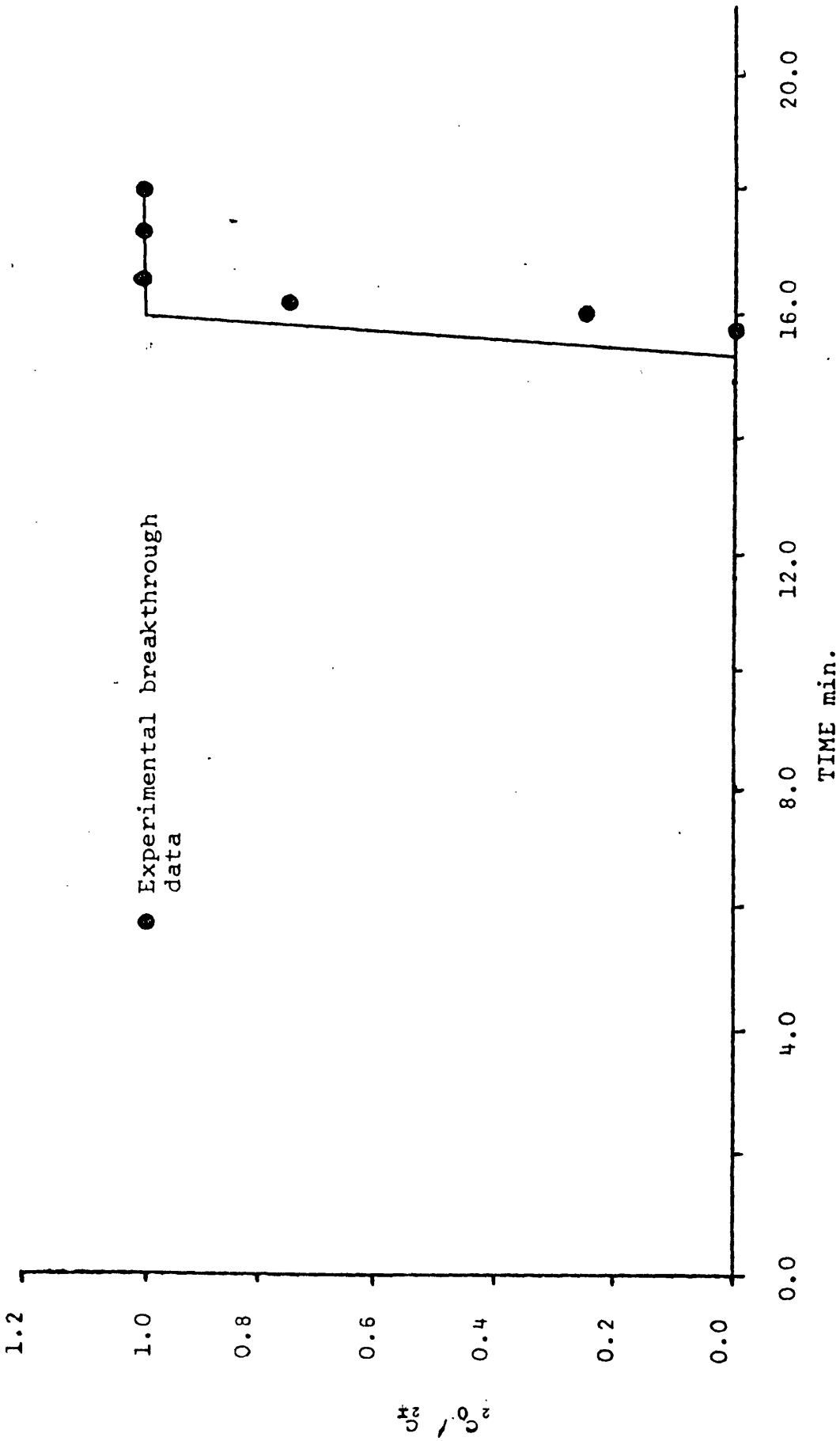
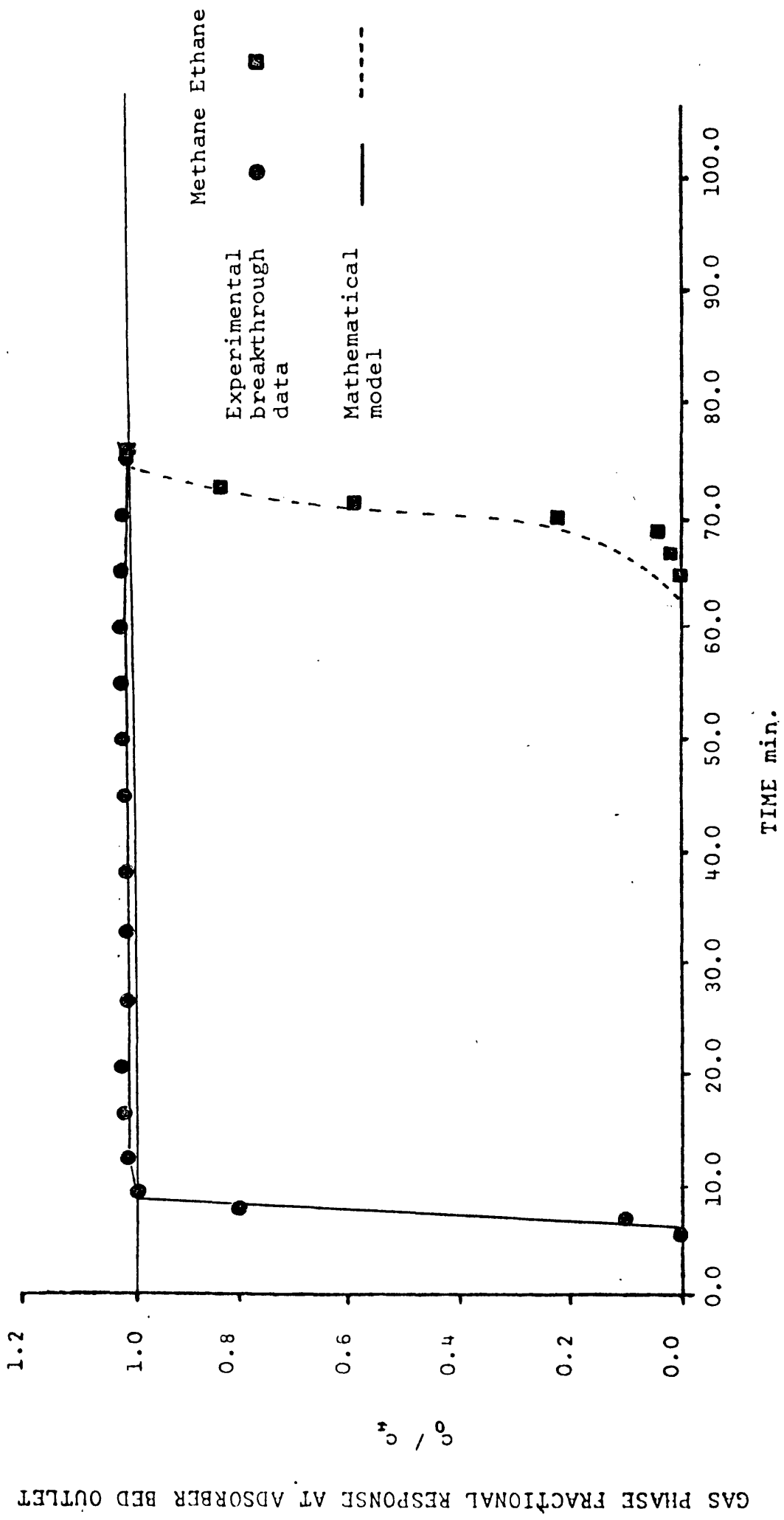


FIG.36

EXPERIMENT NO.6 ETHANE ON ACTIVATED CARBON,  $Y_2=0.0988$ ,  $C_2=1.81$  g mol/cm<sup>3</sup> × 10<sup>5</sup>



**FIG.37** EXPERIMENT NO.7 METHANE-ETHANE ON 5A MOLECULAR SIEVE,  $Y=0.205$ ,  $C_0=3.11$ ,  $C_1=0.64$  g mol/cm<sup>3</sup>10<sup>5</sup>



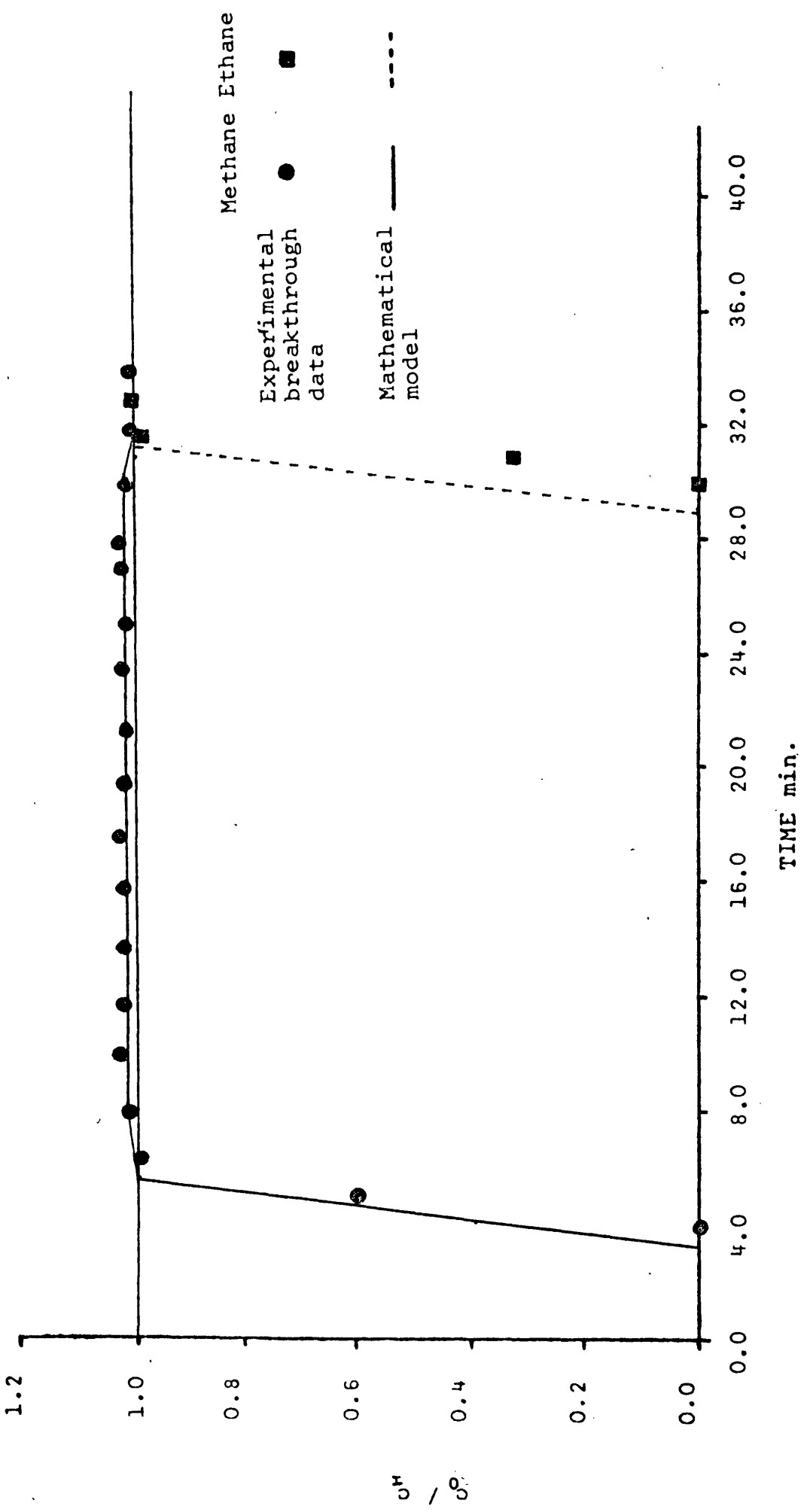


**FIG.38** EXPERIMENT NO.8 METHANE-ETHANE ON 5A MOLECULAR SIEVE,  $Y=0.082$ ,  $C_1=0.98$ ,  $C_2=0.61$  g mol/cm<sup>3</sup>10<sup>5</sup>

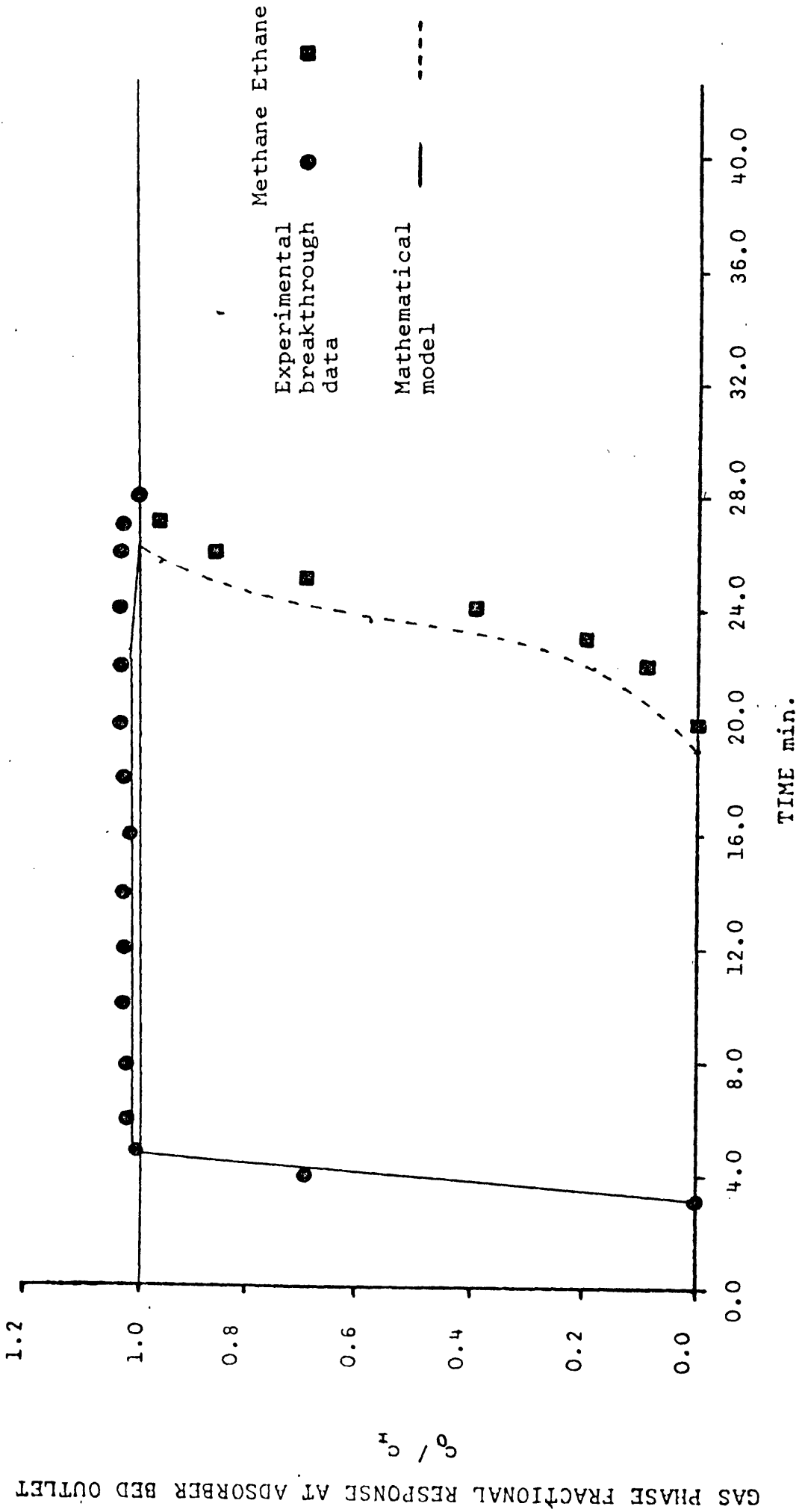


FIG.3.9 EXPERIMENT NO. 9 METHANE ETHANE ON 5A MOLECULAR SIEVE,  $Y=0.270$ ,  $C_1=5.66$ ,  $C_2=0.61$  g mol/cm<sup>3</sup>10<sup>5</sup>

EXPERIMENT NO. 10

SYSTEM: METHANE ETHANE ON 5A MOLECULAR SIEVE

ADSORBATE M.F. IN TOTAL FLOW: 0.0129

M.F. METHANE IN ADSORBATE: 0.743

ADSORPTION TEMPERATURE: 20.0 C

WEIGHT OF ADSORBENT: 3.022 gm

INITIAL OUTLET FLOWRATE: 187.0 cm<sup>3</sup>/min

FINAL OUTLET FLOWRATE:

ADSORPTION CELL TOTAL PRESSURE: 50.0 psig

GAS PHASE ADSORBATE CONCENTRATIONS AT BED INLET

$c_{1i}$ -METHANE	$c_{2i}$ -ETHANE	
0.222	0.0767	g mol/cm <sup>3</sup> × 10 <sup>5</sup>

TABLE 13

EXPERIMENT NO. 11

SYSTEM: METHANE ETHANE ON 5A MOLECULAR SIEVE

ADSORBATE M.F. IN TOTAL FLOW: 0.0129

M.F. METHANE IN ADSORBATE: 0.743

ADSORPTION TEMPERATURE: 20.0°C

WEIGHT OF ADSORBENT: 3.022 gm

INITIAL OUTLET FLOWRATE: 100.0 cm<sup>3</sup>/min

FINAL OUTLET FLOWRATE:

ADSORPTION CELL TOTAL PRESSURE: 50.0 psig

GAS PHASE ADSORBATE CONCENTRATIONS AT BED INLET

$c_{1i}$ -METHANE	$c_{2i}$ -ETHANE	
0.222	0.0767	g mol/cm <sup>3</sup> × 10 <sup>5</sup>

TABLE 14

EXPERIMENT NO. 12

SYSTEM: METHANE ETHANE ON 5A MOLECULAR SIEVE

ADSORBATE M.F. IN TOTAL FLOW: 0.185

M.F. METHANE IN ADSORBATE: 0.856

ADSORPTION TEMPERATURE: 20.0<sup>0</sup> C

WEIGHT OF ADSORBENT: 3.022 gm

INITIAL OUTLET FLOWRATE: 200.0 cm<sup>3</sup>/min

FINAL OUTLET FLOWRATE:

ADSORPTION CELL TOTAL PRESSURE: 50.0 psig

GAS PHASE ADSORBATE CONCENTRATIONS AT BED INLET

$\frac{C_1}{1}$ -METHANE	$\frac{C_2}{2}$ -ETHANE	
3.65	0.61	g mol/cm <sup>3</sup> × 10 <sup>5</sup>

TABLE 15

EXPERIMENT NO.13

SYSTEM: METHANE ETHANE ON 5A MOLECULAR SIEVE

ADSORBATE M.F. IN TOTAL FLOW: 0.185

M.F. METHANE IN ADSORBATE: 0.856

ADSORPTION TEMPERATURE: 20.0° C

WEIGHT OF ADSORBENT: 3.022 gm

INITIAL OUTLET FLOWRATE: 100.0 cm<sup>3</sup>/min

FINAL OUTLET FLOWRATE:

ADSORPTION CELL TOTAL PRESSURE: 50.0 psig

GAS PHASE ADSORBATE CONCENTRATIONS AT BED INLET

$c_1$ -METHANE	$c_2$ -ETHANE	
3.65	0.61	g mol/cm <sup>3</sup> *10 <sup>5</sup>

TABLE 16

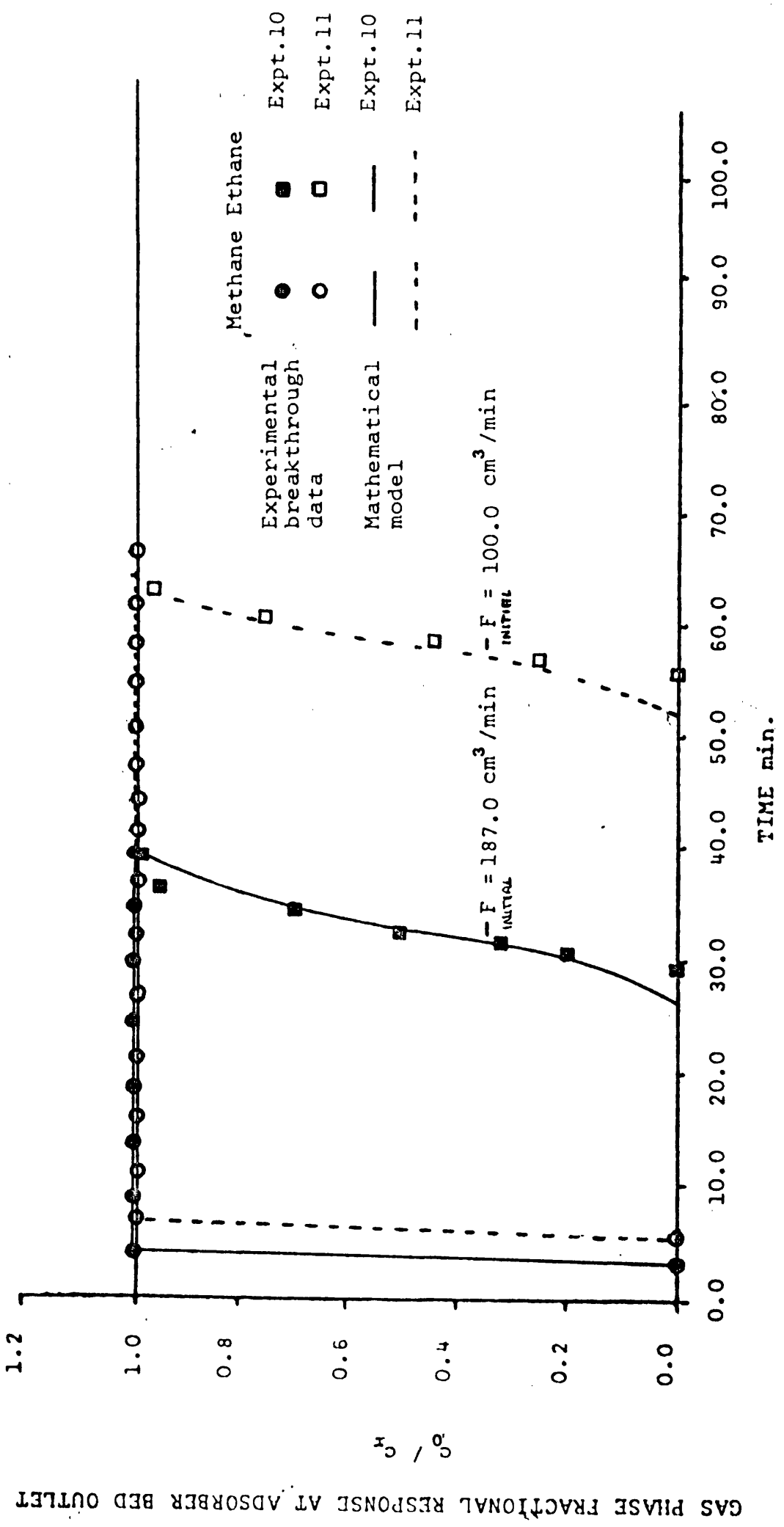


FIG.40 EXPERIMENTS NO.10,11 METHANE-ETHANE ON 5A MOLECULAR SIEVE,  $Y_T = 0.0129$ ,  $S_T = 0.222$ ,  $S_T = 0.0767$   
 $\frac{g}{mol} / \frac{cm^3}{cm^3} \times 10^5$

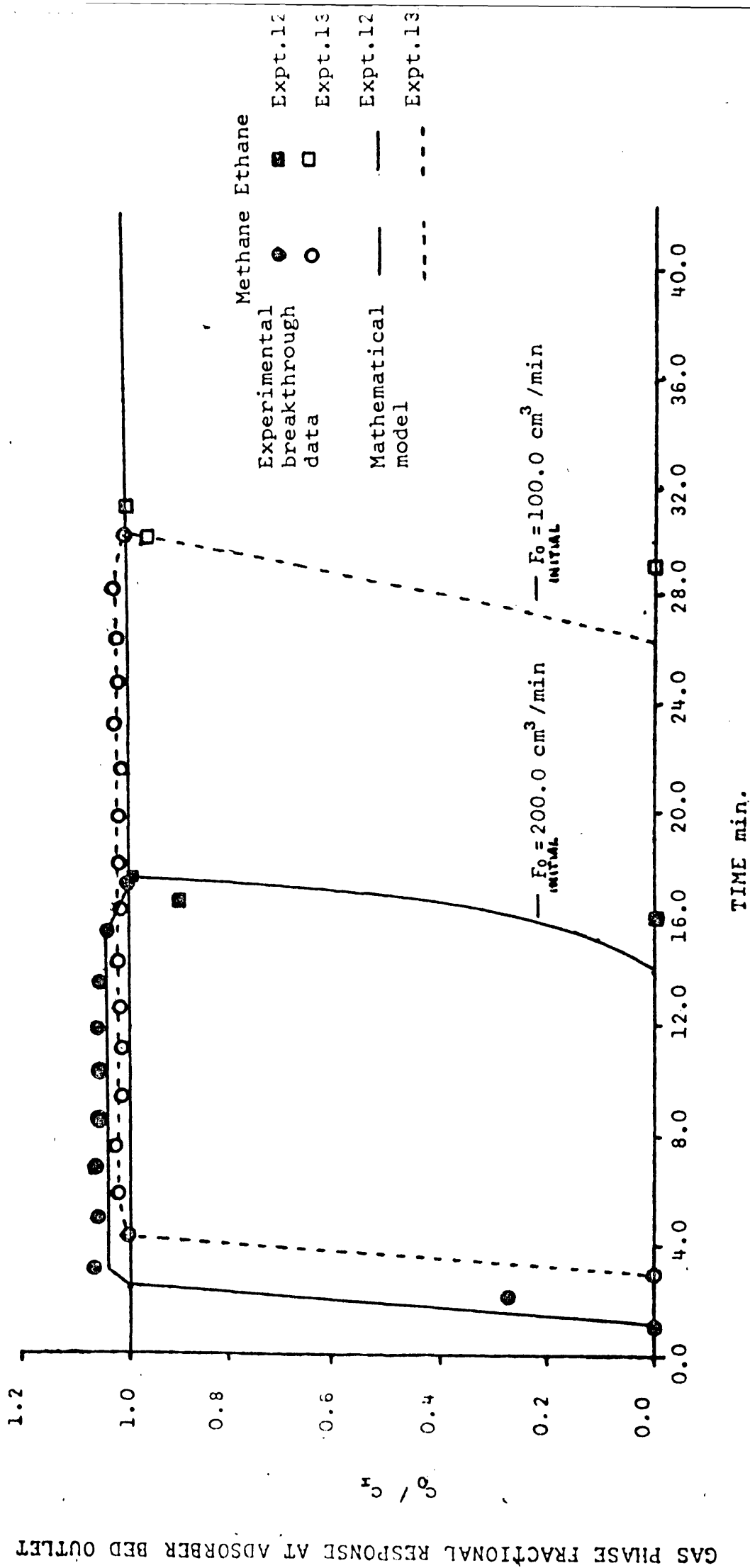


FIG. 41 EXPERIMENTS NO. 12, 13 METHANE-ETHANE ON 5A MOLECULAR SIEVE,  $Y = 0.1846$ ,  $C_2 = 3.65$ ,  $C_1 = 0.61$  g mol/cm<sup>3</sup> × 10<sup>5</sup>



GAS PHASE			ADSORBED PHASE
CONCENTRATION		MOLE FRACTION	MOLE FRACTION
METHANE	ETHANE	METHANE	ETHANE
gmol/cm <sup>3</sup> × 10 <sup>5</sup>			
15.07	0.446	0.97	0.31
4.19	0.446	0.90	0.67
1.39	0.446	0.75	0.87
0.446	0.446	0.50	0.97

TABLE.17

EXPERIMENT NO. 14,15,16

SYSTEM: METHANE-ETHANE ON 5A MOLECULAR SIEVE

ADSORBATE M.F. IN TOTAL FLOW: 0.055

M.F. METHANE IN ADSORBATE: 0.535

ADSORPTION TEMPERATURE: 20.0°C

WEIGHT OF ADSORBENT: 1.105 gm

INITIAL OUTLET FLOWRATE: 50.0 cm<sup>3</sup> / min

FINAL OUTLET FLOWRATE: 50.0 cm<sup>3</sup> / min

ADSORPTION CELL TOTAL PRESSURE: 50.5 psig.

GAS PHASE ADSORBATE CONCENTRATIONS AT BED INLET

c -METHANE	c -ETHANE	
0.536	0.466	g mol/cm <sup>3</sup> × 10 <sup>5</sup>

TABLE 18

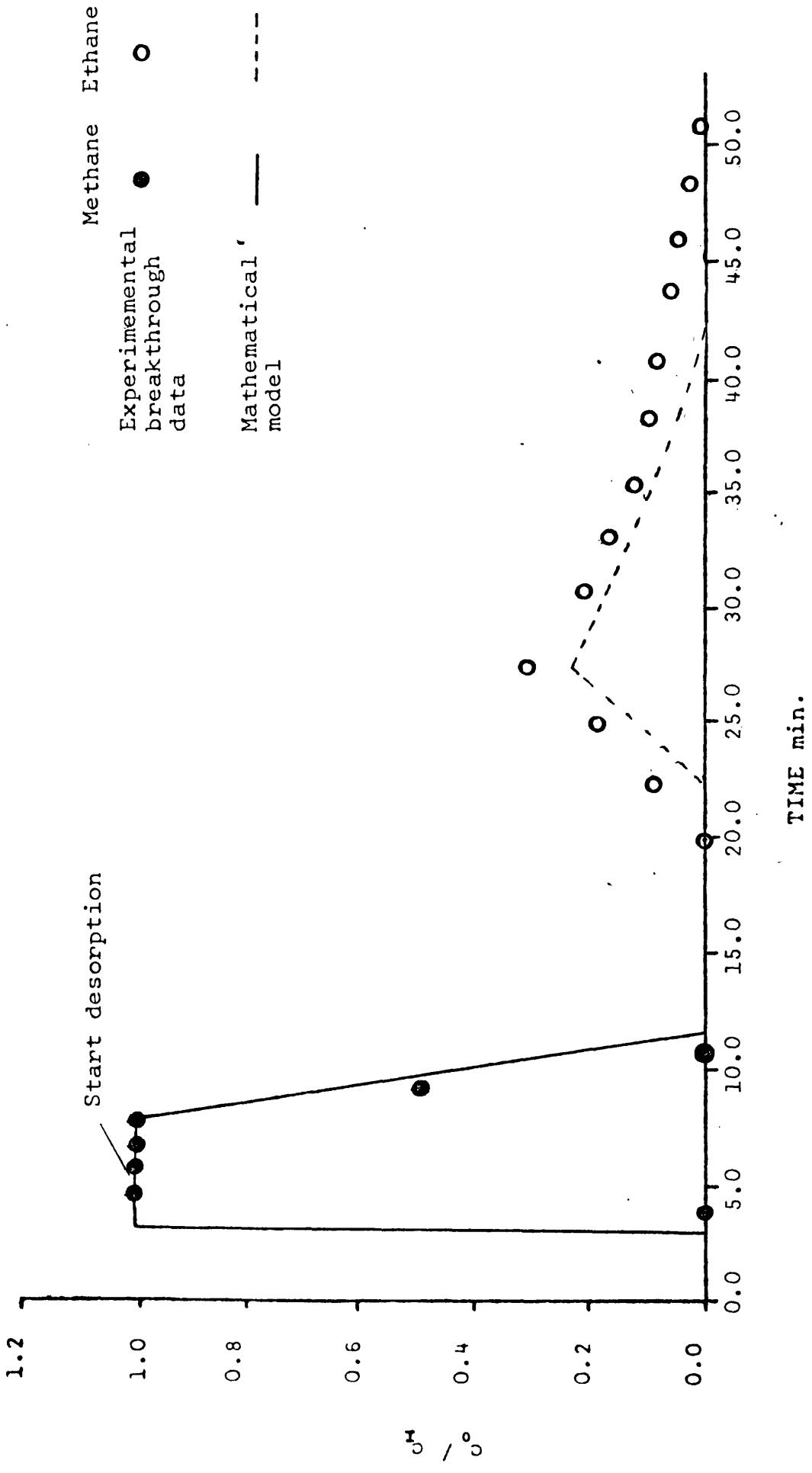
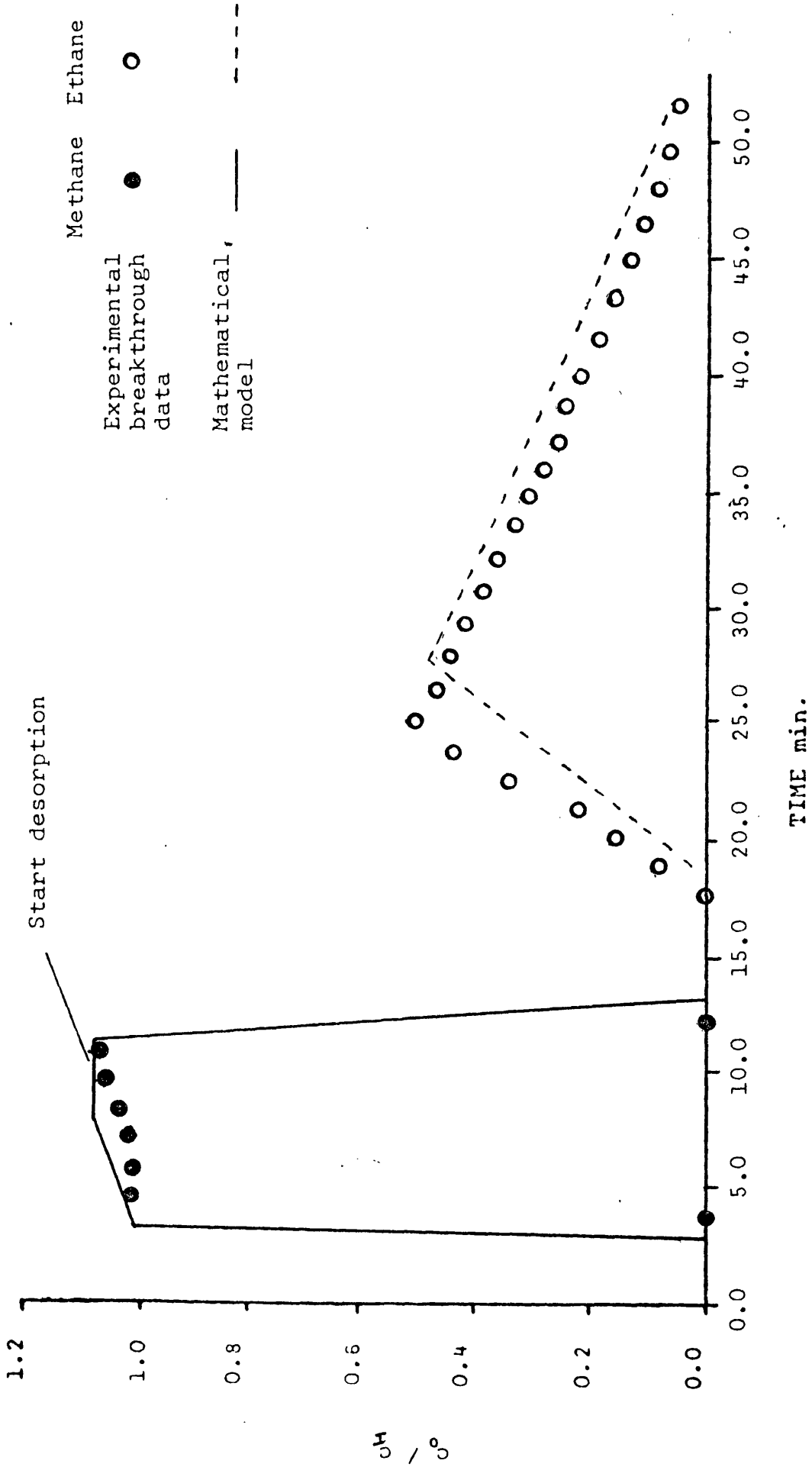


FIG.42 EXPERIMENT NO.14 METHANE-ETHANE ADSORPTION-DESORPTION CYCLE ON 5A MOLECULAR SIEVE  
 $\bar{Y}=0.109, C_1=1.073, C_2=0.932 \text{ g mol/cm}^3 \times 10^5$



**FIG. 43** EXPERIMENT NO. 15 METHANE-ETHANE ADSORPTION-DESORPTION CYCLE ON 5A MOLECULAR SIEVE  
 $\frac{Y}{T} = 0.109, C_1 = 1.073, C_2 = 0.932 \text{ g mol/cm}^3 \times 10^5$

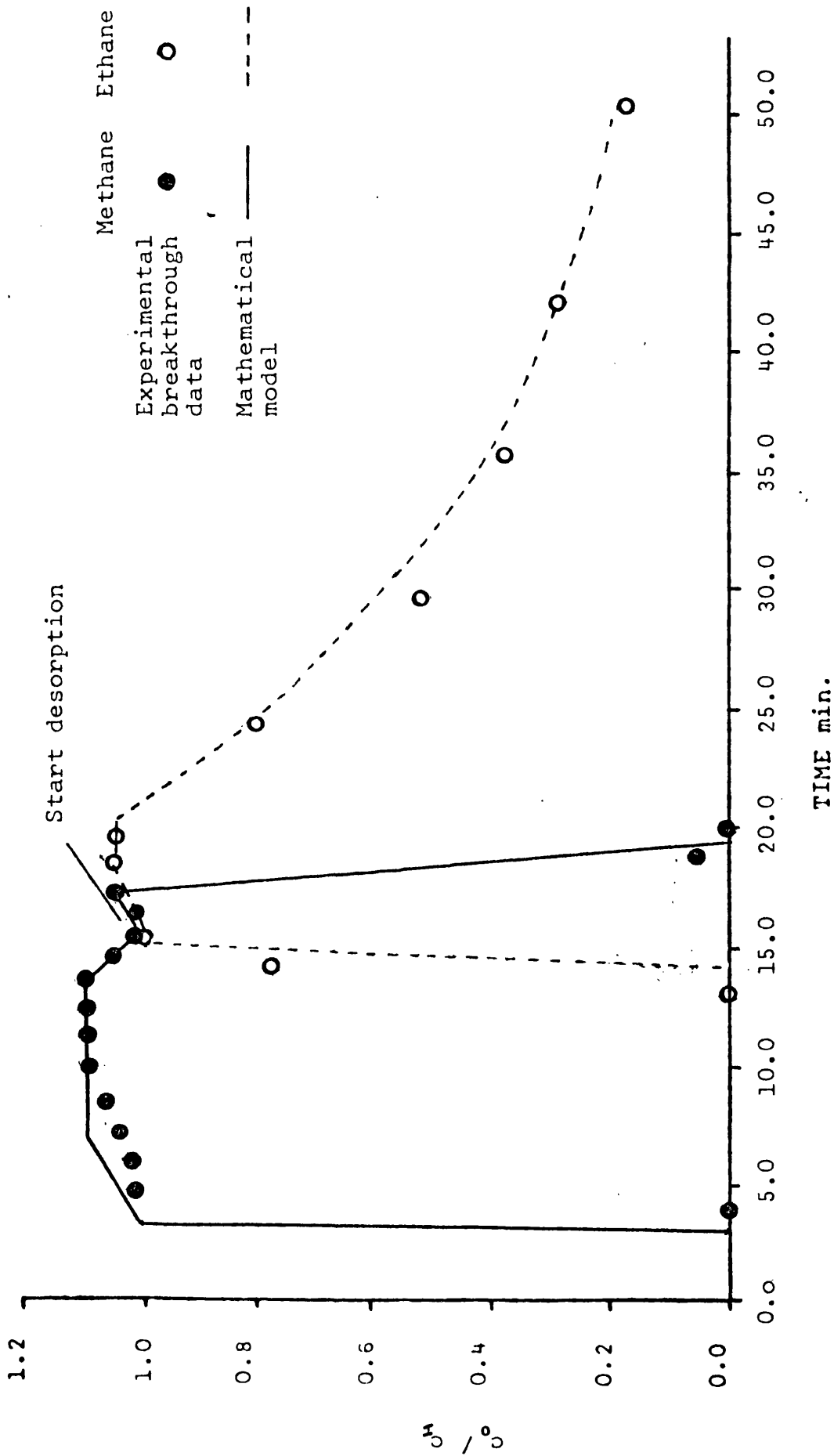


FIG. 44

EXPERIMENT NO. 16 METHANE-ETHANE ADSORPTION-DESORPTION CYCLE ON 5A MOLECULAR SIEVE

$$\bar{Y} = 0.109, \bar{C}_2 = 1.073, \bar{C}_1 = 0.932 \text{ g mol/cm}^3 \times 10^5$$

COMPUTER SIMULATION NO.1

SYSTEM: METHANE-ETHANE ON 5A MOLECULAR SIEVE

ADSORBATE M.F. IN TOTAL FLOW: 0.1

M.F. METHANE IN ADSORBATE: 0.97

ADSORPTION TEMPERATURE: 20.0°C

WEIGHT OF ADSORBENT: 1.105 gm

INITIAL OUTLET FLOWRATE: 50.0 cm<sup>3</sup>/min

FINAL OUTLET FLOWRATE: 50.0 cm<sup>3</sup>/min

ADSORPTION CELL TOTAL PRESSURE 510.0psig

GAS PHASE ADSORBATE CONCENTRATION AT BED INLET

${}^1C_F$ -METHANE	${}^2C_F$ -ETHANE	gmol/cm <sup>3</sup> *10 <sup>6</sup>
15.07	0.466	

TABLE 19

COMPUTER SIMULATION NO.2

SYSTEM: METHANE-ETHANE ON 5A MOLECULAR SIEVE

ADSORBATE M.F. IN TOTAL FLOW: 0.1

M.F. METHANE IN ADSORBATE: 0.9

ADSORPTION TEMPERATURE: 20.0° C

WEIGHT OF ADSORBENT: 1.105 gm

INITIAL OUTLET FLOWRATE: 50.0 cm<sup>3</sup>/min

FINAL OUTLET FLOWRATE: 50.0 cm<sup>3</sup>/min

ADSORPTION CELL TOTAL PRESSURE: 153.0 psig

GAS PHASE ADSORBATE CONCENTRATION AT BED INLET:

$c_1$ -METHANE	$c_2$ -ETHANE	
4.19	0.446	gmol/cm <sup>3</sup> ×10 <sup>5</sup>

TABLE 20

COMPUTER SIMULATION NO.3

SYSTEM: METHANE-ETHANE ON 5A MOLECULAR SIEVE

ADSORBATE M.F. IN TOTAL FLOW: 0.1

M.F. METHANE IN ADSORBATE: 0.75

ADSORPTION TEMPERATURE: 20.0° C

WEIGHT OF ADSORBENT: 1.105 gm

INITIAL OUTLET FLOWRATE: 50.0 cm<sup>3</sup>/min

FINAL OUTLET FLOWRATE: 50.0 cm<sup>3</sup>/min

ADSORPTION CELL TOTAL PRESSURE: 60.0 psig

GAS PHASE ADSORBATE CONCENTRATION AT BED INLET:

$\frac{C_1}{Z}$ -METHANE	$\frac{C_2}{Z}$ -ETHANE	
1.39	0.446	gmol/cm <sup>3</sup> ×10 <sup>5</sup>

TABLE 21



COMPUTER SIMULATION NO.4

SYSTEM: METHANE-ETHANE ON 5A MOLECULAR SIEVE

ADSORBATE M.F. IN TOTAL FLOW: 0.1

M.F. METHANE IN ADSORBATE: 0.5

ADSORPTION TEMPERATURE: 20.0° C

WEIGHT OF ADSORBENT: 1.105 gm

INITIAL OUTLET FLOWRATE: 50.0 cm<sup>3</sup>/min

FINAL OUTLET FLOWRATE: 50.0 cm<sup>3</sup>/min

ADSORPTION CELL TOTAL PRESSURE: 30.0 psig

GAS PHASE ADSORBATE CONCENTRATION AT BED INLET:

$\frac{C_1}{C_2}$ -METHANE	$\frac{C_1}{C_2}$ -ETHANE	
0.466	0.466	gmol/cm <sup>3</sup> × 10 <sup>5</sup>

TABLE 22

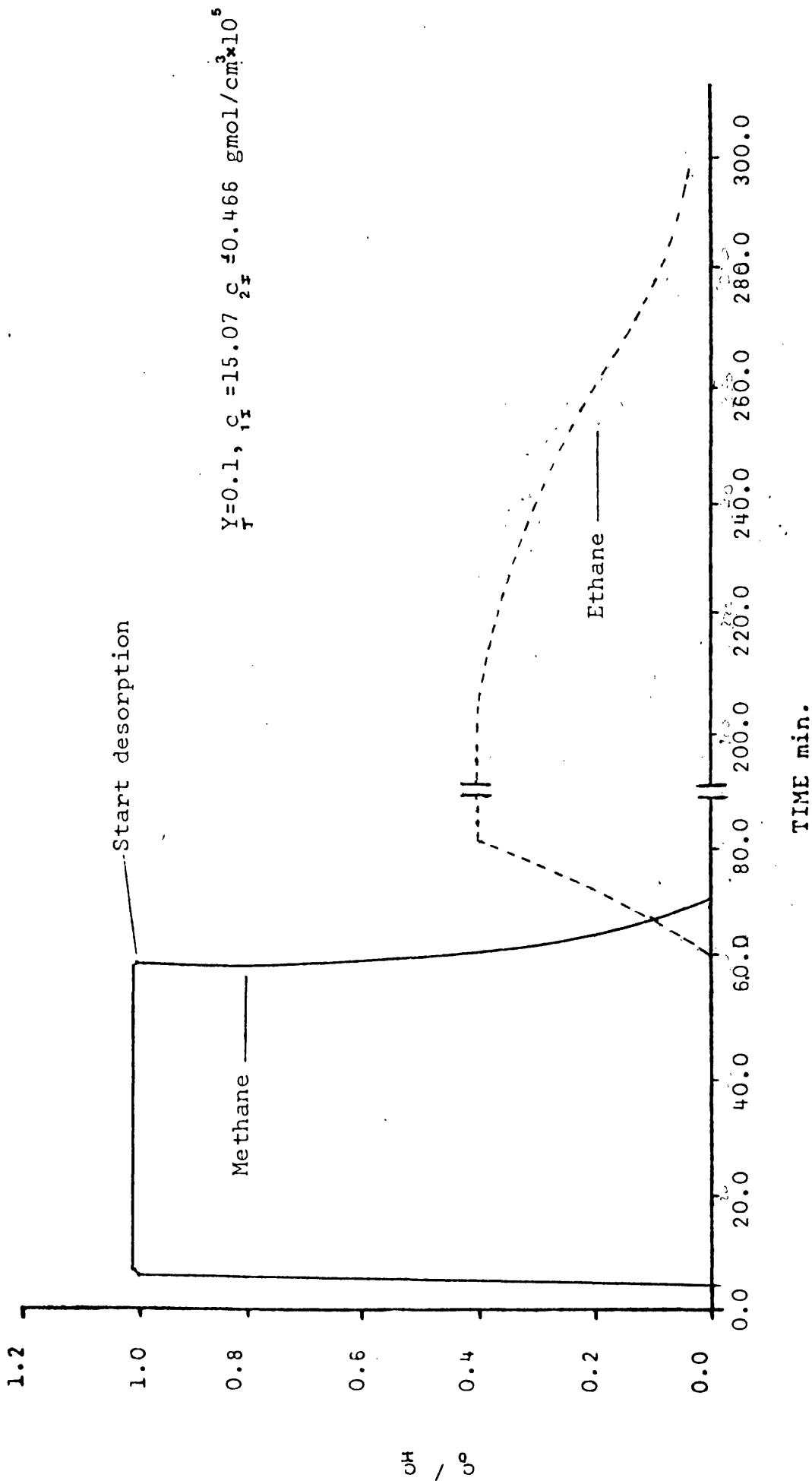


FIG.45 COMPUTER SIMULATION NO.1 METHANE-ETHANE ON 5A MOLECULAR SIEVE

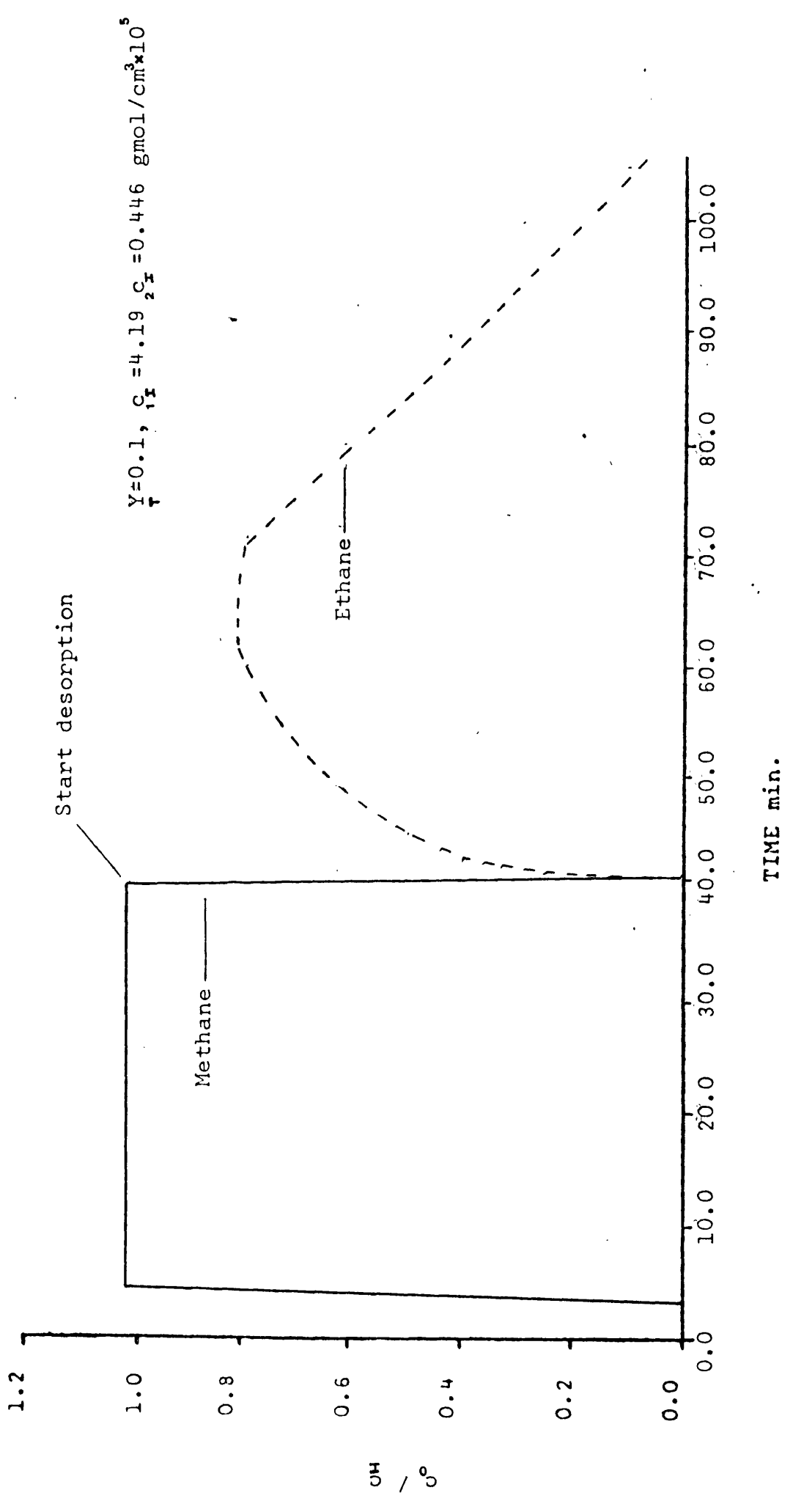


FIG.46 COMPUTER SIMULATION NO.2 METHANE-ETHANE ON 5A MOLECULAR SIEVE

GAS PHASE FRACTIONAL RESPONSE AT ADSORBENT BED OUTLET

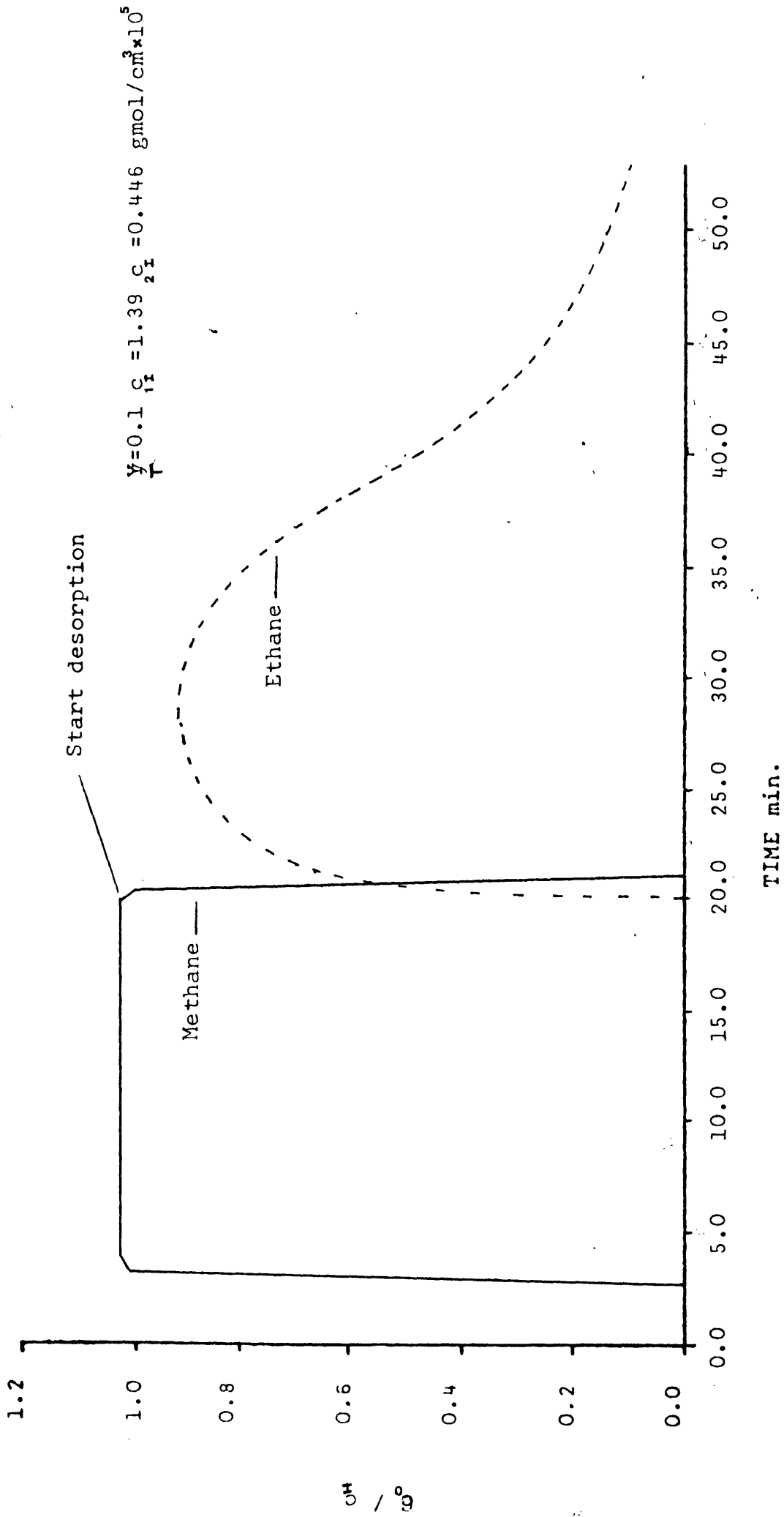


FIG.47 COMPUTER SIMULATION NO.3 METHANE-ETHANE ON 5A MOLECULAR SIEVE

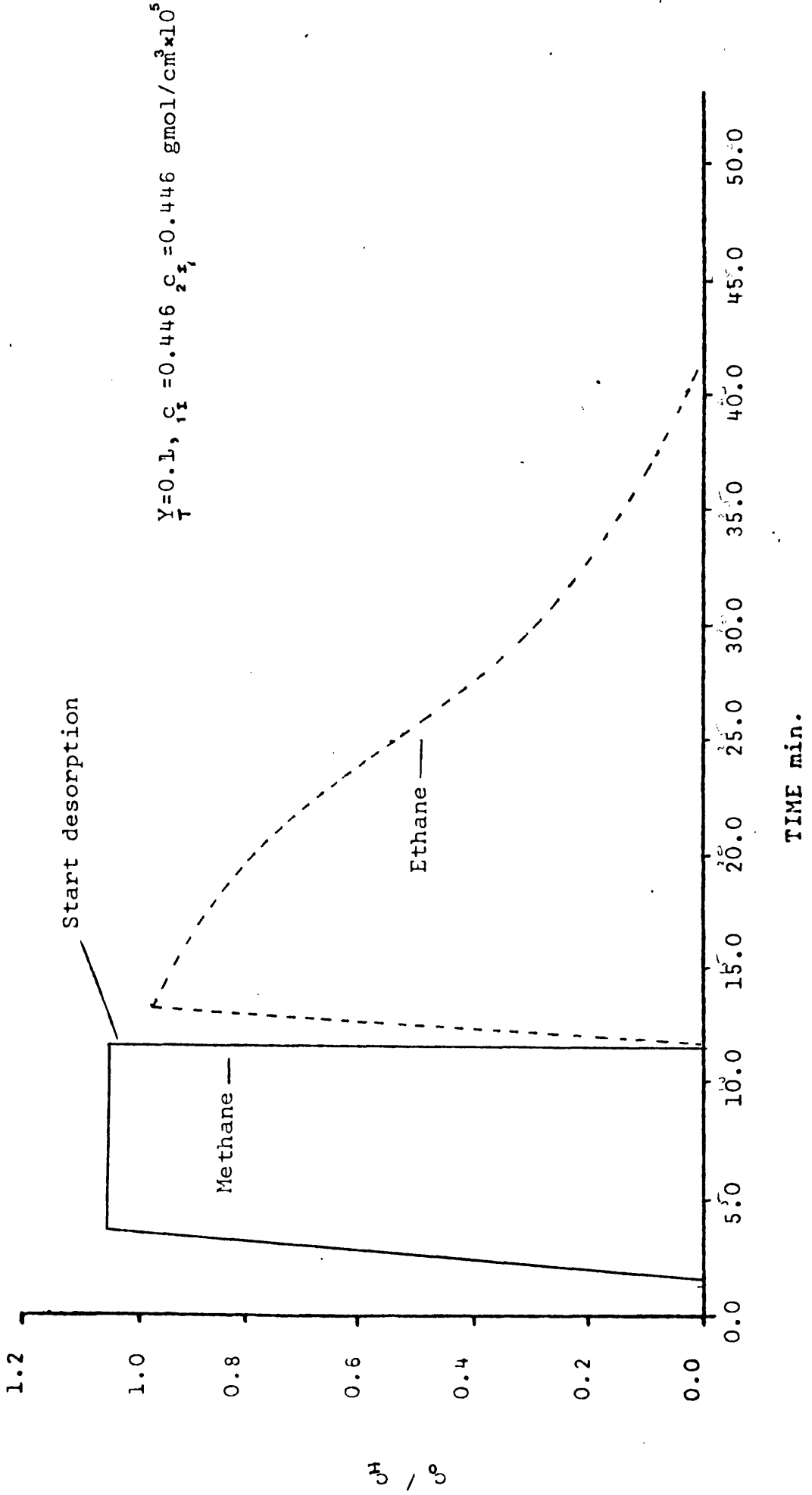


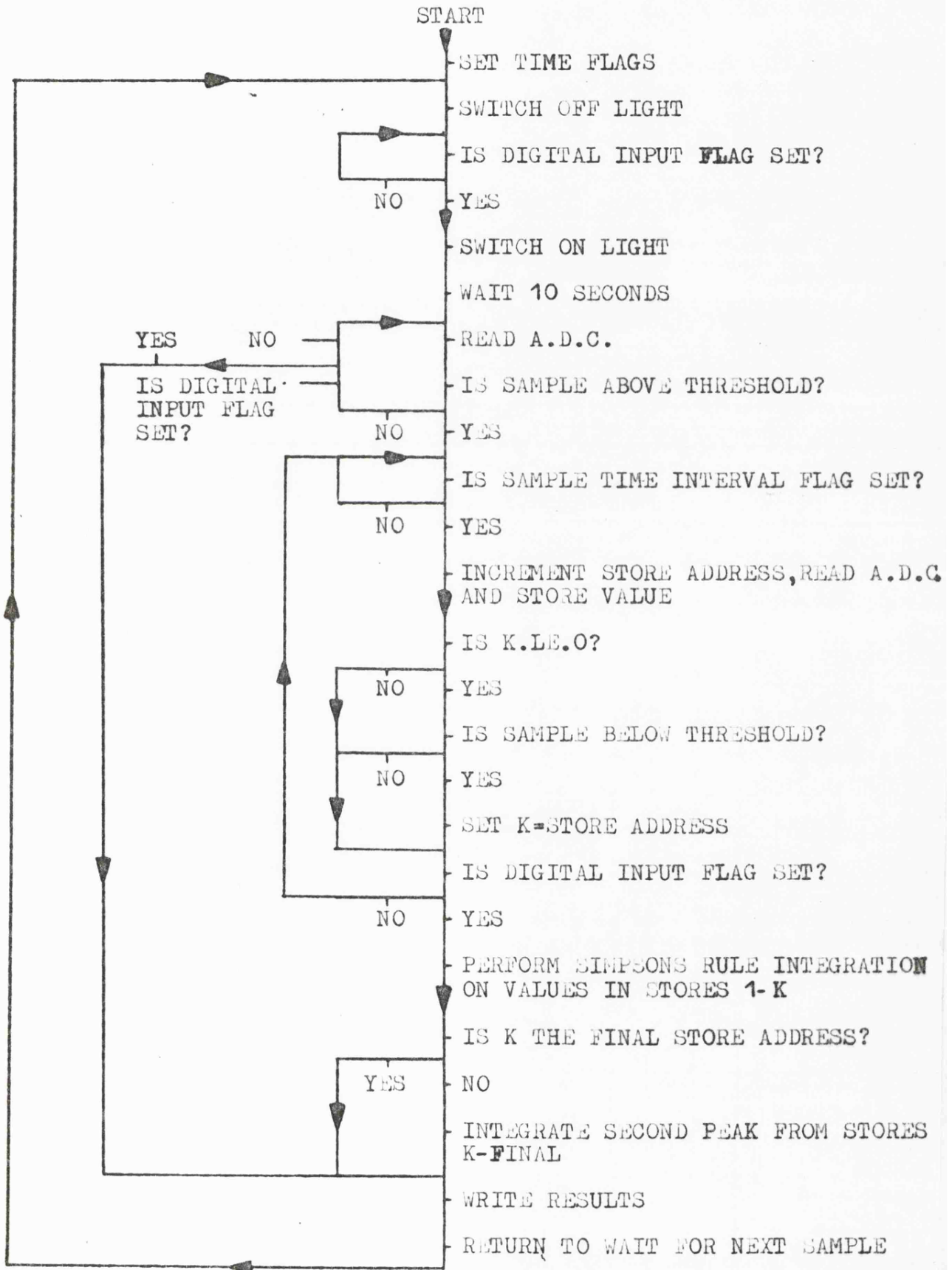
FIG. 48 COMPUTER SIMULATION NO. 4 METHANE-ETHANE ON 5A MOLECULAR SIEVE

APPENDIX ONE

APPENDIX 1

REAL-TIME PEAK HEIGHT DATA ACQUISITION PROGRAM

LINE DIAGRAM



\*\*\*\*\*  
C-SYSTEM 4 COMPATIBLE FOCAL 1976

01.01 C-AESORBER EFFLUENT SAMPLE CHROMATOGRAM INTEGRATION  
01.03 C-TWO COMPONENT A.D.C.  
01.05 C-METHANE-ETHANE MIXTURES  
01.07 S C=FLAG(PST,4,1,2,50)  
01.09 S A=0;S X=0  
01.11 S C=FOUT(ODIG,0,1,1);S N=0;S K=0  
01.13 I (FIN(ODIG,0,1))1.17  
01.15 G 1.13  
01.17 S C=FOUT(ODIG,0,1,0)  
01.19 I (FLAG(50))1.23  
01.21 G 1.19  
01.23 I (.0244-FIN(PAIC,5))1.27  
01.25 I (FIN(ODIG,0,1))2.11;G 1.27  
01.27 I (FLAG(2))1.31  
01.29 G 1.27  
01.31 S N=N+1;S F(N)=FIN(PAIC,5)  
01.33 I (K)1.35,1.35,1.39  
01.35 I (E(N)-.0244)1.37,1.37,1.39  
01.37 S K=N  
01.39 I (FIN(ODIG,0,1))2.01;G 1.27  
  
02.01 S L=K;S J=1;S P=J+1  
02.03 S E=2;F M=J,2,L;D 3.03  
02.05 S E=4;F M=P,2,L;D 3.03  
02.07 I (N-L-1)2.11;S J=K+1;S P=J+1;S X=A  
02.09 S L=N;S A=0;G 2.03  
02.11 I (-X)2.15  
02.13 T %,A,X1;G 1.09  
02.15 T ,X,A1;G 1.09  
  
03.03 S A=A+E\*(E(M)-0.02)

\*\*\*\*\*

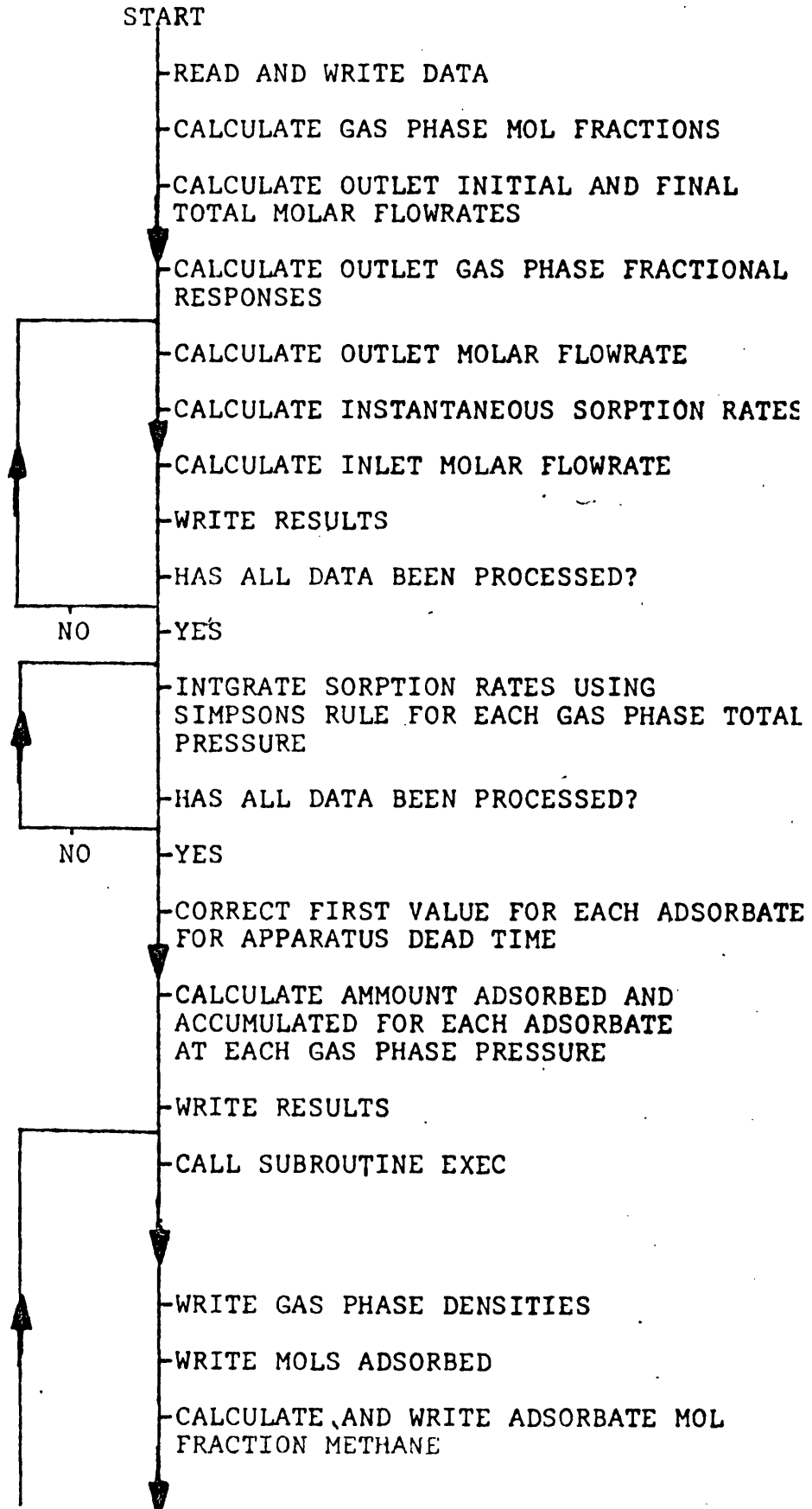


APPENDIX TWO

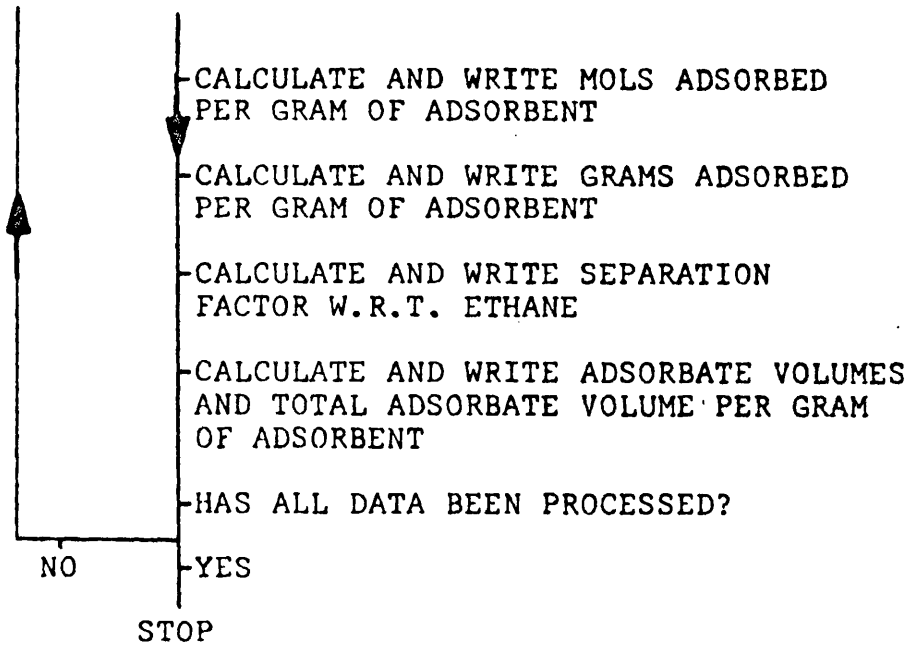
APPENDIX 2

LINE DIAGRAM OF ADSORPTION DATA ANALYSIS PROGRAM

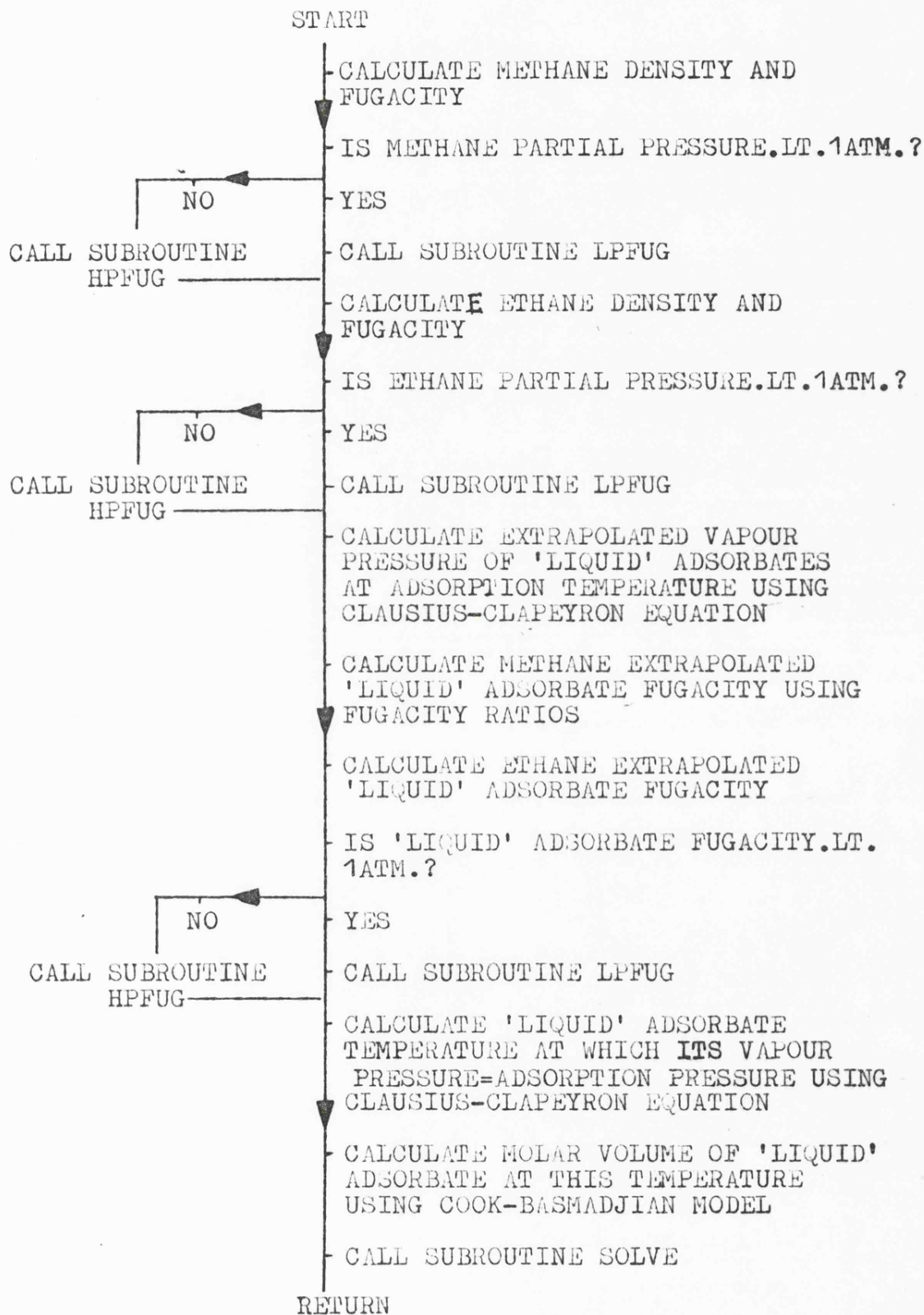
MAIN PROGRAM



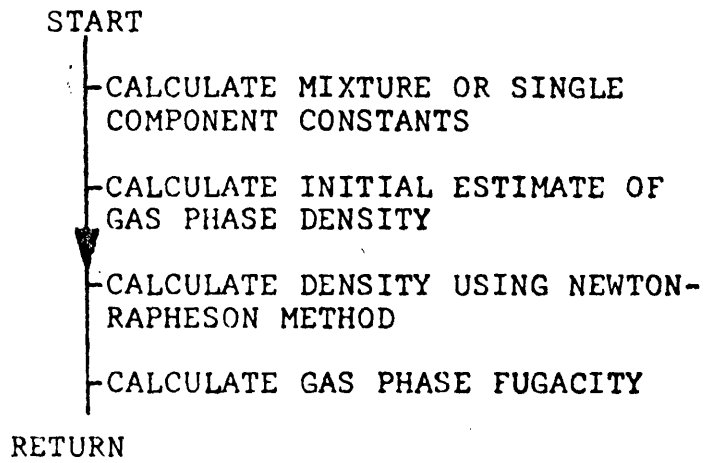
MAIN PROGRAM-CONTINUED



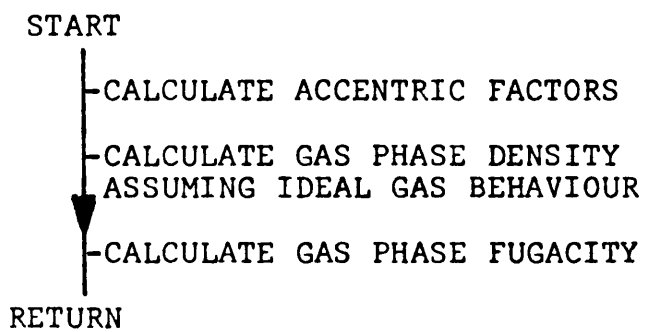
SUBROUTINE EXEC



SUBROUTINE HPFUG



SUBROUTINE LPFUG



SUBROUTINE SOLVE

START

| CALCULATE THEORETICAL ADSORBED PHASE  
| MOL FRACTIONS FROM POLANYI POTENTIAL  
| THEORY USING FALSE POSITION

| CALCULATE POLANYI ADSORPTION  
| POTENTIAL

RETURN





C TIME-TIME OF CHANGE OF GAS PHASE PRESSURE IN NUMBERS OF SAMPLES  
 C PAMBHG-AMBIENT PRESSURE MM.HG.  
 C DT-TIME BETWEEN SAMPLES SEC.  
 C WT-WEIGHT OF DRY ADSORBENT  
 C F1-INITIAL OUTLET FLOWRATE ML./MIN.  
 C F2-FINAL OUTLET FLOWRATE ML./MIN.  
 C DFLOW -FRACTIONAL CHANGE IN OUTLET FLOW  
 C FCAL-FLOWRATE AT DEADTIME CALIBRATION MOL./MIN.  
 C E-BED+MACRO-PORE VOIDAGE ML./GM.  
 C DEATHM-APPARATUS DEAD TIME MIN.  
 C AT1,2,3-CHROMATOGRAPH ATTENUATIONS  
 C ACH4,E-CHROMATOGRAPH AREAS FOR CH4 CALIBRATION/EXPERIMENTAL MIX  
 C AC2H6,E- DITTO FOR C2H6  
 C Q-INITIAL OUTLET FLOWRATE MOL./SEC.  
 C VLMOI 1,2-ADSORBATE MOLAR VOLUME ML./MDL.  
 C AM1,2-AMOUNT ADSORBED MOL.  
 C ADWT1,2-WEIGHT ADSORBED GMS./GM.  
 C SEPFCT-SEPARATION FACTOR C2H6/CH4  
 C CH4MF-MOL.FRACTION CH4 IN ADSORBED PHASE  
 C N-NUMBER OF SAMPLES  
 C NT-NUMBER OF PRESSURES  
 C LQ,LP-STORE ADDRESSES TO IDENTIFY COMPONENTS  
 C LQ=1 FOR CH4; =2 FOR C2H6  
 C LP=2 FOR LQ=1; =1 FOR LQ=2  
 C  
 C

```

0001      COMMON FC1, FC2, VLMDL1, VLMDL2, PF(2), ROW(2)
0002      DIMENSION AREAS(2, 500), Y(2, 500), FLWOUT(500), FLOWIN(500)
0003      DIMENSION ADRATE(2, 500), PADSIG(20), TIME(20), ADS(2, 20)
0004      CALL HEADER
0005      READ(1, 100)N, NT, L0, LP
0006      RFAD(1, 101)(AREAS(L0, L), AREAS(LP, L), L=1, N)
0007      READ(1, 102)ACH4E, AC2H6E
0008      READ(1, 102)ACH4, AC2H6
0009      READ(1, 102)AT1, AT2, AT3
0010      READ(1, 102)(PADSIG(L), L=1, NT)
0011      READ(1, 102)(TIME(L), L=1, NT)
0012      READ(1, 102)TADSK, TAMBK, PAMBHG, F1, F2, WT, DT, FGCDEF
0013      DO 1 L=1, NT
0014      PADSIG(L)=(PADSIG(L)+14. 69)/14. 69
0015      DO 1 M=1, 2
0016      ADS(M, L)=0.
0017      1 CONTINUE

0018      CALCULATE GAS PHASE MOL. FRACTIONS
0019      ACH4=ACH4*AT3
0020      AC2H6=AC2H6*AT3
0021      ACH4E=ACH4E*AT1
0022      AC2H6E=AC2H6E*AT1
0023      IF(L0-2)2, 3, 3
0024      2 CONTINUE
0025      IF(AC2H6)4, 4, 5
0026      5 CONTINUE
0027      THCMF=ACH4E/ACH4+AC2H6E/AC2H6
0028      Y1=ACH4E/(ACH4*THCMF)
0029      GOTO6
0030      4 CONTINUE

```

```

0030      Y1=1.
0031      THCMF=ACH4E/ACH4
0032      GOTO6
0033      3 CONTINUE
0034      Y1=0.
0035      THCMF=AC2H6E/AC2H6
0036      6 CONTINUE
C
C      WRITE EXPERIMENTAL CONDITIONS
C
0037      WRITE(6,103)DT
0038      WRITE(6,104)THCMF
0039      WRITE(6,105)(TIME(L),L=1,NT)
0040      WRITE(6,106)TADSK
0041      WRITE(6,107)(PADSIG(L),L=1,NT)
0042      WRITE(6,108)TAMBK,PAMBHG
0043      WRITE(6,109)Y1
0044      WRITE(6,110)WT
C
C      CALCULATF OUTLET INITIAL AND FINAL MOLAR FLOWRATES
C
0045      WRITE(6,111)F1,F2

FORTRAN 1V      D06-01  SOURCE LISTING      PAGE 003

0046      F3=F1
0047      F1=F1*PAMBHG*273 1/(TAMBK*760.)
0048      F1=F1/22400.
0049      F2=F1*F2/F3

```

```

0050 WRITE(6,112)F1,F2
0051 WRITE(6,113)((AREAS(M,L),L=1,N),M=1,2)
C
C CALCULATE OUTLET GAS FRACTIONAL RESPONSES
C
0052 DO 7 M=1,2
0053 IF(AREAS(M,N).LT.0.01)GOTO7
0055 DO 7 L=1,N
0056 Y(M,L)=AREAS(M,L)/AREAS(M,N)
0057 7 CONTINUE
0058 WRITE(6,114)(Y(1,L),L=1,N)
0059 WRITE(6,115)(Y(2,L),L=1,N)
0060 Q=F1/60.
0061 DEADTM=1.61*(7.94+0.432*WT)/7.94
0062 FCAL=0.000975
0063 Z1=THCMF*Y1
0064 Z2=THCMF*(1.-Y1)
0065 DQ=(F2-F1)/F1
C
C CALCULATE INSTANTANEOUS RATE OF SORPTION
C AND INLET AND OUTLET MOLAR FLOWRATES
C AT EACH SAMPLE TIME BY SOLUTION OF THE MASS BALANCE
C FOR EACH COMPONENT
C
0066 DO 8 M=1,N
0067 DFLOW=1.+(Y(1,M)+Y(2,M))*DQ/Z.
0068 Y(1,M)=Y(1,M)*Z1
0069 Y(2,M)=Y(2,M)*Z2
0070 ADRATE(2,M)=Q*((Z1-Y(1,M))*Z2+(Z2-Y(2,M))*(1.-Z1))
0071 ADRATE(2,M)=ADRATE(2,M)/((1.-Z2)*(1.-Z1)-Z1*Z2)
0072 ADRATE(2,M)=ADRATE(2,M)*DFLOW
0073 ADRATE(1,M)=Q*((Z1-Y(1,M))+ADRATE(2,M)*Z1)/((1.-Z1)
0074 ADRATE(1,M)=ADRATE(1,M)*DFLOW
0075 FLWOUT(M)=F1*DFLOW

```

```

0076 FLOWIN(M)=FLOWOUT(M)+(ADRATE(1,M)+ADRATE(2,M))*60.
0077 8 CONTINUE
0078 WRITE(6,116)(ADRATE(1,M),M=1,N)
0079 WRITE(6,117)(ADRATE(2,M),M=1,N)
0080 WRITE(6,118)(FLOWOUT(L),L=1,N)
0081 WRITE(6,119)(FLOWIN(L),L=1,N)
C
C INTEGRATE SORPTION RATES USING SIMPSONS RULE TO GIVE
C MOLS. OF GAS ADSORBED AND ACCUMULATED FOR EACH GAS PHASE PRESSURE
C
0082 DO 9 L=1,2
0083 K=2.
0084 NK=0.
0085 11 CONTINUE
0086 NK=NK+1
0087 NP=TIME(NK)+0.005
0088 S=1.
0089 DO 10 M=K,NP
0090 ADS(L,NK)=ADS(L,NK)+(3.+S)*ADRATE(L,M)

```

FORTRAN IV D06-01 SOURCE LISTING PAGE 004

```

0091 S=-S
0092 10 CONTINUE
0093 K=NP+1
0094 IF(NK-NT)11,9,9
0095 9 CONTINUE
C
C CORRECTION FOR APPARATUS DEAD VOLUME AND INITIAL OUTLET FLOWRATE
C DIFFERENT FROM THAT AT DEAD VOLUME CALIBRATION
C

```

```

0096 ADS(1,1)=(ADS(1,1)+ADRATE(1,1))*DT/3.
0097 ADS(1,1)=ADS(1,1)-ADRATE(1,1)*60.*DEADTM*FCAL/F1
0098 ADS(2,1)=(ADS(2,1)+ADRATE(2,1))*DT/3.
0099 ADS(2,1)=ADS(2,1)-ADRATE(2,1)*60.*DEADTM*FCAL/F1
0100 DO 12 L=1,2
0101 DO 12 M=2,NT
0102 ADS(L,M)=ADS(L,M)*DT/3.
0103 ADS(L,M)=ADS(L,M-1)+ADS(L,M)
0104 12 CONTINUE
0105 WRITE(6,120)(ADS(1,L),L=1,NT)
0106 WRITE(6,121)(ADS(2,L),L=1,NT)
C
C CALCULATE GAS PHASE DENSITIES AND FUGACITIES
C
C CALCULATE POLYMER ADSORPTION POTENTIALS AND 'LIQUID' ADSORBATE
C MOLAR VOLUMES
C
0107 DO 13 L=1,NT
0108 P=PADSIG(L)*THCMF
0109 CALL EXEC(P,TADSK,Y1,FGCOEF)
0110 ROW(1)=ROW(1)/1000
0111 ROW(2)=ROW(2)/1000.
C
C WRITE RESULTS
C
0112 WRITE(6,123)VLMOL1,VLMOL2
0113 WRITE(6,122)ROW(1),ROW(2)
0114 WRITE(6,124)ADS(1,L),ADS(2,L)
0115 CH4MF=ADS(1,L)/(ADS(1,L)+ADS(2,L))
0116 WRITE(6,125)CH4MF
0117 ADS(1,L)=ADS(1,L)/WT
0118 ADS(2,L)=ADS(2,L)/WT
0119 WRITE(6,126)ADS(1,L),ADS(2,L)
0120 ADWT1=ADS(1,L)*16.
0121 ADWT2=ADS(2,L)*30.

```

```

0122 WRITE(6,127)ADWT1,ADWT2
0123 IF(Y1.LT.0.001.OR.Y1.GT.0.999)GOTO14
0125 SEPFCT=ADS(2,L)*ROW(1)/(ADS(1,L)*ROW(2))
0126 WRITE(6,128)SEPFCT
0127 14 CONTINUE
0128 ADS(1,L)=ADS(1,L)*VLMOL1
0129 ADS(2,L)=ADS(2,L)*VLMOL2
0130 AMTOT=ADS(1,L)+ADS(2,L)
0131 WRITE(6,129)ADS(1,L),ADS(2,L),AMTOT
0132 13 CONTINUE
0133 100 FORMAT(1H ,I3)
0134 101 FORMAT(1H ,ZE0.0)
0135 102 FORMAT(1H ,F16.8)

```

FORTRAN IV D06-01 SOURCE LISTING PAGE 005

```

0136 103 FORMAT(1H ,//,' SAMPLE INTERVAL ',F8.2,' SECONDS')
0137 104 FORMAT(1H ,//,' TOTAL HYDROCARBON MOL FRACTION IN TOTAL FLOW ',//,
1E12.4,//)
0138 105 FORMAT(1H ,//,' PRESSURE CHANGE TIMES IN NO. OF INTERVALS',//,(5F1
16.3))
0139 106 FORMAT(1H ,//,' ADSORPTION TEMPERATURE ',F16.3,' DEG. K',//)
0140 107 FORMAT(1H ,//,' ADSORPTION PRESSURES ATMS.',//,(5F16.3))
0141 108 FORMAT(1H ,//,' AMBIENT TEMP',F8.3,' DEG. K AMBIENT PRESSURE
1',F8.3,' MM. MERCURY',//)
0142 109 FORMAT(1H ,//,' MOL. FRACTION METHANE IN TOTAL ADSORBATE',F8.3,//)
0143 110 FORMAT(1H ,//,' WEIGHT OF ADSORBENT ',F8.3,' GMS.')
0144 111 FORMAT(1H ,//,' AMBIENT FLOWRATE MLS./MIN.',//,' INITIAL',E12.4,'
1 FINAL', E12.4,//)
0145 112 FORMAT(1H ,//,' AMBIENT FLOWRATE MOL./MIN.',//,' INITIAL',E12.4,'
1 FINAL', E12.4,//)

```

```

0146 113 FORMAT(1H , //, ' AREAS FROM CHROMATOGRAM-PDPSE ', //, (8E13. 6))
0147 114 FORMAT(1H , //, ' METHANE BREAKTHROUGH DATA ', //, (8E12. 4))
0148 115 FORMAT(1H , //, ' ETHANE BREAKTHROUGH DATA ', //, (8E12. 4))
0149 116 FORMAT(1H , ' RATE OF SORPTION OF METHANE AT EACH SAMPLE TIME', //,
1(8E12. 4))
0150 117 FORMAT(1H , ' RATE OF SORPTION OF ETHANE AT EACH SAMPLE TIME', //,
1(8E12. 4))
0151 118 FORMAT(1H , //, ' OUTLET FLOWRATE MOL. /MIN. AT EACH SAMPLE TIME '
1, //, (8E12. 4))
0152 119 FORMAT(1H , //, ' CALCULATED INLET FLOWRATE MOL. /MIN. AT EACH SAM
1PLE TIME ', //, (8E12. 4))
0153 120 FORMAT(1H , //, ' AMOUNT ADSORBED AND ACCUMULATED
1 MOL. ', //, (8E12. 4))
0154 121 FORMAT(1H , //, ' ETHANE ', //, ' AMOUNT ADSORBED AND ACCUMULATED
1 MOL. ', //, (8E12. 4))
0155 122 FORMAT(1H , ' GAS PHASE DENSITIES IN ADSORBER MOL. /CC. ', //, ' METHAN
1E', E12. 4, ' ETHANE', E12. 4)
0156 123 FORMAT(1H , //, ' MOLAR VOLUMES CC. /MOL. ', //, ' METHANE ', F8. 3, '
1 ETHANE
', F8. 3, //)
0157 124 FORMAT(1H , //, ' MOL. OF GAS ADSORBED', //, ' METHANE', E12. 4, '
1 ETHANE', E12. 4, //)
0158 125 FORMAT(1H , //, ' MOL. FRACTION METHANE IN ADSORBED PHASE', F8. 3)
0159 126 FORMAT(1H , //, ' MOL. OF GAS ADSORBED/GM. OF ADSORBENT', //, ' METHANE
1', E12. 4, ' ETHANE', E12. 4)
0160 127 FORMAT(1H , //, ' WT. OF ADSORBATE/GM. ', //, ' METHANE', E12. 4, '
1 ETHANE', E12. 4)
0161 128 FORMAT(1H , //, ' SEPARATION FACTOR C2H6/CH4 ', E12. 4)
0162 129 FORMAT(1H , //, ' ADSORBATE VOLUMES CC. /GM. ADSORBENT', //, ' METHANE
1 ', E12. 4, ' ETHANE
', E12. 4, ' TOTAL
', E12. 4)
0163 STOP
0164 END

```



0001

SUBROUTINE EXEC(P,T,Y,FGCOCF)

C  
C  
C  
C  
C  
C  
C  
C  
C  
C  
C  
C  
C  
C  
C  
C  
C  
C  
C  
C  
C  
C

EXECUTIVE SUBROUTINE FOR CALCULATION OF GAS PHASE DENSITIES,  
FUGACITIES,POLANYI ADSORPTION POTENTIALS AND 'LIQUID'  
ADSORBATE MOLAR VOLUMES

PC-CRITICAL PRESSURE ATMS.  
P-GAS PHASE PRESSURE ATMS.  
TRANK-TEMPERATURE DEG. R  
FGCOCF-FUGACITY COEFFICIENT F/P  
F1,2-GAS PHASE FUGACITY ATMS.  
FS1,2-LIQUID FUGACITY ATM.  
BNMV1,2-NORMAL BOILING POINT MOLAR VOLUME ML./MOL.  
Y-GAS PHASE MOL. FRACTION

0002  
0003  
0004  
0005  
0006  
0007  
0008  
0009  
0010

COMMON FC1,FC2,VLMOL1,VLMOL2,PF(2),ROW(2)  
BNMV1=16.0/0.427  
BNMV2=30.0/0.545  
PC1=673./14.69  
PC2=710./14.69  
P3=P\*14.69  
C=2.0  
Y1=Y  
WRITE(6,100)P3,Y

C  
C  
C  
C  
C  
C

SELECT EQUATION FOR CALCULATION OF DENSITY AND FUGACITY

C  
C

```
0011 N=1
0012 M=2
0013 IF(P*Y/PC1-0.02)1,1,2
0014 1 CONTINUE
0015 CALL LPFUG(T, Y, C, P, N, M)
0016 F1=PF(N)
0017 GOTD3
0018 2 CONTINUE
0019 CALL HPFUG(T, Y, C, P, N, M)
0020 F1=PF(N)
0021 3 CONTINUE
0022 Y=1. -Y
0023 N=2
0024 M=1
0025 IF(P*Y/PC2-0.02)4,4,5
0026 4 CONTINUE
0027 CALL LPFUG(T, Y, C, P, N, M)
0028 IF(C-1.)6,6,7
0029 7 CONTINUE
0030 F2=PF(N)
```

FORTRAN IV D06-01 SOURCE LISTING

PAGE 002

```
0031 GOTD9
0032 5 CONTINUE
0033 CALL HPFUG(T, Y, C, P, N, M)
```

```

0034 IF(C-1.)6,6,8
0035 8 CONTINUE
0036 F2=PF(N)
0037 9 CONTINUE
0038 Y=1.-Y
0039 IF(NP.GT.0.)GOTO10

C
C CALCULATE EXTRAPOLATED VAPOUR PRESSURE OF 'LIQUID'
C ADSORBATE AT ADSORPTION TEMPERATURE
C USING CLAUSIUS-CLAPEYRON EQUATION
C
0041 NP=0
0042 C=1.0
0043 TRANK1=T*460./273.13
0044 P1=(EXP((-1865./TRANK1)+11.95))/14.69
0045 P2=(EXP((-3306./TRANK1)+12.61))/14.69

C
C CALCULATE EXTRAPOLATED VAPOUR PRESSURE FUGACITIES
C
C METHANE-USING F/P VS. PR CHART
C
0046 FS1=P1*FGCOEF

C
C ETHANE-USING B R W EQUATION
C
0047 P=P7
0048 IF(P2/PC2-0.02)4,4,5
0049 6 CONTINUE
0050 FS2=PF(2)
0051 NP=NP+1
0052 10 CONTINUE
0053 WRITE(6,101)F1,F2,P1,P2,FS1,FS2

C
C CALCULATE 'LIQUID' ADSORBATE TEMPERATURE AT WHICH
C VAPOUR PRESSURE = ADSORPTION PRESSURE

```

USING CLAUSIUS-CLAPEYRON EQUATION

CALCULATE MOLAR VOLUME OF 'LIQUID' ADSORRATE AT  
THIS TEMPERATURE USING THE MODEL OF COOK AND  
BASMADJIAN

```

0054 Y=Y1
0055 P=P3/14.69
0056 FC1=0.0
0057 FC2=0.0
0058 VLMOL1=0.
0059 VLMOL2=0.
0060 IF(Y.LT.0.001)GOTO11
0061 FC1=FS1/F1
0062 IF(P*Y-1)12,12,13
0063 13 CONTINUE
0064 TRANK1=1./(-.000536*ALOG(P*Y*14.69)+.006399)
0065

```

FORTRAN IV D06-01 SOURCE LISTING PAGE 003

```

0066 VLMOL1=EXP(0.4211*ALOG(TRANK1)+1.3731)
0067 GOTO14
0068 12 CONTINUE
0069 VLMOL1=BNMV1
0070 14 CONTINUE
0071 IF(Y.GT.0.99)GOTO15
0072 11 CONTINUE
0073 FC2=FS2/F2
0074

```

```

0075 IF(P*(1.-Y)-1.)16,16,17
0076 CONTINUE
0077 TRANK3=1./(-0.0003024*ALOG(P*(1.-Y)*14.69)+0.003815)
0078 VLMOL2=EXP(0.69644*ALOG(TRANK3)-0.07357)
0079 GOTO15
0080 16 CONTINUE
0081 VLMOL2=BNMVZ
0082 15 CONTINUE
C
C CALCULATE POLANYI ADSORPTION POTENTIALS, THEORETICAL 'LIQUID'
C ADSORBATE MOL. FRACTIONS
C
C CALL SOLVE(BNMV1,BNMVZ,T,Y)
C RETURN
0083 100 FORMAT(1H1,/,/, ' TOTAL H/C PRESSURE',F16.3, ' PSIA. ',/,/, ' MOL FRAC
0084 TION METHANE IN TOTAL ADSORBATE',F8.4,/,/,)
0085 101 FORMAT(1H,/,/, ' GAS PHASE FUGACITIES',2E12.4, ' ATMS',/,/, ' LIQUID
0086 1 VAPOUR PRESSURES',2E12.4, ' ATMS. ',/,/, ' LIQUID FUGACITIES',2E12.4,
0087 2' ATMS. ',/,/)
END

```

```

0001      SUBROUTINE HFUG(T, Y, C3, P, N, M)
C
C      SUBROUTINE TO CALCULATE GAS PHASE DENSITIES AND FUGACITIES AT
C      REDUCED PRESSURES>0.02
C
C
C      Y-GAS PHASE MOL. FRACTION
C      T-TEMPERATURE DEG. K
C      R-GAS CONSTANT LTR ATM /MOL DEG. K
C      PF1, 2-FUGACITY ATM.
C      D=INITIAL ESTIMATE OF DENSITY MOL. /LTR.
C      DI-NEXT ESTIMATE OF DENSITY MOL. /LTR.
C      PRESQ-CALCULATED PRESSURE ATM.
C      DF-FIRST DIFFERENTIAL OF PRESQ W R T. DENSITY
C
C
C      COMMON FC1, FC2, VLMOL1, VLMOL2, PF(2), ROW(2)
C      DIMENSION A01(2), B01(2), C01(2), A1(2), B1(2), C1(2), G1(2), AA1(2)
C
C      SET COMPONENT PARAMETERS
C
C      IF(NP.GT.0.)GOTO1
C      A01(1)=1.885
C      A01(2)=4.155556
C      B01(1)=0.0426
C      B01(2)=0.062772
C      C01(1)=0.02257*(10.0**6.0)
C      C01(2)=0.179597*(10.0**6.0)
C      A1(1)=0.04940
C      A1(2)=0.34516
C      P1(1)=0.00338004
C      B1(2)=0.011122

```

```

0016 C1(1)=0.0024545*(10.0**6.0)
0017 C1(2)=0.032767*(10.0**6.0)
0018 AA1(1)=0.00024359
0019 AA1(2)=0.00024389
0020 G1(1)=0.0060
0021 G1(2)=0.0118
0022 R=0.08207
0023 NP=NP+1
0024 1 CONTINUE
0025 IF(C3-1.)2,2,3
0026 3 CONTINUE
0027 Y1=1.-Y
0028 GOTO4
0029 2 CONTINUE
0030 Y=1.
0031 D=0.03
0032 4 CONTINUE
0033 B0=Y*B01(N)+Y1*B01(M)
0034 A0=(Y*SQRT(A01(N))+Y1*SQRT(A01(M)))**2.0
0035 C0=(Y*SQRT(C01(N))+Y1*SQRT(C01(M)))**2.0
0036 B=(Y*(B1(N)**0.333)+Y1*(B1(M)**0.333))**3.0
0037 C=(Y*(C1(N)**0.333)+Y1*(C1(M)**0.333))**3.0

```

```

0038 A=(Y*(A1(N)**0.333)+Y1*(A1(M)**0.333))**3.0
0039 AA=(Y*(AA1(N)**0.333)+Y1*(AA1(M)**0.333))**3.0

```

```

0040 G=(Y*SQRT(G1(N))+Y1*SQRT(G1(M)))**2.0
0041 Z=0.0
C
C SOLVE B. R. W. EQUATION IMPLICITLY FOR DENSITY USING NEWTON-RAPHESON
C METHOD
C
0042 8 CONTINUE
0043 Z=Z+1.0
0044 IF(Z.GT.100.)GOTO11
0045 S=-G*(D**2.0)
0046 PRESC=R*T*D+(B0*R*T-AD-CD)/(T**2.0)*(D**2.0)
0047 PRESC=PRESC+(B*R*T-A)*(D**3.0)+A*AA*(D**6.0)
0048 PRESC=PRESC+(C*(D**3.0)/(T**2.0))*(1.0-S)*EXP(S)
0049 DF=R*T+(B0*R*T-AD-CD)/(T**2.0)**2.0*D+6.0*A*AA*(D**5.0)
0050 DF=DF+3.0*(D**2.0)*(B*R*T-A)
0051 DF=DF+3.0*(D**2.0)*C*(1.0-S)*EXP(S)/(T**2.0)
0052 DF=DF+(C*(D**3.0)/(T**2.0))*EXP(S)*2.0*G*D
0053 DF=DF-2.0*G*C*(D**3.0)*(1.0-S)*EXP(S)/(T**2.0)
0054 DI=D--(PRESC-P)/DF
0055 IF(DI)5,5,6
C
C NEW ESTIMATE OF INITIAL DENSITY
C
0057 5 CONTINUE
0058 D=D*0.95
0059 GOTO8
0060 6 CONTINUE
0061 D=DI
0062 IF(ABS(P-PRESC).LE.(0.001*P))GOTO7
0064 GOTO8
C
C CALCULATE FUGACITIES FROM DENSITY
C
0065 7 CONTINUE
0066 S=-G*(D**2.0)

```



```

0067 V=R*T*ALOG(D*R*T*Y)+(R0+B01(N))*R*T*D
0068 V=V-2.0*PI*(SQRT(A0*A01(N))+SQRT(C0*C01(N)))/(T**2.0)
0069 W=R*T*((B**2.0)*B1(N)**0.333)+((A**2.0)*A1(N)**0.333)
0070 W=W*3.0*(D**2.0)/2.0
0071 U=A*((AA**2.0)*AA1(N)**0.333)+AA*((A**2.0)*A1(N)**0.333)
0072 U=U*0.60*(D**5.0)
0073 VV=3.0*(D**2.0)*((1.0-EXP(S))/(-S)-EXP(S)/2.0)/(T**2.0)
0074 VV=VV*((C**2.0)*C1(N)**0.333)
0075 VW=(1.0-EXP(S))/(-S)-EXP(S)+S*EXP(S)/2.0
0076 VW=VW*2.0*C*(D**2.0)*SQRT(G1(N)/G)/(T**2.0)
0077 PF(N)=EXP((V+U+W+VV-VW)/(R*T))
0078 IF(C3-1.)9,9,10
0079 10 CONTINUE
0080 ROW(N)=D*Y
0081 9 CONTINUE
0082 RETURN
0083 11 CONTINUE
0084 WRITE(6,100)
0085 100 FORMAT(1H , //, ' SUBROUTINE HFFUG STOPS AFTER 100. ITERATIONS')
0086 STOP

```



```

0016 1 CONTINUE
0017 W=W1(N)
0018 Y=1.0
0019 3 CONTINUE
0020 PR=P/PC(N)
0021 TR=TRANK/TC(N)
C
C CALCULATE FUGACITIES
C
0022 A=(0.1445+0.073*W)/TR-(0.33-0.46*W)/(TR**2.0)
0023 A=A-(0.1385+0.5*W)/(TR**3.0)-(0.0121+0.097*W)/(TR**4.0)
0024 A=PR*(A-(0.007*W)/(TR**9.0))
0025 PF(N)=P*Y*EXP(A)
0026 RETURN
0027 END

```



```

0019 X2=X
0020 N=1
0021 9 CONTINUE
0022 XNEW=ABS(E1)*(X2-X1)/(ABS(E1)+ABS(E2))+X1
0023 IF(ABS(XNEW-X).LE.(0.001*X))GOTO12
0025 X=XNEW
0026 IF(X.LT.0.001.OR.X.GT.0.99)GOTO14
0028 GOTO1
0029 3 CONTINUE
0030 IF(F)6,12,7
0031 6 CONTINUE
0032 E1=F
0033 X1=X
0034 GOTO9
0035 7 CONTINUE
0036 E2=F
0037 X2=X
0038 GOTO9
0039 10 CONTINUE
0040 X=Y
0041 IF(X-0.4)11,11,12

```

C

PAGE 002

FORTRAN IV D06-01 SOURCE LISTING

C CALCULATE POLANYI ADSORPTION POTENTIAL

C

0042 11 CONTINUE  
0043 Z=T\*ALOG(FC2)/BNMV2

```

0044      GOTD13
0045      12 CONTINUE
0046      Z=T*ALOG(FC1*X)/BNMV1
0047      13 CONTINUE
0048      WRITE(6,100)Z,X
0049      RETURN
0050      14 CONTINUE
0051      WRITE(6,101)X
0052      RETURN
0053      100 FORMAT(1H ,//, ' POLANYI ADSORPTION POTENTIAL',E12.4, '//, ' MOL. FRA
ACTION METHANE IN ADSORBED PHASE',/, ' CALCULATED FROM POLANYI POTEN
TIAL',E12.4, '//)
0054      101 FORMAT(1H ,//, ' SUBROUTINE SOLVE FAILS AT X= ',E12.4)
0055      END

```

0001

SUBROUTINE HEADER

C  
C  
C

SUBROUTINE TO PRINT HEADINGS AND TITLE

0002

DIMENSION TITLE(72)

0003

WRITE(6,1)

0004

WRITE(6,2)

0005

WRITE(6,3)

0006

WRITE(6,4)

0007

WRITE(6,5)

0008

WRITE(6,6)

0009

WRITE(6,7)

0010

WRITE(6,8)

0011

WRITE(6,9)

0012

WRITE(6,10)

0013

READ(1,11)(TITLE(L),L=1,72)

0014

WRITE(6,11)(TITLE(L),L=1,72)

0015

1 FORMAT(1H1,19X,'AAA DDD SSSSS 000 RRRR PPPP TTTT IIII 0  
100 N N DDD AAA TTTT AAA')

0016

2 FORMAT(1H ,19X,'A A D D S O O R R P P T I O  
1 O N N D D A A T A A')

0017

3 FORMAT(1H ,19X,'AAAAA D D SSSSS 0 O RRRR PPPP T I O  
1 O N N N D D AAAAA T AAAAA')

0018

4 FORMAT(1H ,19X,'A A D D S O O R R P P T I O  
1 O N N N D D A A T A A')

0019

5 FORMAT(1H ,19X,'A A DDD SSSSS 000 R R P T IIII 0  
100 N N DDD A A T A A')

0020

6 FORMAT(1H ,//,42X,'AAA N N AAA L Y Y SSSSS IIIII SSSS  
1S')

0021

7 FORMAT(1H ,41X,'A A N N A A L Y Y S I S')

0022

8 FORMAT(1H ,41X,'AAAAA N N AAAAA L Y SSSSS I SSSSS')

0023

9 FORMAT(1H ,41X,'A A N N N A A L Y S I S')

0024

10 FORMAT(1H ,41X,'A A N N A A LLLL Y SSSSS IIIII SSSSS',/  
1//)

0025

11 FORMAT(1H ,72A1)

0026

RETURN

0027

END

AAA DDD SSSSS 000 RRRR PPPP TTTT IIIII 000 N N N  
 A A D D S O O R R P P T I O O NN N  
 AAAAA D D SSSSS O O RRRR PPPP T I O O N N N  
 A A D D S O O R R P T I O O N NN  
 A A DDD SSSSS 000 R R P T IIIII 000 N N

DDD AAA TTTT AAA  
 D D A A T A A  
 D D AAAAA T AAAAA  
 D D A A T A A  
 DDD A A T A A

AAA N N AAA L Y Y SSSSS IIIII SSSSS  
 A A NN N A A L Y Y S S I S  
 AAAAA N N AAAAA L Y SSSSS I SSSSS  
 A A N NN A A L Y Y S S I S  
 A A N N A A LLLL Y SSSSS IIIII SSSSS

RUN 10 CH4-C2H6 ON 5A MOLECULAR SIEVE

SAMPLE INTERVAL

60.00 SECONDS

TOTAL HYDROCARBON MOI. FRACTION IN TOTAL FLOW

0.2053E+00

PRESSURE CHANGE TIMES IN NO. OF INTERVALS

78.000	124.000	166.000	204.000	242.000
--------	---------	---------	---------	---------

ADSORPTION TEMPERATURE

293.100 DEG. K



ADSORPTION PRESSURES ATMS.  
4. 404            7. 807            11. 211            18. 018            28. 229

AMBIENT TEMP 292. 800    DEG. K    AMBIENT PRESSURE 753. 000    MM. MERCURY

MOL. FRACTION METHANE IN TOTAL ADSORBATE    0. 829

WEIGHT OF ADSORBENT    2. 400    GMS.

AMBIENT FLOWRATE MLS. /MIN.

INITIAL    0. 2350E+02    FINAL    0. 2740E+02

AMBIENT FLOWRATE MOL. /MIN.

INITIAL    0. 9695E-03    FINAL    0. 1130E-02



















0. 1125E-02	0. 1125E-02	0. 1124E-02	0. 1124E-02	0. 1123E-02	0. 1122E-02	0. 1122E-02	0. 1122E-02	0. 1122E-02
0. 1122E-02	0. 1123E-02	0. 1122E-02	0. 1122E-02	0. 1123E-02	0. 1120E-02	0. 1122E-02	0. 1122E-02	0. 1122E-02
0. 1122E-02	0. 1120E-02	0. 1122E-02	0. 1123E-02	0. 1125E-02	0. 1126E-02	0. 1128E-02	0. 1130E-02	0. 1130E-02
0. 1130E-02	0. 1131E-02	0. 1130E-02	0. 1130E-02	0. 1132E-02	0. 1138E-02	0. 1145E-02	0. 1151E-02	0. 1151E-02
0. 1152E-02	0. 1150E-02	0. 1149E-02	0. 1138E-02	0. 1134E-02	0. 1131E-02	0. 1130E-02	0. 1129E-02	0. 1129E-02
0. 1129E-02	0. 1128E-02	0. 1129E-02	0. 1128E-02	0. 1128E-02	0. 1128E-02	0. 1128E-02	0. 1127E-02	0. 1127E-02
0. 1128E-02	0. 1127E-02	0. 1127E-02	0. 1127E-02	0. 1126E-02	0. 1126E-02	0. 1126E-02	0. 1126E-02	0. 1126E-02
0. 1126E-02	0. 1127E-02	0. 1126E-02	0. 1127E-02	0. 1126E-02	0. 1129E-02	0. 1129E-02	0. 1129E-02	0. 1131E-02
0. 1131E-02	0. 1130E-02							

METHANE

AMMOUNT ADSORBED AND ACCUMULATED MOLS.

0. 5889E-03 0. 8879E-03 0. 1067E-02 0. 1301E-02 0. 1586E-02

ETHANE

AMMOUNT ADSORBED AND ACCUMULATED MOLS.

0. 2647E-02 0. 3154E-02 0. 3469E-02 0. 3689E-02 0. 3854E-02

TOTAL H/C PRESSURE 13.279 PSIA

MOL FRACTION METHANE IN TOTAL ADSORBATE 0.8290

GAS PHASE FUGACITIES 0.7478E+00 0.1533E+00 ATMS

LIQUID VAPOUR PRESSURES 0.2410E+03 0.2517E+02 ATMS

LIQUID FUGACITIES 0.1747E+03 0.2186E+02 ATMS

POLANYI ADSORPTION POTENTIAL 0.2577E+02

MOL FRACTION METHANE IN ADSORBED PHASE  
CALCULATED FROM POLANYI POTENTIAL 0.1154E+00

MOLAR VOLUMES CC./MOL

METHANE 37.471 ETHANE 55.046

GAS PHASE DENSITIES IN ADSORBER MOL. /CC.

METHANE 0. 3115E-04 ETHANE 0. 6427E-05

MOI S. OF GAS ADSORBED

METHANE 0. 5889E-03 ETHANE 0. 2647E-02

MOL. FRACTION METHANE IN ADSORBED PHASE 0. 182

MOI S. OF GAS ADSORBED/GM. OF ADSORBENT

METHANE 0. 2454E-03 ETHANE 0. 1103E-02

WT. OF ADSORBATE/GM.

METHANE 0. 3926E-02 ETHANE 0. 3308E-01

SEPARATION FACTOR C<sub>2</sub>H<sub>6</sub>/CH<sub>4</sub> 0. 2178E+02

ADSORBATE VOLUMES CC./GM. ADSORBENT

METHANE 0. 9195E-02 ETHANE 0. 6070E-01 TOTAL 0. 6990E-01

TOTAL H/C PRESSURE 23.543 PSIA

MOL FRACTION METHANE IN TOTAL ADSORBATE 0.8290

GAS PHASE FUGACITIES 0.1325E+01 0.2699E+00 ATMS

LIQUID VAPOUR PRESSURES 0.2410E+03 0.2517E+02 ATMS.

LIQUID FUGACITIES 0.1747E+03 0.2186E+02 ATMS.

POLANYI ADSORPTION POTENTIAL 0.2262E+02

MOL FRACTION METHANE IN ADSORBED PHASE  
CALCULATED FROM POLANYI POTENTIAL 0.1367E+00

MOLEAR VOLUMES CC./MOL.

METHANE 37.369 ETHANE 55.046

GAS PHASE DENSITIES IN ADSORBER MOL. /CC.

METHANE 0.5547E-04 ETHANE 0.1139E-04

MOLES OF GAS ADSORBED

METHANE 0.8879E-03 ETHANE 0.3154E-02

MOL. FRACTION METHANE IN ADSORBED PHASE 0.220

MOLES OF GAS ADSORBED/GM. OF ADSORBENT  
METHANE 0.3700E-03 ETHANE 0.1314E-02

WT. OF ADSORBATE/GM.

METHANE 0.5919E-02 ETHANE 0.3942E-01

SEPARATION FACTOR C<sub>2</sub>H<sub>6</sub>/CH<sub>4</sub> 0.1729E+02

ADSORBATE VOLUMES CC./GM. ADSORBENT  
METHANE 0.1383E-01 ETHANE 0.7233E-01 TOTAL 0.8615E-01

TOTAL H/C PRESSURE 33.807 PSIA.  
MOL FRACTION METHANE IN TOTAL ADSORBATE 0.8290

GAS PHASE FUGACITIES 0.1900E+01 0.3849E+00 ATMS  
LIQUID VAPOUR PRESSURES 0.2410E+03 0.2517E+02 ATMS.  
LIQUID FUGACITIES 0.1747E+03 0.2186E+02 ATMS.

POLANYI ADSORPTION POTENTIAL 0.2063E+02

MOL. FRACTION METHANE IN ADSORBED PHASE  
CALCULATED FROM POLANYI POTENTIAL 0.1520E+00

MOLAR VOLUMES CC./MOL.  
METHANE 38.023 ETHANE 55.046

GAS PHASE DENSITIES IN ADSORBER MOL./CC.  
METHANE 0.7980E-04 ETHANE 0.1636E-04

MOLES OF GAS ADSORBED

METHANE 0.1067E-02 ETHANE 0.3469E-02

MOI. FRACTION METHANE IN ADSORBED PHASE 0.235

MOLES OF GAS ADSORBED/GM. OF ADSORBENT

METHANE 0.4446E-03 ETHANE 0.1445E-02

WT. OF ADSORBATE/GM.

METHANE 0.7113E-02 ETHANE 0.4336E-01

SEPARATION FACTOR C2H6/CH4 0.1586E+02

ADSORBATE VOLUMES CC./GM. ADSORBENT

METHANE 0.1690E-01 ETHANE 0.7957E-01 TOTAL 0.9647E-01



TOTAL H/C PRESSURE 54.334 PSIA.

MOL FRACTION METHANE IN TOTAL ADSORBATE 0.8290

GAS PHASE FUGACITIES 0.3046E+01 0.6104E+00 ATMS.

LIQUID VAPOUR PRESSURES 0.2410E+03 0.2517E+02 ATMS.

LIQUID FUGACITIES 0.1747E+03 0.2186E+02 ATMS.

POLANYI ADSORPTION POTENTIAL 0.1804E+02

MOL. FRACTION METHANE IN ADSORBED PHASE  
CALCULATED FROM POLANYI POTENTIAL 0.1749E+00

MOLAR VOLUMES CC./MOL.

METHANE 38.942 ETHANE 55.046

GAS PHASE DENSITIES IN ADSORBER MOL./CC.

METHANE 0.1287E-03 ETHANE 0.2630E-04

MOLES OF GAS ADSORBED

METHANE 0.1301E-02 ETHANE 0.3689E-02

MOI. FRACTION METHANE IN ADSORBED PHASE 0.261

MOLES OF GAS ADSORBED/GM. OF ADSORBENT

METHANE 0.5422E-03 ETHANE 0.1537E-02

WT. OF ADSORBATE/GM.

METHANE 0.8675E-02 ETHANF 0.4612E-01

SEPARATION FACTOR C<sub>2</sub>H<sub>6</sub>/CH<sub>4</sub> 0.1388E+02

ADSORBATE VOLUMES CC./GM ADSORBENT

METHANF 0.2111E-01 ETHANE 0.8462E-01 TOTAL 0.1057E+00

TOTAL H/C PRESSURE 85.126 PSIA.

MOL FRACTION METHANE IN TOTAL ADSORBATE 0.8290

GAS PHASE FUGACITIES 0.4754E+01 0.9543E+00 ATMS

LIQUID VAPOUR PRESSURES 0.2410E+03 0.2517E+02 ATMS.

LIQUID FUGACITIES 0.1747E+03 0.2186E+02 ATMS.

POLANYI ADSORPTION POTENTIAL 0.1551E+02

MOL FRACTION METHANE IN ADSORBED PHASE  
CALCULATED FROM POLANYI POTENTIAL 0.1977E+00

MOL AIR VOLUMES CC./MOL.

METHANE 39.885 ETHANE 55.046

GAS PHASE DENSITIES IN ADSORBER MDL./CC.

METHANE 0.2029E-03 ETHANE 0.4185E-04

MOI.S OF GAS ADSORBED

METHANE 0.1586E-02 ETHANE 0.3854E-02

MOI. FRACTION METHANE IN ADSORBED PHASE 0.291

MOI.S OF GAS ADSORBED/GM. OF ADSORBENT

METHANE 0.6607E-03 ETHANE 0.1606E-02

WT. OF ADSORBATE/GM.

METHANE 0.1057E-01 ETHANE 0.4818E-01

SEPARATION FACTOR C<sub>2</sub>H<sub>6</sub>/CH<sub>4</sub> 0.1178E+02

ADSORBATE VOLUMES CC./GM. ADSORBENT

METHANE 0.2635E-01 ETHANE 0.8841E-01 TOTAL 0.1148E+00

APPENDIX THREE

C  
C PROGRAM TO MODEL FIXED-BED SINGLE OR BINARY ADSORPTION OF  
C METHANE AND/OR ETHANE ON 5A MOLECULAR SIEVE OR ACTIVATED  
C CARBON  
C  
C  
C

C THE MODEL SOLVES THE P.D.E.'S FOR CASES WHERE THE GAS-SOLID  
C MASS TRANSFER RATE IS GIVEN IN TERMS OF A DRIVING FORCE  
C BETWEEN THE GAS PHASE AND THE AVERAGE ADSORBENT ADSORBATE  
C CONCENTRATION OR FOR EQUILIBRIUM CONTROL  
C  
C  
C  
C

C CASES CAN BE SOLVED WHERE THE ADSORBATE CONCENTRATION  
C IS A SIGNIFICANT PROPORTION OF THE TOTAL GAS PHASE  
C CONCENTRATION IN THE BED AND HENCE AN AXIAL FLOW PROFILE EXISTS  
C  
C  
C  
C

C NON-STEP CHANGES IN ADSORBATE CONCENTRATION AND THE VARIATION  
C IN OUTLET FLOWRATE WITH GAS PHASE ADSORBATE CONCENTRATION  
C ARE ALSO INCLUDED  
C  
C  
C  
C

C AREAS-CHROMATOGRAM PEAK AREAS FROM P. D. P. 8  
C C-GAS PHASE ADSORBATE CONC. GMUL/CC  
C FLOW-INTERSTITIAL LINEAR FLOWRATE CM/S  
C

C Y-BED OUTLET GAS PHASE FRACTIONAL RESPONSE  
C ACH4, AC2H6-KATHEROMETER RESPONSE CHECK PEAK AREAS  
C ACH4E, AC2H6-FINAL PEAK AREA  
C PADSIG-TOTAL PRESSURE IN ADSORPTION CELL P. S. I. G.  
C TADSK-ADSORPTION CELL TEMPERATURE DEG. K  
C TAMBK-AMBIENT TEMPERATURE DEG. K  
C PAMBHC-AMBIENT PRESSURE MM. HG  
C F-CELL OUTLET FLOWRATE CC/MIN.  
C WT-WEIGHT OF ADSORBENT GM  
C AT1, 2, 3-CHROMATOGRAPH ATTENUATION SETTINGS  
C DTEXP-TIME INTERVAL BETWEEN CELL EFFLUENT ANALYSES  
C THCMF-TOTAL ADSORBATE MOL FRACTION OF GAS PHASE  
C Y1-MOL FRACTION OF METHANE IN TOTAL ADSORBATE  
C DT1-MODEL TIME INCREMENT FOR METHANE S  
C DT2-MODEL TIME INCREMENT FOR ETHANE S  
C ROWB-ADSORBENT BED BULK DENSITY GM/CC  
C ROWP-ADSORBENT PELLET DENSITY GM/CC  
C EMAC-ADSORBENT PELLET MACRO-PURE VOIDAGE  
C EBED-ADSORBENT BED TOTAL VOIDAGE  
C DEADTM TIME FOR STEP CHANGE IN GAS CONC. TO REACH GAS SAMPLE POINT  
C WITHOUT ADSORPTION MIN.  
C T-TIME S  
C AX-CROSS-SECTIONAL AREA OF ADSORPTION CELL CM\*\*2  
C RL-ADSORBENT BED LENGTH CM  
C DZ-MODEL BED LENGTH INCREMENT CM  
C FM-CELL OUTLET FLOWRATE GMOL/S  
C ROW-GAS PHASE DENSITY IN CELL GMOL/CC

```
C F1-CELL LINEAR INTERSTITIAL FLOWRATE AT OUTLET CM/S
C C2-GAS PHASE MOL FRACTION OF ETHANE AT ANY POINT ALONG CELL AXIS
C C1 GAS PHASE MOL FRACTION OF METHANE AT ANY POINT ALONG CELL AXIS
C D01,2- INCREASE IN SOLID PHASE ADSORBATE CONC. GMOL
C A1,2 B1,2-LANGMUIR CONSTANTS
C FRI,2-GAS PHASE FRACTIONAL RESPONSE AT CELL OUTLET AT ANY TIME
C Z1,2-ADSORBATE MOL FRACTION IN TOTAL GAS PHASE AT CELL INLET
C STEPS-NUMBER OF STEPS IN FINITE DIFF. RAMP
C STEP1,2-STEP SIZE GMOL/CC
C R1,2-RATE OF ADSORPTION GMOL/S
C FLOWOUT CELL OUTLET INTERSTITIAL LINEAR FLOWRATE AT ANY TIME CM/S
C DFLOW-CHANGE IN INTERSTITIAL LINEAR FLOWRATE ACROSS CELL CM/S
C COUTT-TOTAL ADSORBATE CONC. AT CELL OUTLET GMOL/CC
C DCONCT-CHANGE IN TOTAL ADSORBATE CONC. ACROSS CELL GMOL/CC
C Z-POSITION ALONG ADSORBENT BED AXIS
C N-NUMBER OF SAMPLES ANALYSED IN EXPERIMENTAL RUN
C NM,MM COUNTERS TO INDICATE COMPOSITION OF GAS PHASE
C NM=1,MM=1-PURE METHANE
C NM=2,MM=2-PURE ETHANE
C NM=1,MM=2-METHANE ETHANE MIXTURE
```

READ DATA



```

0001 DIMENSION AREAS(2,200), C(4,750), FLOW(755), Y(2,200)
0002 DIMENSION TITL(72)
0003 INTEGER Z
0004 CALL ASSIGN (1, 'L200,200JK1.DAT',15)
0005 CALL ASSIGN (6, 'L200,200JK2.RES',17)
0006 READ(1,100)(TITL(L),L=1,72)
0007 WRITE(6,100)(TITL(L),L=1,72)
0008 READ(1,99)N
0009 READ(1,99)NR,NM
0010 READ(1,101)(AREAS(1,L),AREAS(2,L),L=1,N)
0011 READ(1,102)ACH4E,AC2H6E
0012 READ(1,102)ACH4,AC2H6
0013 READ(1,102)AT1,AT2,ATS
0014 READ(1,102)PADCIG
0015 READ(1,102)TAUSEK, TAMBK, PAMBHG, F, WT, DTEXP
0016 READ(1,99)NZ
0017 READ(1,102)DT1,DT2

C
C CALCULATE GAS PHASE INLET CONCENTRATIONS
C
ACH4=ACH4*ATS
AC2H6=AC2H6*ATS
ACH4E=ACH4E*AT1
AC2H6E=AC2H6E*AT2
THEMF=ACH4E/ACH4+AC2H6E/AC2H6
Y1=ACH4E/(ACH4+THEMF)

```

```

0018
0019
0020
0021
0022
0023

```





```
0067      STEPS=90.*23.4/(D11*F)
0068      STEP1=C(1,1)/STEPS
0069      STEP2=C(3,1)/STEPS
0070      NT=0
0071      CMAX1=C(1,1)
0072      CMAX2=C(3,1)
0073      C(1,1)=0.
0074      C(3,1)=0.
0075      WRITE(6,116)
0076      2 CONTINUE
0077      Z=2
0078      INCREMENT TIME
0079      T=T+DT1
0080      CALCULATE RAMP ADSORBATE INLET GAS PHASE CONCENTRATION
0081      C(1,1)=C(1,1)+STEP1
0082      C(3,1)=C(3,1)+STEP2
0083      IF(C(1,1).GT.CMAX1 OR C(3,1).GT.CMAX2)GOTO3
0084      GOTO 4
0085      3 CONTINUE
0086      C(1,1)=CMAX1
0087      C(3,1)=CMAX2
0088      4 CONTINUE
0089      CALCULATE OUTLET FLOWRATE AT TIME T AS A FUNCTION OF GAS PHASE
```

```

C
C
0088      UNTIL COMPUTATION AT T-DT
C
0089      DFLOWT=1. +0.35*(FR1+FR2)*THCRH/Z.
C
C
0090      CALCULATE INLET GAS PHASE FLOWRATE AT TIME T FROM MASS BALANCES
C
0091      FOR EACH COMPONENT AT T-DT
C
0092      A=FR1*Z1
0093      B=FR2*Z2
0094      R2=0*((Z1-A)*Z2:(Z2-B)*(1.-Z1))
0095      R2=R2/((1.-Z2)*(1.-Z1)-Z1*Z2)
0096      R2=R2*DFLOWT
0097      R1=0*((Z1-A)+R2*Z1)/(1.-Z1)
0098      R1=R1*DFLOWT
0099      FLOWT=F1*DFLOWT
0100      DFLOW=(R1+R2)/DIV
0101      COUTT=C(1,NZ)+C(3,NZ)
0102      DCONCT=C(1,1)+C(3,1)-COUTT
C
C
0103      CALCULATE AXIAL FLOWRATE PROFILE AT TIME T
C
C
0104      ASSUME CONSTANT AXIAL FLOWRATE IF THE CHANGE IN FLOWRATE
0105      ACCROSS THE BED IS SMALL
C
0106      IF(DCONCT.GT.1.0E-20)GOTO5
0107      DO 6 L=1,NZ
0108      FLOW(L)=FLOWT

```

```
0104      6 CONTINUE
0105      5 CONTINUE
0106      IF(NFLOW)7,7,8
C
C      USE LINEAR PROFILE FOR FIRST TIME INTERVAL
C
0107      7 CONTINUE
0108      DO 9 L=1,NZ
0109      FLOW(L)=BFLOW*(NZ-L)/(NZ-1)+FLOWOUT
0110      9 CONTINUE
0111      NR=DT2/DT1+0.05
0112      NFLOW=1
0113      GOTO10
C
C      ASSUME EQUAL FRACTIONAL AXIAL CONCENTRATION AND FLOWRATE
C      PROFILES AT T-DT
C
0114      8 CONTINUE
0115      DO 10 L=1,NZ
0116      FLOW(L)={(C(1,L)+C(3,L)-COUT)/DCONS}*DFLOW+FLOWOUT
0117      10 CONTINUE
0118      FLOW(NZ+1)=FLOW(NZ)+(FLOW(NZ)-FLOW(NZ-1))
C
C      CALCULATE SOLID SURFACE EQUILIBRIUM CONCENTRATION
C      AT BED AXIAL POSITION Z FOR METHANE
C
0119      IF(C(1,Z-1).EQ.0.0.AND.C(3,Z-1).EQ.0.0)GOTO11
0121      C1=C(1,Z-1)/(C(1,Z-1)+C(3,Z-1))
0122      GOTO12
0123      11 CONTINUE
```

```

0124 C1=1.0E-10
0125 12 CONTINUE
0126 A1=C1*0.00035/(1.-0.8801*C1)
0127 B1=-42600.*C1+46970.
0128 EQUAD1=C(1,Z-1)*A1*B1/(1.+B1*C(1,Z-1))
C
C CALCULATE GAS PHASE CONCENTRATION AT Z FROM
C OVERALL MASS BALANCE FOR METHANE
C
0129 DD1=EQUAD1-C(2,Z)
0130 RHS1=C(1,Z)+DT1*FLOW(Z)*C(1,Z-1)/DZ-DD1*ROWB/EBED
0131 DIV1=DT1*(FLOW(Z)+(FLOW(Z+1)-FLOW(Z-1))/Z)/DZ+1.
0132 C(1,Z)=RHS1/DIV1
C
C CALCULATE SOLID PHASE ADSORBED CONCENTRATION
C
0133 C(2,Z)=C(2,Z)+DD1
C
C HAS SOLUTION REACHED BED EXIT
C
0134 IF(Z.EQ.NZ)GOTO13
C
C NO. INCREMENT Z
C
0136 Z=Z+1
0137 GOTO10
C

```

```

C      YES ; CALCULATE GAS PHASE FRACTIONAL BREAKTHROUGH
0138      13 CONTINUE
0139      FR1=C(1,NZ)/C(1,1)
0140      NT=NT+1
C
C      IS IT TIME FOR ETHANE CALCULATION
C
C      NO; DO ANOTHER METHANE
C
C      IF (NT.LT.NR)GOTO2
0141      NT=0
0142      Z=2
0143      14 CONTINUE
0144      YES; DO AN ETHANE
C
C      CALCULATE SOLID SURFACE EQUILIBRIUM CONCENTRATION
C      AT BED AXIAL POSITION Z FOR ETHANE
C
0146      IF(C(1,Z-1).EQ.0.0.AND.C(3,Z-1).EQ.0.0)GOTO15
0148      C2=C(3,Z-1)/(C(1,Z-1)+C(3,Z-1))
0149      GOTO16
0150      15 CONTINUE
0151      C2=1.0E-10
0152      16 CONTINUE
0153      A2=C2*0.02951/(1.+10.6*C2)
0154      B2=-139200.*C2+251400.
0155      EQUAD2=C(3,Z-1)*A2*B2/(1.+B2*C(3,Z-1))

```



```

C
C
C
0156 C CALCULATE GAS PHASE CONCENTRATION AT Z FROM
0157 C OVERALL MASS BALANCE FOR ETHANE
0158 C
0159 C  $DO2=EQ(AD2-C(4,Z))$ 
0160 C  $RHS2=C(3,Z)+DT2*FLOW(Z)*C(3,Z-1)/DZ-DO2*ROWB/EBED$ 
0161 C  $DIV2=DT2*(FLOW(Z)+(FLOW(Z+1)-FLOW(Z-1))/Z)/DZ+1$ 
0162 C  $C(3,Z)=RHS2/DIV2$ 
0163 C CALCULATE SOLID PHASE ADSORBATE CONCENTRATION
0164 C  $C(4,Z)=C(4,Z)+DO2$ 
0165 C
0166 C HAS SOLUTION REACHED BED EXIT
0167 C
0168 C IF(Z.EQ.NZ)GOTO17
0169 C
0170 C NO: INCREMENT Z
0171 C
0172 C  $Z=Z+1$ 
0173 C GOTO14
0174 C
0175 C 17 CONTINUE
0176 C  $FR1=C(1,NZ)/C(1,1)$ 
0177 C  $FR2=C(3,NZ)/C(3,1)$ 
0178 C
0179 C YES: IS T EQUAL TO EXPERIMENTAL SAMPLE TIME
0180 C
0181 C NO : RETURN TO BED INLET
0182 C
0183 C

```

```

0168      IF (NTOT.GT.(T/DTEXP+0.0001))GOTO2
C
C      YES: WRITE MODEL AND EXPERIMENTAL RESULTS
C
0170      TMIN=T/60.
0171      WRITE(6,117)Y(1,NTOT),FR1,Y(2,NTOT),FR2,TMIN
0172      NTOT=NTOT+1
C
C      CHECK FOR BREAKTHROUGH OF BOTH SPECIES OR TIME OUT
C
C
C      IF COMPLETE - STOP
C
0173      IF (FR1.GT.0.99.AND.FR2.GT.0.99) STOP
C
C      RETURN TO BED INLET
C      GOTO2
0175      99 FORMAT(1H , I4)
0176      100 FORMAT(1H , 72A1)
0177      101 FORMAT(1H , 8F6.4)
0178      102 FORMAT(1H , F16.8)
0179      103 FORMAT(1H , //, ' TOTAL HYDROCARBON MOL. FRACTION IN TOTAL FLOW ', //
0180             1, E12.4, //)
0181      104 FORMAT(1H , //, ' ADSORPTION TEMPERATURE ', F16.3, ' DEG. K ', //)
0182      105 FORMAT(1H , //, ' ADSORPTION PRESSURE ', F16.3, ' PSIG. ', //)
0183      106 FORMAT(1H , //, ' AMBIENT TEMP. ', F8.3, ' DEG. K   AMBIENT PRESSURE
0184             1, F8.3, ' MM. MERCURY', //)
0185      107 FORMAT(1H , //, ' MOL. FRACTION METHANE IN TOTAL ADSORBATE ', F8.3, //)
0186      108 FORMAT(1H , //, ' WEIGHT OF ADSORBENT ', F8.3, ' GMS. ', //)
0187      109 FORMAT(1H , //, ' EXPERIMENTAL SAMPLE TIME INTERVAL ', E12.4 , ' SEC.

```



RUN 7 METHANE-ETHANE ON 5A MOLECULAR SIEVE

TOTAL HYDROCARBON MOL. FRACTION IN TOTAL FLOW

0.2050E+00

ADSORPTION TEMPERATURE 293.100 DEG. K

ADSORPTION PRESSURE 50.000 PSIG.

AMBIENT TEMP. 292.800 DEG. K AMBIENT PRESSURE 753.000 MM. MERCURY

MOL. FRACTION METHANE IN TOTAL ADSORBATE 0.829

WEIGHT OF ADSORBENT 2.400 GMS.

EXPERIMENTAL SAMPLE TIME INTERVAL 0.6000E+02 SEC.

MATHEMATICAL MODEL TIME INCREMENTS 0.1000E+01 0.2000E+02 SEC.



INLET GAS PHASE CONCENTRATIONS  
 METHANE 0.3116E-04 MOL./CC.  
 ETHANE 0.6428E-05 MOL./CC.

FRACTIONAL BREAKTHROUGH DATA

METHANE		ETHANE		
EXPTL.	MODEL	EXPTL.	MODEL	TIME(MIN)
0.0000E+00	0.8323E-31	0.0000E+00	0.9960E-31	0.2080E+01
0.0000E+00	0.5760E-31	0.0000E+00	0.8676E-31	0.2413E+01
0.0000E+00	0.3226E-31	0.0000E+00	0.7949E-31	0.3030E+01
0.0000E+00	0.2354E-31	0.0000E+00	0.1184E-30	0.4080E+01
0.0000E+00	0.2028E-31	0.0000E+00	0.4561E-31	0.5080E+01
0.0000E+00	0.4517E-15	0.0000E+00	0.4236E-16	0.6080E+01
0.1079E+00	0.1052E+01	0.0000E+00	0.6271E-02	0.7080E+01
0.7733E+00	0.1043E+01	0.0000E+00	0.8144E-02	0.8080E+01
0.9545E+00	0.1042E+01	0.0000E+00	0.8365E-02	0.9030E+01
0.9644E+00	0.1043E+01	0.0000E+00	0.8739E-02	0.1008E+02
0.9673E+00	0.1042E+01	0.0000E+00	0.9182E-02	0.1108E+02
0.9683E+00	0.1042E+01	0.0000E+00	0.9804E-02	0.1208E+02
0.9792E+00	0.1042E+01	0.0000E+00	0.1053E-01	0.1308E+02
0.9822E+00	0.1042E+01	0.0000E+00	0.1132E-01	0.1408E+02
0.9861E+00	0.1042E+01	0.0000E+00	0.1216E-01	0.1508E+02
0.9832E+00	0.1042E+01	0.0000E+00	0.1303E-01	0.1608E+02
0.9832E+00	0.1042E+01	0.0000E+00	0.1393E-01	0.1708E+02
0.9861E+00	0.1042E+01	0.0000E+00	0.1484E-01	0.1808E+02
0.9881E+00	0.1042E+01	0.0000E+00	0.1577E-01	0.1908E+02
0.9792E+00	0.1042E+01	0.0000E+00	0.1672E-01	0.2008E+02
0.9921E+00	0.1042E+01	0.0000E+00	0.1768E-01	0.2108E+02
0.9990E+00	0.1042E+01	0.0000E+00	0.1865E-01	0.2208E+02
0.9941E+00	0.1042E+01	0.0000E+00	0.1964E-01	0.2308E+02

0. 9970E+00	0. 1042E+01	0. 0000E+00	0. 2064E-01	0. 2408E+02
0. 9990E+00	0. 1041E+01	0. 0000E+00	0. 2166E-01	0. 2508E+02
0. 9950E+00	0. 1041E+01	0. 0000E+00	0. 2269E-01	0. 2608E+02
0. 1007E+01	0. 1042E+01	0. 0000E+00	0. 2373E-01	0. 2708E+02
0. 1009E+01	0. 1042E+01	0. 0000E+00	0. 2478E-01	0. 2808E+02
0. 1009E+01	0. 1042E+01	0. 0000E+00	0. 2585E-01	0. 2908E+02
0. 1000E+01	0. 1042E+01	0. 0000E+00	0. 2694E-01	0. 3008E+02
0. 1004E+01	0. 1041E+01	0. 0000E+00	0. 2805E-01	0. 3108E+02
0. 1007E+01	0. 1041E+01	0. 0000E+00	0. 2917E-01	0. 3208E+02
0. 1009E+01	0. 1042E+01	0. 0000E+00	0. 3029E-01	0. 3308E+02
0. 1008E+01	0. 1043E+01	0. 0000E+00	0. 3142E-01	0. 3408E+02
0. 1015E+01	0. 1042E+01	0. 0000E+00	0. 3258E-01	0. 3508E+02
0. 1015E+01	0. 1041E+01	0. 0000E+00	0. 3377E-01	0. 3608E+02
0. 1016E+01	0. 1040E+01	0. 0000E+00	0. 3500E-01	0. 3708E+02
0. 1021E+01	0. 1041E+01	0. 0000E+00	0. 3622E-01	0. 3808E+02
0. 1016E+01	0. 1042E+01	0. 0000E+00	0. 3743E-01	0. 3908E+02
0. 1017E+01	0. 1043E+01	0. 0000E+00	0. 3864E-01	0. 4008E+02
0. 1019E+01	0. 1042E+01	0. 0000E+00	0. 3990E-01	0. 4108E+02
0. 1020E+01	0. 1040E+01	0. 0000E+00	0. 4124E-01	0. 4208E+02
0. 1026E+01	0. 1039E+01	0. 0000E+00	0. 4263E-01	0. 4308E+02
0. 1024E+01	0. 1040E+01	0. 2400E-01	0. 4401E-01	0. 4408E+02
0. 1018E+01	0. 1042E+01	0. 2500E-01	0. 4530E-01	0. 4508E+02
0. 1027E+01	0. 1043E+01	0. 2100E-01	0. 4658E-01	0. 4608E+02
0. 1030E+01	0. 1042E+01	0. 1700E-01	0. 4799E-01	0. 4708E+02
0. 1030E+01	0. 1039E+01	0. 1800E-01	0. 4953E-01	0. 4808E+02
0. 1026E+01	0. 1038E+01	0. 1800E-01	0. 5118E-01	0. 4908E+02
0. 1029E+01	0. 1040E+01	0. 2900E-01	0. 5276E-01	0. 5008E+02
0. 1035E+01	0. 1043E+01	0. 2300E-01	0. 5408E-01	0. 5108E+02
0. 1031E+01	0. 1044E+01	0. 3100E-01	0. 5538E-01	0. 5208E+02
0. 1039E+01	0. 1042E+01	0. 2300E-01	0. 5693E-01	0. 5308E+02
0. 1047E+01	0. 1038E+01	0. 2700E-01	0. 5881E-01	0. 5408E+02
0. 1042E+01	0. 1036E+01	0. 2100E-01	0. 6092E-01	0. 5508E+02
0. 1041E+01	0. 1039E+01	0. 2500E-01	0. 6280E-01	0. 5608E+02

0. 1025E+01	0. 1043E+01	0. 1500E-01	0. 6404E-01	0. 5708E+02
0. 1025E+01	0. 1045E+01	0. 1400E-01	0. 6515E-01	0. 5808E+02
0. 1030E+01	0. 1043E+01	0. 1200E-01	0. 6681E-01	0. 5908E+02
0. 1032E+01	0. 1036E+01	0. 2800E-01	0. 6928E-01	0. 6008E+02
0. 1033E+01	0. 1034E+01	0. 3000E-01	0. 7237E-01,	0. 6108E+02
0. 1035E+01	0. 1038E+01	0. 3300E-01	0. 7489E-01	0. 6208E+02
0. 1030E+01	0. 1044E+01	0. 2100E-01	0. 7590E-01	0. 6308E+02
0. 1040E+01	0. 1048E+01	0. 2700E-01	0. 7620E-01	0. 6408E+02
0. 1005E+01	0. 1044E+01	0. 3400E-01	0. 7758E-01	0. 6508E+02
0. 1042E+01	0. 1033E+01	0. 3300E-01	0. 8122E-01	0. 6608E+02
0. 1044E+01	0. 1032E+01	0. 2500E-01	0. 8672E-01	0. 6708E+02
0. 1053E+01	0. 1035E+01	0. 2700E-01	0. 9153E-01	0. 6808E+02
0. 1052E+01	0. 1044E+01	0. 2200E-01	0. 9361E-01	0. 6908E+02
0. 1050E+01	0. 1053E+01	0. 4800E-01	0. 9148E-01	0. 7008E+02
0. 1046E+01	0. 1044E+01	0. 2360E+00	0. 9040E-01	0. 7108E+02
0. 1062E+01	0. 1029E+01	0. 6010E+00	0. 9708E-01	0. 7208E+02
0. 1051E+01	0. 1031E+01	0. 8680E+00	0. 1099E+00	0. 7308E+02
0. 1048E+01	0. 1028E+01	0. 9600E+00	0. 1326E+00	0. 7408E+02
0. 1050E+01	0. 1025E+01	0. 9790E+00	0. 2245E+00	0. 7508E+02
0. 1051E+01	0. 1014E+01	0. 9920E+00	0. 7771E+00	0. 7608E+02
0. 1057E+01	0. 1001E+01	0. 9920E+00	0. 9923E+00	0. 7708E+02